JUSTUS-LIEBIG-
UNIVERSITÄT
GIESSEN

Molecular Analysis of a Major Carpel Developmental Regulator: CRABS CLAW's Protein Domains and Non-Cell-Autonomous Action

Inaugural-Dissertation in fulfillment of

the requirements for the degree

Doctor of Science (Dr. rer. nat.)

Submitted to the Institute of Botany,

Justus-Liebig Universität Gießen

By
M. Sc. Thomas Groß
Friedberg, Germany

Gießen, 2019

Reviewers: Prof. Dr. Annette Becker

Institute of Botany

Justus-Liebig-University Giessen

Heinrich-Buff-Ring 38

35392 Giessen

Prof. Dr. Sandra Hake

Institute for Genetics

Justus-Liebig-University Giessen

Heinrich-Buff-Ring 58-62

35392 Giessen

For my family and Mathieu

„Die Neugier ist die mächtigste Antriebskraft im Universum, weil sie die beiden größten Bremskräfte im Universum überwinden kann: die Vernunft und die Angst.“

Walter Moers - Die Stadt der träumenden Bücher

Content

Summary

CRABS CLAW is a small protein belonging to the YABBY family, a plant specific protein family. In *Arabidopsis thaliana* it is expressed in the developing carpels and regulates the apical fusion of the two carpels, transmitting tract development, lateral growth, and nectary formation. The expression of CRC is rather complex with multiple expression domains throughout the young gynoecium and as for other YABBY proteins a non-cell-autonomous action has been described. However, only few regulators of CRC expression and target genes are described and the mode of non-cell-autonomous action is still unknown. This dissertation aims to identify transcriptional regulators, responsible for the proper temporal and spatial expression of CRC, the specification of CRC's place in the adaxial-abaxial regulatory network and to clarify the means of its non-cell-autonomous action. The regulation of CRC expression has been analyzed via a large scale Yeast-1-Hybrid screen and identified over 100 potential regulators of CRC expression, integrating CRC tightly into the carpel developmental regulatory protein network.

Further analysis of CRC function through expression analysis led to the identification of target genes of CRC like mir165/166, members of the *KANADI* gene family, and the HD ZIP III gene family. Both gene families are major players in the adaxial-abaxial regulatory network, involved in the development of all lateral plant organs such as leaves and floral organs. CRC supports KANADI action and activates the expression of other involved factors. In addition, CRC directly targets members of the HD ZIP III family. However, CRC's position in the adaxial-abaxial regulatory network seems to be not conserved in other eudicots. CRC exhibits a non-cell-autonomous action which is conferred by at least two signaling pathways. Abaxial polarity is regulated by the activation of the mobile miRNA165/166. At the same time, localizations of GFP tagged CRC revealed the CRC protein to be mobile as it migrates into the adaxial domain in young gynoecia. In older gynoecia it was excluded from the adaxial domain.

This study identified multiple unique features of CRC compared to its relatives. Its thightly controlled expression by over 100 putative regulators, integration in complex co-expression networks, adaxial and abaxial target genes, and its two mode non-cell-autonomous action indicate the important role in the complicated carpel development.

Zusammenfassung

CRABS CLAW ist ein kleines Protein der pflanzenspezifischen YABBY Protein Familie. In *Arabidopsis thaliana* ist es in den entwickelnden Fruchtblättern exprimiert und reguliert die apikale Fusion der Fruchtblätter, die Entwicklung des Transmissionskanal (einem Bereich des Septums), die Begrenzung des lateralen Wachstums des Gynoeceums, und die Bildung der Nektarien. Die Expression von CRC ist auf mehrere Bereiche im Fruchtblatt aufgeteilt und ebenso wurde ein nicht-zell-autonomer Effekt wie für andere YABBY Proteine beschrieben. Jedoch sind nur einige wenige Regulatoren der CRC Expression und Zielgene von CRC bekannt, sowie die Natur des mobilen Signals des nicht-zell-autonomen Effektes unbekannt ist. Daher zielt diese Dissertation darauf, zusätzliche transkriptionelle Regulatoren, die für die korrekte zeitliche und räumliche Expression von CRC nötig sind, zu identifizieren, sowie CRCs Position im adaxialen-abaxialen Netzwerk zu identifizieren und die Art und Weise des nicht-zell-autonomen Effektes zu klären. Die Expression von CRC wurde durch eine groß angelegte Hefe-1-Hybrid Analyse näher untersucht und über 100 mögliche Regulatoren der CRC Expression wurden identifiziert. Dies festigt CRCs Position im gen-regulatorischen Netzwerk der Fruchtblattentwicklung.

Eine weitere Analyse der CRC Funktionen mittels Expressionsanalyse führte zu der Identifikation mehrerer Zielgene wie mir165/166, Mitglieder der *KANADI* Genfamilie und Mitglieder der HD ZIP III Genfamilie. Beide Genfamilien sind Hauptkomponenten des adaxial–abaxialen Regulationsnetzwerkes. Dabei unterstützt CRC die Funktion der KAN Proteine und reguliert die Expression anderer involvierter Gene. Zusätzlich reguliert CRC direkt die Expression einiger HD ZIP III Gene. Wobei die Regulation der adaxial-abaxialen Regulatoren durch CRC zwischen verschiedenen Eudikotylen nicht komplett konserviert ist.

CRC weist eine nicht-zell-autonome Funktion auf, die durch mindestens zwei Signalübertragungswege vermittelt wird. Zum einen reguliert CRC die abaxiale Polarität durch die Aktivierung der mobilen miRNA165/166 und zum anderen durch direkten Transport des CRC Proteins. Lokalisierungen von mit GFP markierten CRC zeigten, dass das CRC Protein in den frühen Stadien des Gyneoceums von der abaxialen Domäne in die adaxiale wandert. In späteren Stadien ist CRC auf die abaxiale Domäne begrenzt.

Diese Studie konnte mehrere einzigartige CRC Charakteristika identifizieren, die CRC von den anderen Mitgliedern der YABBY Familie unterscheidet. Seine stark kontrollierte Expression durch mehr als 100 mögliche Regulatoren, die Integration in ein kompliziertes Co-Expressions Netzwerk, adaxiale und abaxiale Zielgene, und mindestens zwei Möglichkeiten zur nicht-zell-autonomen Regulation, zeigen eindringlich die wichtige Rolle CRCs in der komplexen Karpellentwicklung auf.

Introduction

Arabidopsis thaliana as a Model Organism

Arabidopsis thaliana, the model plant for plant science and especially in flower development for the last 35 years (Koornneef and Meinke, 2010), is one of the best analyzed plants due to multiple favorable traits. The duration between germination and flowering/seed production is rather short with approximately 6 weeks. *A. thaliana* is easy to cultivate both on petri dishes filled with medium or on soil and only moderate climate and light conditions are necessary. The *A. thaliana* genome, sequenced in 2000 as the first plant genome (The Arabidopsis Genome Initiative, 2000), is diploid and has a size of 1n ~ 135 Mbp distributed over 5 chromosomes. Even though, there are lager genome sizes of 1n ~ 157 Mbp published (Bennett *et al.*, 2003), compared to other plants, it is a rather small genome, easy to manipulate (Johnston *et al.*, 2005). Furthermore, multiple genetic manipulation methods have been established for *A. thaliana* which generated different mutant collections (Koornneeff *et al.*, 1982) and T-DNA insertion line collections (Alonso *et al.*, 2003). Additionally, a vast bioinformatics support is present for *Arabidopsis* like the TAIR database (Lamesch *et al.*, 2012). Moreover, *A. thaliana* is mostly self-pollinating, thus introduced mutations are rapidly homozygous and phenotypes can be analyzed.

Flower Development of *A. thaliana*

There are multiple pathways regulating flowering time like the number of leaves, the availability of sucrose, the phytohormone gibberellin, and vernalization (figure 1). However, the most prominent cue to induce the transition from the vegetative growth phase to the generative phase in which flowers are formed is by day length through the proteins CONSTANS (CO) and FLOWERING LOCUS T (FT). During the day, the CO protein, a B-box-type zinc-finger protein, accumulates in the companion cells of the leaf phloem and is degraded after dusk (Putterill *et al.*, 1995; Suárez-López *et al.*, 2001; An *et al.*, 2004). Only in long day

conditions (>12 hours of light), the CO protein level can rise enough to induce the expression of FT, a Raf kinase inhibitor (Samach *et al.*, 2000; Suárez-López *et al.*, 2001). The FT protein is then transported via the phloem to the shoot apical meristem (SAM) (Notaguchi *et al.*, 2008). There, FT interacts with the bZIP protein FLOWERING LOCUS D and both activate the expression of *APETALA1* and *LEAFY* which transform the SAM into an inflorescence meristem (IM) that produces floral meristems (FM) (Abe *et al.*, 2005; Wigge *et al.*, 2005).

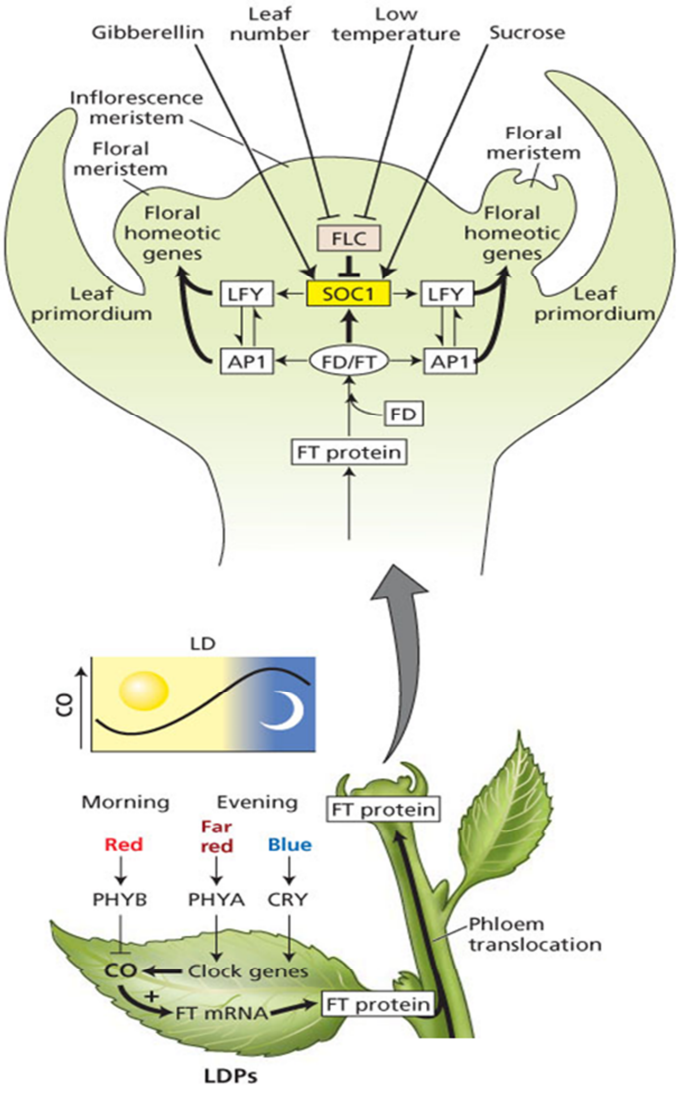

Figure 1: Regulation of flowering time in *A. thaliana*. Different signaling pathways are integrated at the SAM, leading to the transition from vegetative to generative phase and to the formation of flowers (after Taiz and Zeiger (2010)).

In general, most flowers of angiosperms are composed out of four whorls of floral organs: the sterile sepals and petals, the stamens which produce the pollen and the carpel(s) which

harbor the ovules and later seeds. In *A. thaliana,* the organ identity of the four sepals, four petals, six stamens, and two carpels (combined in one gynoecium) is mostly regulated by complexes of different MADS (MCM1, AGAMOUS, DEFICIENS, SRF) box transcription factors (TFs), summarized in the so called ABCE model (figure 2).

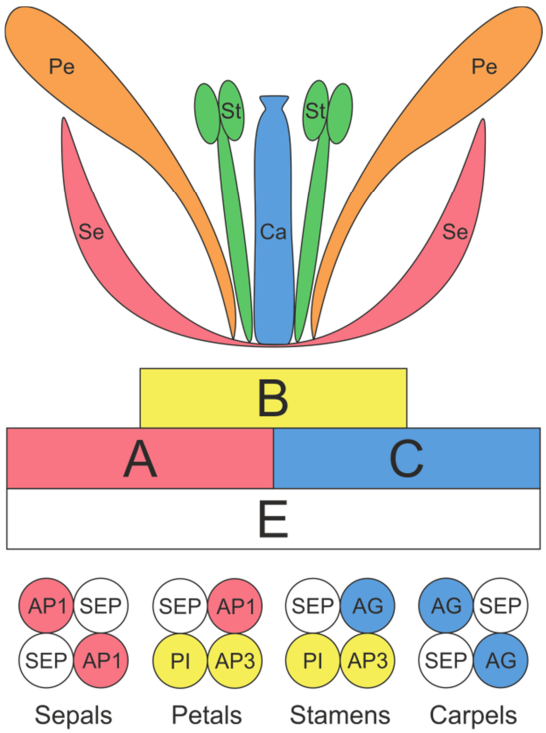

Figure 2: ABCE model of flower development in *A. thaliana*, after which the identity of the four whorls is determined by the presence of certain MADS box protein complexes, so called tetrads. Se: Sepals, Pe: Petals, St; Stamens, Ca: Carpels. Based on Irish (2017) and Theißen *et al.* (2016).

Combinations of four MADS box proteins, so called floral quartets are responsible for the homeotic identity of each whorl. Sepal identity is conferred by a heterotetramer of class A MADS box TFs (APETALA 1, AP1) and class E MADS box TFs (SEPALLATA 1/2/3/4). Classes A, B (PISTILLATA, PI; APETALA 3, AP3), and E confer petal identity, and stamen identity is regulated by a combination out of classes B, C (AGAMOUS, AG), E. Lastly, a combination of classes C and E confers carpel identity. The A class protein AP1 is supported by APETALA 2, a member of the AP2/ETHYLENE RESPONSIVE ELEMENT BINDING PROTEIN family. Mutations in one of the different MADS box TFs lead to an expanded activity range of the neighboring MADS box TFs and homeotic conversions happen. In *ag* mutants the activity range of AP1 and PI is expanded and super numerous sepals and petals are formed instead of stamens

and carpels. Nevertheless, the fine tuning of the developmental processes relies on genes, downstream of the MADS box TFs, like CRABS CLAW (CRC).

CRC - a Major Carpel Developmental Regulator

The *A. thaliana* protein CRABS CLAW (AT1G69180), the first identified member of the YABBY protein family, is involved in multiple steps during the development of one of the most important plant organs: the carpel (Bowman and Smyth, 1999). The eponymous phenotype of the *crc-1* mutant is the shortened and widened gynoecium whose tip resembles the claw of a yabby crab, because the two carpels remain unfused in the apex (figure 3). Here, the carpels are not able to produce a fused replum zone, a continuous false septum, and unified stylus tissue.

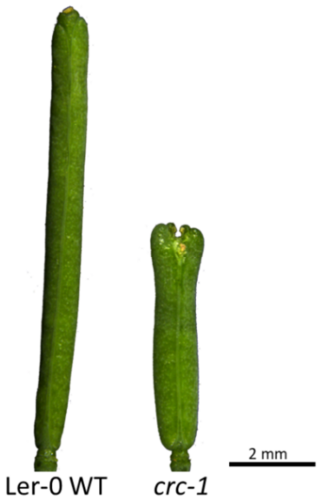

Figure 3: The *crc-1* phenotype in *A. thaliana*. Comparison of a wild type *A. thaliana* Ler-0 silique with a *crc-1* silique in the same ecotype. The picture was taken using a Leica M165C stereoscope.Scale bar represents 2 mm.

Furthermore, CRC specifies abaxial - adaxial polarity in concert with KANADI proteins and probably antagonistic to members of the HD-ZIP III protein family (Eshed *et al.*, 1999; Reinhart *et al.*, 2013; Tatematsu *et al.*, 2015); it is involved in nectary formation, and in the

termination of the floral meristem as a direct target of AG and redundantly to REBELOTE, SQUINT, and ULTRAPETALA 1 (Prunet *et al.*, 2008; Prunet *et al.*, 2009). The protein itself is structured into three domains (figure 4): A C2C2 zinc finger domain in the N-terminal region, a serine-proline rich domain in the central region, and a helix-loop-helix domain (YABBY domain) in the C-terminal region with sequence similarity the high mobility group (HMG) box (Bowman and Smyth, 1999).

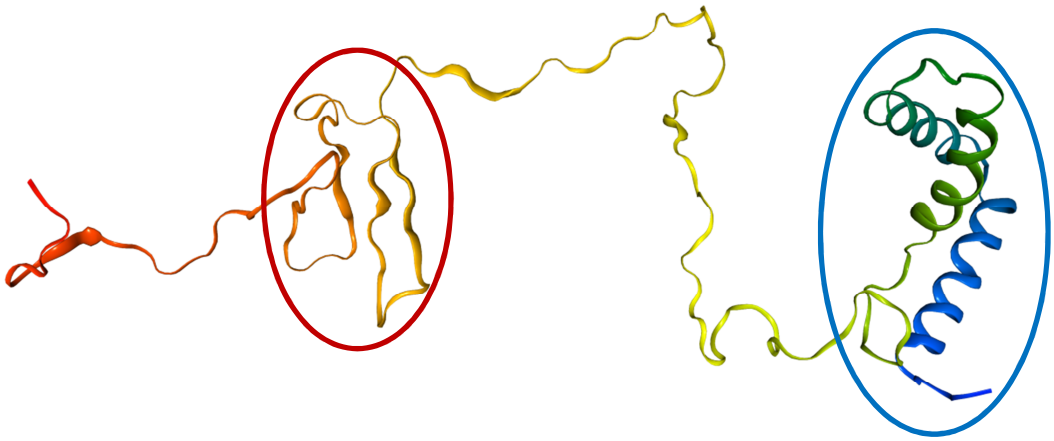

Figure 4: Three dimensional prediction model of the CRC protein. The model was made with the online prediction tool RaptorX (Källberg *et al.*, 2012) and visualized with NGL viewer (Rose and Hildebrand, 2015). Zinc finger (red circle) and YABBY domain (blue circle) are highlighted.

Both, the zinc finger domain and the YABBY domain are possible DNA binding domains but in the analyzed YABBY proteins (like OsYAB4 from *Oryza sativa*) so far the YABBY domain was the main DNA interacting domain (Shamimuzzaman and Vodkin, 2013; Yang *et al.*, 2016; Gross *et al.*, 2018). Shamimuzzaman and Vodkin (2013) were able to identify typical zinc finger binding motifs for YABBY proteins in *Glycine max*, but it seems that the YABBY domain is able to bind to these motifs too (Yang *et al.*, 2016). Additionally, Franco-Zorrilla *et al.* (2014) identified a DNA binding motif for two vegetative YABBY proteins (FIL and YAB5) from *A. thaliana* which differs in sequence from the previous shown DNA binding motifs (Shamimuzzaman and Vodkin, 2013). The lack of a DNA binding motif for CRC has impeded the identification of direct target genes of CRC for a long time. So far only four direct target genes are known. Han *et al.* (2012) identified by microarray based expression analysis *KETOACYL-CoA SYNTHASE 7* (*KCS7*) and *KCS15*; two genes that are involved in the synthesis

of very long chain fatty acids (VLCFAs), as to be regulated by CRC in developing fruits. These VLCFAs are part of cuticle waxes, seed storage lipids, and interestingly, serve as the substrate for the generation of signal molecules (Joubès *et al.*, 2008). The third gene, *TORNADO 2* (*TRN2*), is a plasma membrane localized ATPase which is responsible for auxin homeostasis in the developing gynoecium (Yamaguchi *et al.*, 2017). CRC represses the expression of *TRN2* synergistically with KNUCKLES and thus influencing auxin distribution and WUSCHEL (WUS) activity in the floral meristem. In addition, CRC activates the expression of *YUCCA4* (*YUC4*), an auxin synthase (Yamaguchi *et al.*, 2018). Recently the analysis of these two genes led to the identification of a CRC DNA binding motif. Based on the work of Shamimuzzaman and Vodkin (2013), putative YABBY binding motifs were identified in the promoter regions of both genes (Yamaguchi *et al.*, 2017; Yamaguchi *et al.*, 2018). Further analyzes showed the interaction of CRC with these motifs and the misregulation of TRN2 and YUC4 expression when these motifs were mutated (Yamaguchi *et al.*, 2017; Yamaguchi *et al.*, 2018). TRN2 and YUC4 directly link CRC and auxin during carpel development, as already hypothesized after rescuing *crc-1* mutants with the application of exogenous auxin by Ståldal *et al.* (2008).

CRABS CLAW Acts as a Bifunctional Transcription Factor in Flower Development

Nearly 20 years after its description, CRCs genetic interactions with other carpel development regulators like SPATULA were well described; however, its biochemical properties and molecular way of action remained unclear. Thus, an analysis of CRC's protein domains in regard to its localization, DNA binding, dimerization, and other molecular properties was performed which resulted in the publication Gross *et al.* (2018) (accessible at: https://www.frontiersin.org/articles/10.3389/fpls.2018.00835/full). In the next paragraphs, I will recapitulate the most important findings.

To analyze the subcellular localization of CRC, the coding sequence (CDS) of CRC was fused to GREEN FLUORESCENT PROTEIN (GFP) and expressed in leaves of *N. benthamiana*. Full

length CRC is exclusively localized to nuclei (figure 5 D and E). Only when the YABBY domain is removed, CRC is present in the cytoplasm (figure 5 F and G) vice versa, when the single YABBY domain is fused to GFP the exclusive nuclear import is restored (figure 5 H and I). Even though, a core nuclear localization signal (NLS) was identified in the N-terminal part of the YABBY domain, additional supporting motifs in the YABBY domain are necessary to induce nuclear import, as the NLS alone is not sufficient to induce nuclear import (figure 5 J and K).

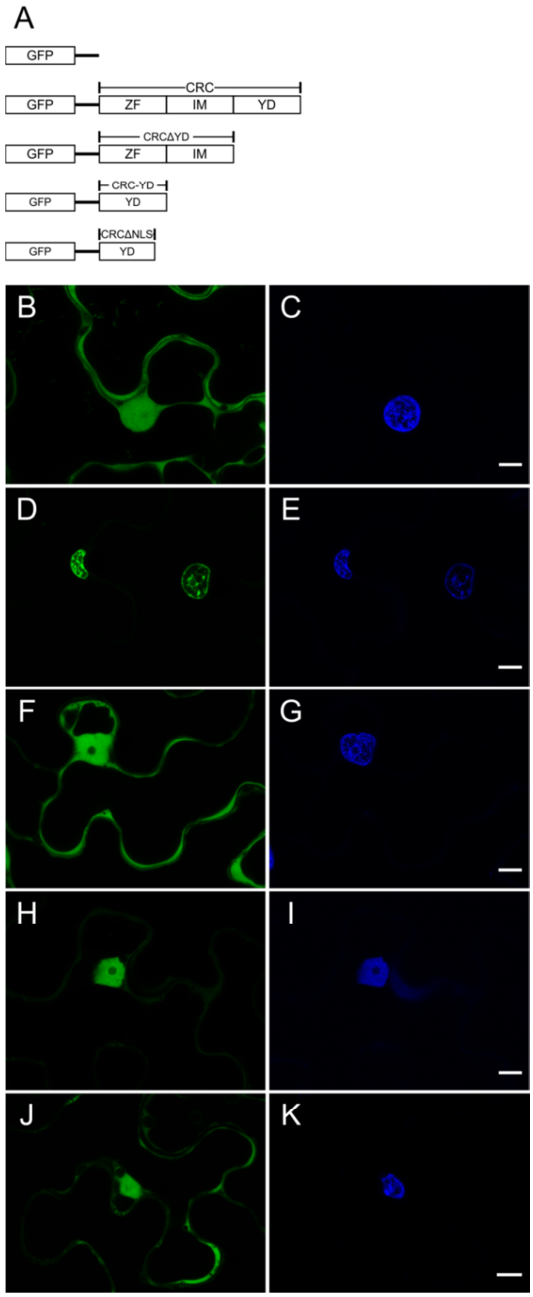

Figure 5: Analysis of the intracellular localization of GFP::CRC employing different CRC deletion variants. GFP fusion proteins were detected by CLSM. False colors were assigned to GFP (green, right panels) and DAPI

(blue, left panels) which stains DNA. A: Schematic representation of the GFP-CRC constructs used in this study. B and C: *pro35S::GFP* (29.26 kDa). D and E: *pro35S::GFP::CRC* (48.97 kDa). F and G: *pro35S::GFP::CRCΔYD* (40.75 kDa). H and I: *pro35S::GFP::CRC-YD* (34.75 kDa). J and K: *pro35S::GFP::CRCΔNLS* (47.97 kDa). ZF: zinc finger domain, IM: intermediate domain, YD: YABBY domain, NLS: nuclear localization signal. All scale bars represent 10 µm. After Gross *et al.* (2018).

The YABBY family has six members (CRC, FILAMENTOUS FLOWER (FIL), YABBY 2, YAB3, INNER NO OUTER (INO), and YAB5) with CRC and INO restricted to flowers. The so called vegetative YABBY proteins (FIL, YAB2, YAB3, and YAB5) are known to interact with each other. To identify if CRC is also interacting with its relatives, I performed a Yeast-2-Hybrid (Y2H) analysis which identified INO as the single YABBY protein interacting with CRC (figure 6). In addition, the formation of CRC homodimers was shown by bimolecular fluorescence complementation (BiFC). Similar to the nuclear localization, the YABBY domain was the responsible protein domain for the homodimerization. Interestingly, the YABBY domain is not only relevant for localization and homodimerization but also for CRC's interaction with DNA. A Yeast-1-Hybrid (Y1H) analysis, using a part of the *KCS15* promoter, revealed that the YABBY domain is the main DNA interacting domain of CRC. However, the YABBY domain is not able to bind to *proKCS15* alone and other parts of CRC might stabilize this protein-DNA interaction to allow the YABBY domain to bind to DNA.

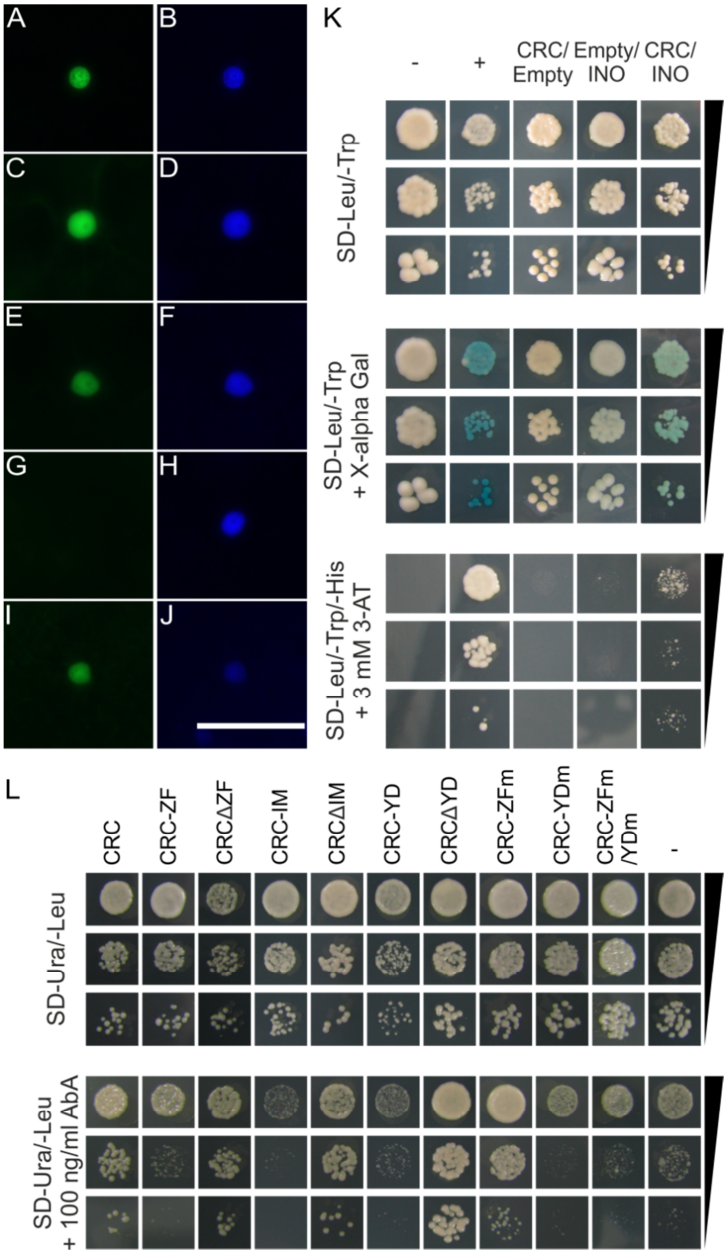

Figure 6: Protein interaction analysis of CRC and analysis of interacting domains. A-J: Protein interaction analysis by BiFC using multiple CRC versions. YFP_C and YFP_N tagged full-length CRC, deletion versions of CRC, and single domains were detected by fluorescence microscopy. A: Combination CRC-YFP_C- /CRC-YFP_N visualizing the YFP signal, B: DAPI staining of the cell shown in A. C: Combination YFP_C-CRCΔZF/YFP_N-CRCΔZF visualizing the YFP signal, D: DAPI staining of the cell shown in C. E: Combination YFP_C-CRCΔIM/YFP_N-CRCΔIM visualizing the YFP signal. F: DAPI staining of the cell shown in E. G: Combination YFP_C-CRCΔYD/YFP_N-CRCΔYD visualizing the YFP signal. H: DAPI staining of the cell shown in G. I: Combination YFP_C-CRC-YD/YFP_N-CRC-YD visualizing the YFP signal. J: DAPI staining of the cell shown in I. ZF: zinc finger domain, IM: intermediate domain, YD: YABBY domain. Scale bar represents 50 µm. K: Y2H analysis of CRC's interaction with INO. Yeast cell suspensions of the respective test strains with an OD_{600} of 0.1, 0.01, and 0.001 plated on SD-Leu/-Trp medium and stained with X-α-Gluc after 5 days of incubation and on SD-Leu/-Trp/-His + 3mM 3-AT. As positive control, a combination of AD-EcSEI/BD-EcDEF2 (Lange et al., 2013) was used and a combination of

the empty vectors pGADT7/pGBKT7 as negative control. L: CRC's DNA binding capabilities in an Y1H analysis. The *S. cerevisiae proKCS15* reporter strain was transformed with full length CRC, single domains, deletion constructs, and mutant versions, fused to the activation domain of GAL4. Yeast cell suspensions of the respective test strains with an OD_{600} of 0.1, 0.01, and 0.001 plated on SD-Ura/-Leu and on SD-Ura/-Leu + 100 ng/ml AbA. As negative controls, the *proKCS15* bait strain was transformed with an empty pGADT7 vector. After Gross *et al.* (2018).

CRC is involved in multiple important steps during carpel development and, thus the question arose how CRC can regulate these different processes. To analyze this in more detail, I established a dominant repressor line (CRC-SRDX) and a dominant activator line (CRC-EDLL) to identify if CRC is an activator of transcription, a repressor of transcription or both. In fact the two lines split the CRC phenotype (figure 7). While the repressor line CRC-SRDX was unable to fuse its carpels, showed an enhanced lateral growth, and also lacked nectaries; the activator line CRC-EDLL exhibited to a higher extend additional carpels compared to *crc-1.* In conclusion, carpel fusion, inhibition of lateral growth, and nectary formation are based on activating processes and termination of the floral meristem is based on repressing processes. This bifunctional character is probably possible due to different interacting proteins. Hence, CRC can have different functions in different tissues and at different time points attributed to varying interaction partners.

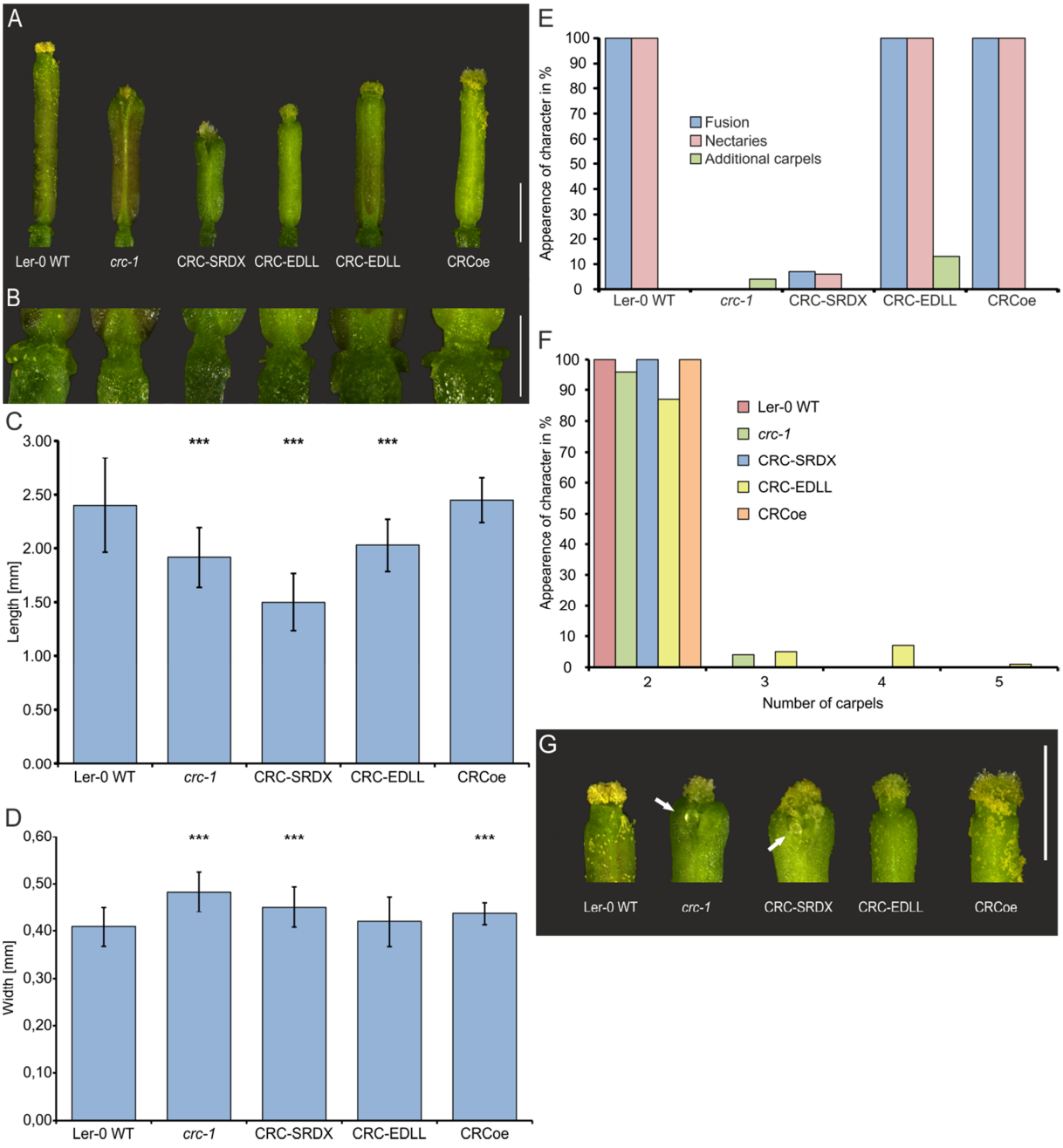

Figure 7: Phenotypic analysis of CRCoe, CRC-SRDX, and CRC-EDLL expressing *A. thaliana* Ler-0 plants. A: Representative gynoecia of Ler-0 wild type, *crc-1*, *proUBQ10::CRC* (CRCoe), *proUBQ10::CRC::SRDX*, and *proUBQ10::CRC::EDLL* plants. Scale bar represents 1 mm. B: Magnification of the gynophore region of the exemplary gynoecia with arrows highlighting the nectaries. Scale bar represents 500 µm. Statistical analysis of gynoecium length (C), width (D), a summary of other described defects of the *crc-1* phenotype (E), and the number of carpels in the analyzed gynoecia of the four plant lines. In each line, except for CRCoe (n = 30), 100 randomly picked gynoecia were analyzed. Both, length and width comparisons (C and D) are mean values with their respective standard deviation. Percent values are shown in E and F. Student's t-test was applied to compare the wild type gynoecia with the other lines and significant differences were marked with up to three asterisks (p<0.001). G: Magnification of the apical region of representative gynoecia of the respective lines showing protruding ovules (arrows). Scale bar represents 1 mm. After Gross *et al.* (2018).

CRC Expression in the Developing Flower

Already in the first description of CRC, Bowman and Smyth (1999) revealed the complex spatial and temporal expression pattern of *CRC*. During carpel development, *CRC* expression is detectable starting in stage 6 (stages according to Smyth *et al.* (1990)) in the gynoecial primordium and forms two distinct domains in the carpels after stages 7-8 (figure 8): An epidermal expression around the circumference of the gynoecium, and an internal expression in four stripes that are close to the developing placenta (Bowman and Smyth, 1999; Lee *et al.*, 2005a). Whereas, the epidermal expression of *CRC* is consistent over the complete length of the carpels, the internal expression forms a basal-apical gradient (figure 8 A-D) and ceases in later developmental stages. The epidermal expression is maintained until the mid of stage 12 in the valves, but it ceases earlier in the future replum (figure 8 G), whereas the expression in the nectaries (figure 8 F) is stable until after anthesis (Bowman and Smyth, 1999). Previous analyzes of the *CRC* promoter by Lee *et al.* (2005a) identified five conserved regions (A-E) that are sufficient to enable a normal *CRC* expression in the developing carpels. Furthermore, putative binding sites of MADS box transcription factors and LEAFY were identified in these regions, especially in the E region, most distant to the start codon. More recent Chip-SEQ data showed that the MADS box transcription factors AG, PI, AP1, and AP3 are able to bind to the *CRC* promoter, especially in the E region, and thus are involved in the regulation *CRC* expression (Lee *et al.*, 2005a; Gomez-Mena *et al.*, 2005; Ó'Maoiléidigh *et al.*, 2013).

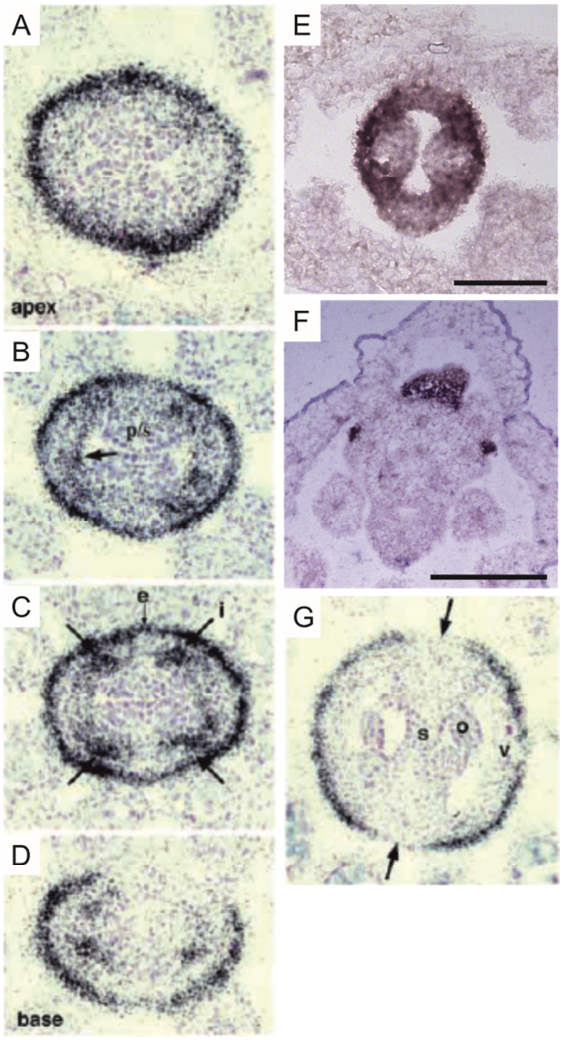

Figure 8: Analysis of the expression pattern of CRC via mRNA in situ hybridization. Crossections of *A. thaliana* flowers and buds in different developmental stages. A-D: serial crosssections of a stage 8-9 gynoecium, showing two expression domains of CRC, an epidermal (e) and an internal (i) (C). Arrows indicate expression in the inner epidermis (B) and four internal patches (C). CRC expression is declining from basal to apical in these regions. No CRC expression can be detected in precursor cells of the placenta (p) and septum (s) (B). E: Transverse section of a stage 7 gynoecium. CRC expression is present throughout the valves and forms two horse shoe shaped expression domains. No expression can be detected in the precurser cells of placenta and septum. Scale bar represent 50 µm. F: CRC expression in the nectaries at the base of the stamens. Scale bar represents 200 µm. G: Cross section of a stage 11 gynoecium. CRC expression is only present in the outer epidermis of the valves (v) and missing from the future replum (arrows). Internal expression or in the septum or ovules (o) cannot be detected. Sections A-D and G were taken from Bowman and Smyth (1999), sections E and F were provided by Anna Barbara Dommes.

CRC Orthologues Show Hints for Non-Cell-Autonomous Action of YABBY Proteins

During their expression analysis of CRC, Bowman and Smyth noticed, that there is a gap between the expression site and the phenotypical affected region. This led to the hypothesis of a non-cell-autonomous action of CRC (Bowman and Smyth, 1999), after which CRC expression and CRC perception can take place in different cells. Further studies with CRC orthologues from other species like *Pisum sativum* (Fourquin *et al.*, 2014), *Eschscholzia californica* (Orashakova *et al.*, 2009), and *Oryza sativa* (Toriba and Hirano, 2014) supported this hypothesis. *PsCRC* is expressed around the main vascular bundle of the developing carpel, but when *PsCRC* expression is downregulated, the carpel is not able to fuse its margins (Fourquin *et al.*, 2014). *EcCRC* is expressed, like in *A. thaliana*, around the circumference of the gynoecium but not in the future replum, placenta, and ovules. However, knock-down experiments have shown that, especially these tissues are affected. The replum is not able to allow dehiscence of the valves and the placenta tissue cannot support ovule formation due to its improper development. In addition, the termination of the floral meristem is disturbed (Orashakova *et al.*, 2009). The *O. sativa* orthologue of CRC, DROOPING LEAF is involved in leaf midrib formation, carpel identity regulation, and awn development. However, it is not expressed in the awn primordium but below and DL mutants are missing most awns (Toriba and Hirano, 2014). FIL, another member of the YABBY protein family, has been shown to exhibit non-cell-autonomous functions (Goldshmidt *et al.*, 2008), however, it seems that not the FIL protein itself is transported but a derived signal. Recent studies have identified members of the miRNA family mir165/166 to be regulated by FIL, which are especially involved in the regulation of adaxial–abaxial polarity (Tatematsu *et al.*, 2015). These miRNAs might be the derived signal of YABBY proteins, responsible for the non-cell-autonomous action.

YABBY Proteins Are Involved in the Adaxial-Abaxial Regulatory Network

During the development of lateral plant organs such as leaves and flowers multiple genes are involved to specify the abaxial (lower/ventral/outer) and adaxial (upper/dorsal/inner) side of lateral plant organs. The adaxial-abaxial regulatory network in leaves has been intensively studied and most of the involved factors are also acting in carpels but still less is known about these regulatory processes in carpels. Thus, the development of adaxial-abaxial polarity in leaves will be presented here.

In leaves, members of the KANADI family (KAN1-4), a group of homeodomain transcription factors, specify the abaxial) side of the leaf (Kerstetter *et al.*, 2001) (figure 9) by counteracting the activity of the five HD ZIP III genes (*REVOLUTA, PHAVOLUTA, PHABULOSA, CORONA,* and *ATHB8*) which specify the adaxial side of the leaf (Emery *et al.*, 2003; Prigge *et al.*, 2005; Reinhart *et al.*, 2013). YABBY proteins support the KANADI proteins in their action and physically interact with them (Sessions and Yanofsky, 1999; Siegfried *et al.*, 1999; Trigg *et al.*, 2017). All three protein groups are integrated in multiple regulatory feedback loops. The abaxial regulatory core proteins, the KAN proteins, are enhancing their own expression and interact with YABBY proteins and the auxin response factors ETTIN (ARF3) and ARF4. Thereby they inhibit the expression of the middle domain regulators WUSCHEL HOMEOBOX 1 (WOX1) and PRESSED FLOWER (PRS, WOX3); more importantly, they inhibit the action of various adaxial regulators such as ASYMMETRIC LEAVES 1 and AS2, ULT1, and members of the HD-ZIP III family (Wu *et al.*, 2008; Merelo *et al.*, 2017). In return, most of the adaxial regulators are downregulating the expression of abaxial factors. HD ZIP III proteins, the adaxial regulatory core proteins, are also enhancing their own expression and also the expression of LITTLE ZIPPER proteins, which in turn dimerize with HD ZIP III proteins and render them unfunctional (Wenkel *et al.*, 2007).

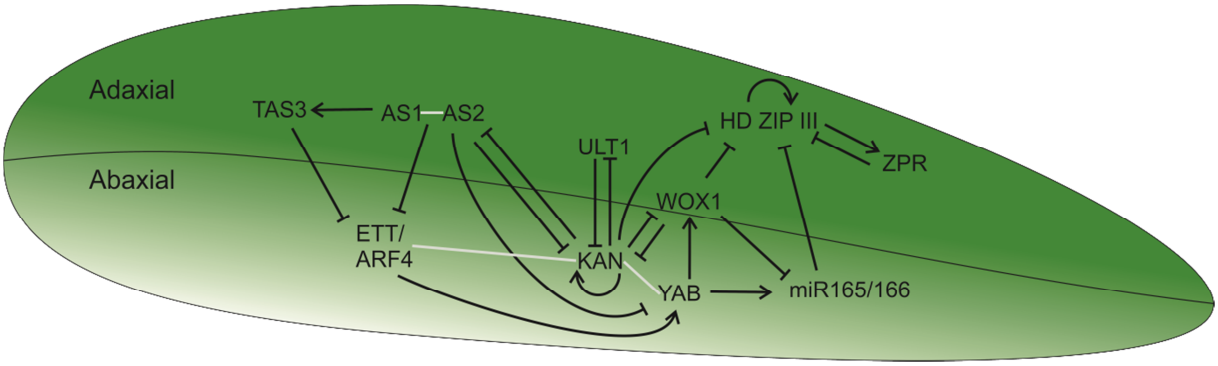

Figure 9: Determination of adaxial-abaxial identity in leaves. White lines represent a physical interaction. Pointed arrows indicate enhancing the action of the target, by activation of transcription. Blunt arrows indicate repression of the target either by repressing its transcription or by enhancing its post-transcriptional degradation. Based on Merelo *et al.* (2017), Reinhart *et al.* (2013), Tatematsu *et al.* (2015), and Garcia *et al.* (2006).

Furthermore, two non-cell autonomous regulatory systems are present. HD-ZIP III transcripts can be detected in the adaxial site of leaves but not in the abaxial side. Further expression analysis showed that this restriction is based on post-transcriptional silencing by miRNA 165/166 (Jung and Park, 2007). These two miRNA families (mir165 with two members and mir166 with seven members) target the identical region of HD-ZIP III transcripts in the 3' region of HD-ZIP III mRNAs (Jung and Park, 2007) and their expression seems to be regulated by YABBY proteins. Tatematsu *et al.* (2015) have shown that FIL is necessary for sufficient expression of miRNA 165/166, and thus the activity range of HD-ZIP III genes is widened in *fil* mutants and leaves are adaxialized. Vice versa, the adaxial factor AS1 is regulating the expression of the *trans*-acting small interfering RNA (tasiRNA) TAS3 which is downregulating the expression of ETTIN and ARF4 and by this, modulating the response to auxin in the developing tissue (Fahlgren *et al.*, 2006).

Symplasmic Transport in Plants

The non-cell-autonomous control of developmental processes in plants is mostly dependent on plasmodesmata (figure 10). These intercellular channels traverse the plant´s cell walls

and mediate intercellular communication by allowing the symplasmic exchange of molecules like sugars, hormones, proteins, mRNAs, and small RNA species (Lucas and Lee, 2004; Benitez-Alfonso *et al.*, 2010; Xu and Jackson, 2010; Furuta *et al.*, 2012; Burch-Smith and Zambryski, 2012; Stahl and Simon, 2013; Kragler, 2013; Ehlers and Westerloh, 2013; Benitez-Alfonso, 2014).

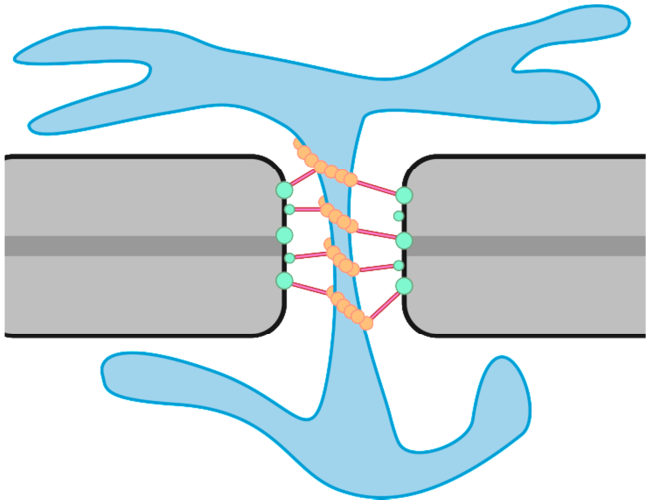

Figure 10: Schematic structure of a simple plasmodesma. Blue: endoplasmatic reticulum (ER), orange: helically structured proteins, green: membrane proteins, red: spoke like proteins, dark grey: middle lamella, light grey: primary cell wall, black: plasma membrane.

In simple and branched plasmodesmal morphotypes, the most significant symplasmic transport takes place through small cytoplasmic micro channels. These channels are left open between proteins which are associated with the plasma membrane, lining the plasmodesmal channels, and with the membrane of the desmotuble, i.e. the central plasmodesmal component derived from the endoplasmic reticulum (ER). Non-targeted transport through plasmodesmata is driven by diffusion and is restricted by the size exclusion limit (SEL) which can be highly variable depending i.e. on the cell type and the developmental stage of the cells (reviewed in Burch-Smith and Zambryski (2012), Ehlers and Westerloh (2013)). The mechanism of targeted symplasmic transport remains unclear, but models suggest that cargo molecules are either delivered via the cytoskeleton, the ER or via diffusion to the plasmodesmata. Receptor proteins and chaperonins may then be necessary for the selective cell-to-cell transport (Lucas and Lee, 2004; Xu *et al.*, 2011; Kragler, 2013).

Remarkably, no common transport motif shared by different cargo molecules has been identified so far (Kragler, 2013).

Several *A. thaliana* transcription factors were shown to act in a non-cell-autonomous manner (table 1). The majority of these proteins is transported in a targeted manner into adjacent cells. They exert non-cell-autonomous control on meristem maintenance and on the development of leaf or root tissues, and inflorescences. The plasmodesma-mediated transport of such non-cell-autonomous proteins (NCAPs) and of small RNAs is supposed to form gradients in the developing plant tissues which are required for positional signaling and proper cell differentiation (Furuta *et al.* (2012), and reviewed in Becker and Ehlers (2016)). Remarkably, unidirectional transport through plasmodesmata has also been described at certain cell interfaces (Christensen *et al.*, 2009; Li *et al.*, 2013).

Table 1: Plasmodesma-mobile transcription factors of *A. thaliana* with known non-cell-autonomous effect.

Transcription factor	Function	Tissue	References
LEAFY	Floral meristem identity	Inflorescence meristem	Sessions *et al.* (2000), Wu *et al.* (2003)
SHOOTMERISTEMLESS	SAM initiation and maintenance	SAM	J-Y Kim *et al.* (2003)
KNOTTED1-LIKE HOMEOBOX PROTEIN 1/ BREVIPEDICELLUS	SAM initiation and maintenance; inflorescence cell fate	SAM	J-Y Kim *et al.* (2003)
SHORT-ROOT	Cell division and endodermis specification	Root	Helariutta *et al.* (2000), Nakajima *et al.* (2001)
CAPRICE	Root hair development	Root	Wada *et al.* (2002)
AGAMOUS	Cell division and cell fate; flower development	Floral meristem	Urbanus *et al.* (2010)
WUSCHEL	SAM maintenance	SAM	Yadav *et al.* (2011)
FLOWERING LOCUS T	Floral meristem induction	Vascular tissue in leaves	Corbesier *et al.* (2007)
TARGET OF MONOPTEROUS 7	Recruitment of the hypophysis	Embryo and the upper cell of the suspensor	Schlereth *et al.* (2010), Lu *et al.* (2018)
SPEECHLESS	Establishment of the stomatal lineage	Young epidermal cells	Guseman *et al.* (2010)
ARABIDOPSIS THALIANA HOMEOBOX PROTEIN 2	Regulates SAM activity	SAM (mobile mRNA)	Thieme *et al.* (2015)

Plasmodesmal transport of developmental regulators needs to be strictly controlled, and it might even be required to form symplasmically isolated spatial domains within the developing tissues by establishing symplasmic barriers (reviewed in Ehlers and Westerloh (2013)). Different mechanisms have been shown to modify the symplasmic networks in the developing tissue: (1) the number of plasmodesmata at a given cell interface can be strictly controlled throughout the development by *de-novo* formation, fission and degradation of cell connections (Ehlers and Westerloh, 2013). (2) Plasmodesmal permeability is regulated by the redox state of the cell (Burch-Smith and Zambryski, 2012). (3) The regulation of callose deposits around the plasmodesmal orifices is also controlling the functional properties of the cell connections, which has recently been shown to play a central role in the maintenance of auxin gradients (Han *et al.*, 2014). (4) Membrane micro domains, like lipid rafts and tetraspanin-enriched membrane regions, may adjust the receptor protein composition in the plasmodesmal channels and, consequently, regulate which cargo molecules can be transported (Faulkner, 2013). It has also been speculated that (plasmodesmal) membrane micro domains may represent specific sites for the formation of higher order protein complexes due to a high spatial receptor protein density (Faulkner, 2013; Stahl *et al.*, 2013). Many transcription factors involved in floral organ specification act in higher order protein complexes, like MADS proteins that act as floral quartets (Theißen, 2001). Their formation may also be supported by such membrane micro domains.

However, flower development has not been in the focus of plasmodesmal research, so far, as only contradictory information on the changes of the plasmodesmal networks during floral development has been published (reviewed in Ehlers and Westerloh (2013)). Publications on non-cell-autonomous control of flower development in *A. thaliana* is restricted to LEAFY, KNOTTED1-LIKE HOMEOBOX PROTEIN 1/BREVIPEDICELLUS (KNAT1/BP), and AGAMOUS (see table 1).

Hypotheses and Aims of This Dissertation

The formation of flowers and especially of the carpel, was one of the crucial steps in the evolution of land plants (Becker *et al.*, 2011). Moreover, the proper development of the complex female reproductive organs is of great importance in an evolutionary, ecological and economical aspect, since the carpel is the prerequisite for the formation of seeds and fruits. CRC is involved in the development of the carpels and thus in the formation of the gynoecium and its function is conserved throughout the dicots to a large extent.

CRC has a complex expression pattern but only few regulators of CRC expression are known. As the complex spatial and temporal expression pattern cannot solely be based on few MADS box transcription factors and LFY, other regulators must be involved as well (I). To identify these other regulators of CRC expression, a large scale Y1H screen of the CRC promoter, including more than 1,500 *A. thaliana* transcription factors, was performed.

Furthermore, by comparing the expression data of the wild type and the phenotypically affected regions in *A. thaliana* and *E. californica* plants with a compromised CRC activity, it is noticeable that expression domains and affected regions are not congruent. This non-cell-autonomous effect gives rise to the hypotheses that either the CRC protein or a derived signal is transported via plasmodesmata (II). As previous studies have shown the effect of YABBY proteins on the expression of mir165/166 in leaves, these miRNAs might be the derived signal. To validate or refute these hypotheses experimentally, I analyzed the CRC protein transport in *A. thaliana* as a possible example for targeted cell-to-cell transport of a transcription factor and also the effect of CRC on the expression of mir165/166 in flowers.

Additionally, a connection between CRC and mir165/166 raises the question if CRC is indirectly regulating the expression of adaxially acting HD ZIP III genes, as by controlling the mir165/166 level, it limits the activity range of HD ZIP III genes. Taken together with the enhancement of the *kan1* or *kan2* phenotype by *crc-1*, this shows the involvement of CRC in the adaxial-abaxial polarity regulation. Hence, CRC might be involved in the regulation of other abaxial factors than mir165/166 like the KAN genes or the middle domain genes WOX1 and PRS (III). By measuring the expression of these putative target genes, CRC's role in the regulation of adaxial-abaxial polarity might be identified.

Multiple studies of CRC orthologues in other eudicot species (e.g. *P. sativum* and *E. californica*) found CRC's functions (e.g. termination of the floral meristem) to be conserved to a large extent. Even though, there are significant morphological differences between the gynoecia of these species, the establishment of adaxial–abaxial polarity is a crucial part of the development of lateral plant organs such as leaves and carpels. Hence, the functions of YABBY proteins and especially of CRC in the establishment of adaxial–abaxial polarity might be identical in these species (IV). Therefore, expression studies of the orthologues of CRC and other abaxial and adaxial regulators in *E. californica* were used to validate or refute this hypothesis that CRC's place in the adaxial–abaxial network remains the same.

Material and Methods

Plant Material and Plant Growth

All seeds of *A. thaliana* wild type (Col-0 and Ler-0) ecotypes were already present in the research group. All used Salk T-DNA insertion lines or mutant lines were obtained from the European Arabidopsis Stock Center (uNASC). Two types of *crc* mutants were used. First the original *crc-1* allele in *A. thaliana* Ler-0 and second a *CRC* knockout SALK line in *A. thaliana* Col-0 (referenced to as *crc*). The *half filled*, *bee1*, *bee3* triple mutant (*hbb*) was a kind gift of Birgit Poppenberger and Martin Yanofsky, the *cal* mutant was a kind gift of Daniel Schubert. All plants were grown on a soil-perlite mixture under standard long day conditions. Plants were watered when necessary and fertilized (WUXAL, Hauert MANNA Düngerwerke GmbH, Nürnberg, Germany) once a week starting 4 weeks after germination.

Protein Structure Prediction

Three dimensional structure of CRC was predicted based on homology using the online prediction tool RaptorX (Källberg *et al.*, 2012). To visualize the predicted model, the protein structure viewer NGL was applied (Rose and Hildebrand, 2015).

Regulation of CRC Expression

Amplification of the CRC Promoter

The CRC promoter (*proCRC*), as described by Bowman and Smyth (1999) and Lee *et al.* (2005a), was amplified (table 2) as a 3.8 kB fragment from genomic DNA (gDNA) of *A. thaliana* Ler-0, isolated with the genomic DNA mini kit for plants (Geneaid, New Taipei City, Taiwan) according to the manufacturer's instructions. Additionally, the promoter was

divided into eight fragments (*proCRC F1 – F8*) and into the five conserved regions (*proCRC A – E*) that were identified by Lee *et al.* (2005a). Detailed sequence information of the different fragments can be found in the electronic appendix. All primer sequences are listed in Appendix table 13. The PCR was set up according to table 2 and run on a thermo cycler starting with an initial denaturation of 98 °C for 1 min, followed by 40 cycles of 10 s 98 °C, 20 s 58 °C, and 30 s per kB for elongation. After 40 cycles, the samples were incubated for 5 min at 72 °C and stored at 12 °C until use.

Table 2: PCR master mix composition for the amplification of *proCRC*.

Substance	Volume per sample [µl]
H_2O	32.5
5x Phusion High Fidelity Buffer	10
10 mM dNTPs	1
10 µM pCRC Fw HindIII	2.5
10 µM pCRC Rv KpnI	2.5
Phusion DNA Polymerase (2 U/µl)	0.5
gDNA Ler-0 (12 ng/µl)	1

The successful amplification was checked via gel electrophoresis. Therefore, 5 µl of the PCR product were mixed with 1 µl 6x loading dye (New England Biolabs GmbH, Frankfurt am Main, Germany) and placed on a 1 % agarose gel, supplemented with 2 µl/100 ml DNA stain G (SERVA Electrophoresis GmbH, Heidelberg, Germany). The gel was subjected to 7 V per cm gel for 35 min. Afterwards the gel was illuminated on a UV table and pictures were taken. The remaining PCR products were purified with the NucleoSpin gel and PCR clean-up kit (Macherey und Nagel, Düren, Germany) according to the manufacturer's instructions. After elution, the concentration of the purified PCR product was measured spectrophotometrically.

Restriction of *proCRC* and pAbAi

The purified CRC promoter versions were digested in a reaction with HindIII and KpnI (all used restriction enzymes were ordered from New England Biolabs). 2 µg of the respective purified promoter fragment were mixed with 5 µl 10x CutSmart buffer (New England

Biolabs), 0.5 µl 20 U/µl HindIII-HF, and 0.5 µl 20 U/µl KpnI-HF and filled up to 50 µl. The restriction reactions were incubated for 1 h at 37 °C and purified with the NucleoSpin gel and PCR clean-up kit. In parallel, the bait DNA vector pAbAi (Takara Clontech, Saint-Germain-en-Laye, France) was digested in a similar reaction (the vector was a kind gift of Paula Elomaa, University of Helsinki) as the promoter fragments. All reactions were filled up to 50 µl with ddH_2O and incubated for 1 hour at 37 °C. To remove the restriction enzymes and short DNA fragments, the PCR purification kit was used again.

Cloning of the CRC Promoter

The purified digested *proCRC* versions and pAbAi were ligated in a reaction with 100 ng pAbAi, the respective *proCRC* version, 2 µl 10x T4 DNA ligase buffer, and 1 µl 2 U/µl T4 DNA ligase (Thermo Scientific, Schwerte, Germany). The amount of the insert in ng was calculated with:

Equation 1: Calculation of the amount (in ng) of insert to add to the ligation mix for an optimal ratio of insert and vector.

$$ng\ Insert = 5 * \frac{(ng\ Vector * kb\ Insert)}{kb\ Vector}$$

Sterilized ddH_2O was used to fill up the reaction to 20 µl and the ligation mix was incubated for 30 min at room temperature. 6 µl ligation mix were added to 100 µl chemo competent *E. coli* DH5α cells. Competent bacteria and DNA were incubated for 20 min and then transferred for 45 s in a 42 °C warm water bath, followed by incubation on ice for 2 min. The transformed bacteria were filled up to 1 ml with SOC medium and incubated for 1 hour at 37 °C and 190 rpm before the cells were plated on LB-agar plates, supplemented with 100 µg/ml ampicillin (SERVA Electrophoresis GmbH, Heidelberg, Germany). All LB-agar plates were incubated over night at 37 °C.

Identification of Positive Clones and Plasmid Isolation

In order to identify *E. coli* DH5α colonies that carry the respective *proCRC* version in pAbAi, a colony PCR was performed (table 3). 20 µl PCR master mix were distributed into reaction tubes and a sterile tooth pick was used to transfer traces of single *E. coli* colonies into it.

Table 3: PCR master mix composition for a colony PCR to detect the presence of *proCRC* in pAbAi.

Substance	Volume per sample [µl]
H_2O	16.4
10x DreamTaq Buffer	2
10 mM dNTPs	0.5
10 µM pAbAi Fw	0.5
10 µM pCRC Rv KpnI	0.5
DreamTaq DNA Polymerase (5 U/µl)	0.1

The PCR was performed on a thermo cycler starting with an initial denaturation of 95 °C for 5 min, followed by 35 cycles of 30 s 93 °C, 30 s 56 °C, and 1 min per kB for elongation. After 35 cycles, the samples were incubated for 5 min at 72 °C and stored at 12 °C until use. The successful amplification was checked on a 1 % agarose gel and positive colonies were grown over-night in liquid LB medium with ampicillin at 37 °C and 190 rpm.

Over-night cultures of these colonies were harvested to isolate their plasmid DNA with the Plasmid EasyPure kit (Macherey und Nagel) according to the manufacturer's instructions. Plasmids were sequenced at StarSEQ GmbH (Mainz, Germany) to rule out amplification errors. Prior to yeast transformation, 8 µg of the respective bait vector were linearized with BstBI in a reaction with 5 µl 10x CutSmart buffer, 20 U BstBI, and ddH_2O was used to fill up to 50 µl. The samples were purified after 2 h at 37 °C with the PCR clean up kit as described before.

Generation of *S. cerevisiae* Y1HG Bait Strains

The yeast strain *S. cerevisiae* Y1HG (Takara Clontech) was used for all Y1H analyses. For each transformation, three 20 ml YPAD (20 g tryptone, 10 g yeast extract, 100 mg adenine

hemisulphate, and 100 ml 20 % glucose) cultures were inoculated with a well grown Y1HG colony and grown over-night at 30 °C and 200 rpm. The OD_{600} was measured of each culture and the best grown culture was used to inoculate 300 ml fresh YPAD medium up to an OD_{600} of 0.2. The 300 ml culture was incubated for 3 h at 30 °C and 200 rpm and harvested by centrifugation at 1000 g for 5 min when OD_{600} reached 0.4 – 0.6.

The yeast pellet was resuspended in 35 ml TE buffer (pH 7) and centrifuged again at the same settings. Resuspension was performed with 0.5 – 1.5 ml TE/LiAc solution and 100 µl of the competent yeast cells were used for each transformation mix. In each transformation mix, 1 µg of linearized pAbAi bait vector, 100 mg single stranded carrier DNA (SERVA Electrophoresis GmbH), and 600 µl PEG solution (480 µl 50 % PEG 4000, 60 µl 10x TE, and 60 µl 1 M LiAc) were mixed and incubated for 30 min at 30 °C and 200 rpm. Afterwards, 80 µl DMSO were added and a heat shock at 42 °C was applied for 15 min, followed by incubation on ice for 2 min. The transformed yeast cells were pelleted by centrifugation at 17.000 g for 5 s and the supernatant was removed. Cells were resuspended in 100 µl TE buffer and plated on SD-Ura plates which were incubated for 3 days at 30 °C. Grown yeast colonies were screened for the integration of the bait plasmid by homologous recombination into the URA3 locus via colony PCR as described before.

Autoactivation Test of Bait Strains

Positively tested colonies were dissolved in 0.9 % NaCl solution and diluted to an OD_{600} of 0.002. Aliquots of 100 µl of the diluted colonies were plated on SD-Ura plates with increasing Aureobasidin A (AbA, Takara Clontech) concentrations (100 ng/ml, 150 ng/ml, 200 ng/ml, 500 ng/ml, and 1000 ng/ml). The plates were incubated at 30 °C for 4 days. Only bait strains whose growth was inhibited by concentrations lower than 1000 ng/ml AbA were used for Y1H analysis. The lowest AbA concentration that was sufficient to suppress yeast growth was used for the following screens.

Transformation of Bait Strains with Prey Libraries

The transformation of the bait strains was performed as described before but the transformed yeast cells were resuspended in 500 µl TE buffer instead of 100 µl. Three different libraries were used to identify transcriptional regulators of CRC: library 1 with 1498 proteins was published by Mitsuda *et al.* (2010); library 2 with eight proteins (for composition see Appendix table 14), a kind gift of Stefan de Folter; library 3 with 20 proteins (for composition see Appendix table 15). For every used prey library, a transformation reaction was set up and 1 µg of plasmid DNA was added. Transformed cells were plated on SD-Leu (libraries 1 and 3) or SD-Trp (library 2) plates supplemented with the before tested Aba concentration and the plates were incubated at room temperature for up to 10 days. Grown colonies were tested by colony PCR for the presence of a prey plasmid and streaked out on fresh selective medium for two times to reduce the risk of having more than on type of library plasmid in the same yeast colony.

Plasmid Isolation from Yeast Cells

Plasmid DNA from yeast was isolated with either the Easy Yeast Plasmid Isolation Kit (Takara Clontech) or as described in Hoffman and Winston (1987). Electrocompetent *E. coli* DB3.1 or XL1-Blue cells were transformed with the isolated plasmid DNA by adding up to 3 µl of the isolated plasmids to 50 µl of electrocompetent cells. After an incubation of 1 min on ice, the transformation mix was transferred to an electroporator cuvette and subjected to 2500 V for up to 6 ms in an Eporator (Eppendorf AG, Hamburg, Germany). 1 ml of SOC medium was added after the electro shock and the cells were incubated at 37 °C and 190 rpm for 1 hour. Afterwards, the transformed cells were grown on LB-agar plates as described before.

Prey Identification

Two *E. coli* colonies per plate were picked and grown over night in liquid LB medium. Their plasmids were isolated as described before. All plasmids were sequenced at StarSEQ GmbH (Mainz, Germany) and the obtained sequences were blasted using NCBI BLAST (Altschul *et al.*, 1990) against the *A. thaliana* nucleotide collection to identify the respective library gene.

Integration of *proCRC* into Greengate System

As *proCRC* exhibits an internal BsaI recognition site, a site-directed mutagenesis (Hemsley *et al.*, 1989) of *proCRC* was performed to remove the BsaI recognition site for the later integration of *proCRC* into the Greengate system (Lampropoulos *et al.*, 2013). The PCR was set up according to table 4 and was run on a thermo cycler starting with an initial denaturation at 98 °C for 1 min, followed by 40 cycles of 10 s 98 °C, 20 s 58 °C, and 30 s per kB for elongation. After 40 cycles, the samples were incubated for 5 min at 72 °C and stored at 12 °C until use.

Table 4: PCR master mix composition for the site directed mutagenesis of *proCRC*.

Substance	Volume per sample [µl]
H_2O	32.5
5x Phusion High Fidelity Buffer	10
10 mM dNTPs	1
10 µM SDM proCRC Fw	2.5
10 µM SDM proCRC Rv	2.5
Phusion DNA Polymerase (2 U/µl)	0.5
pAbAi *proCRC* (5 ng/µl)	1

The amplified modified pAbAi *proCRC* was purified as described before, phosphorylated with T4-Polynucleotidekinase (T4-PNK, NEB), and digested with DpnI to remove the original methylated template DNA according to the manufacturer's instructions. The linear pAbAi *proCRC* was religated using T4-DNA ligase (Thermo Fisher Scientific) and transformed into chemocompetent *E. coli* DH5α cells as described before.

Plasmids from positively tested colonies were isolated as described before and checked for the removal of the BsaI recognition site by sequencing. The promoter was then amplified from pAbAi *proCRC* using primers with BsaI recognition sites and cloned into pGGA000 as described before.

Construction of *proCRC:GUS* Reporter

In order to analyze the activity range of *proCRC*, a β-glucuronidase (GUS) based expression analysis was performed. To assemble the construct *proCRC:N-Dummy:GUS:C-Dummy:*Ter_{RBCS}*;pMAS:Basta:*Ter_{MAS} in the plant transformation vector pGGZ003, Greengate reactions were set up to table 5 and as described in Lampropoulos *et al.* (2013), with 150 ng of each module vector, 100 ng of the destination vector pGGZ003, 20 U BsaI-HF but with only 5 U T4-DNA ligase.

Table 5: Composition of the Greengate reactions for the construct pGGZ003 *proCRC:N-Dummy:GUS:C-Dummy:*Ter_{RBCS}*;*pro_{MAS}*:Basta:*Ter_{MAS}.

Vector/Substance	Insert	Amount
pGGA000	proCRC	150 ng
pGGB003	N-Dummy	150 ng
pGGC051	GUS	150 ng
pGGD002	C-Dummy	150 ng
pGGE009	UBQ10 terminator	150 ng
pGGF001	pMAS:Basta:tMAS	150 ng
pGGZ003		100 ng
10x CutSmart buffer		1.5 µl
10 mM ATP		1.5 µ
T4-DNA ligase (5 U/µl)		1 µl
BsaI-HF (20 U/µl)		1 µl
H_2O		Up to 15 µl

The ligated pGGZ003 *proCRC:N-Dummy:GUS:C-Dummy:*Ter_{UBQ10}*;pMAS:Basta:*Ter_{MAS} was transformed into *E. coli* DH5α and verified by sequencing as described before.

Stable Transformation of *A. thaliana*

Electrocompetent *A. tumefaciens* GV3101 pSOUP$^+$ (a strain that contains the helper plasmid pSOUP) cells were transformed with 100 ng purified plasmid DNA by electroporation as described before for *E. coli*. A floral dip transformation of *A. thaliana* Col-0 wild type plants was performed, based on the floral dip protocol by Davis *et al.* (2009). For each *A. tumefaciens* strain, an over-night culture of 5 ml YEBS medium (supplemented with 50 µg/ml rifampicin, 50 µg/ml gentamicin, and 100 µg/ml spectinomycin) was started. A 50 ml YEBS culture (supplemented with gentamicin and spectinomycin) was inoculated with 1 ml of the over-night culture and incubated for 8 h at 28 °C and 200 rpm. The 50 ml densely grown culture was added to 450 ml fresh YEBS medium (without antibiotics) and incubated over-night at the same conditions as before. Afterwards, 12.5 g sucrose and 500 µl 20 mg/ml acetosyringone in DMSO were added and the culture was incubated for additional 4 hours. To the 500 ml culture, 100 µl of Silwet L-77 were added and the inflorescences of 4 weeks old *A. thaliana* Col-0 wildtype plants were submersed for 1 min in the bacterial suspension. Dipped plants were grown for additional three weeks under long day conditions and their seeds were harvested. Putative transgenic seeds were sown on soil and seven days after germination, the seedlings were sprayed with 300 µM Basta for selection every second day. Genomic DNA was isolated as described in Wang *et al.* (1993) and Collard *et al.* (2007) and used for a genotyping PCR (table 6).

Table 6: Master mix composition for a genotyping PCR to identify transgenic *A. thaliana* plants.

Substance	Volume per sample [µl]
H_2O	14.9
10 x DreamTaq Buffer	2
10 mM dNTPs	0.5
10 µM proCRC F8 Fw	0.5
10 µM GUS Rv	0.5
DreamTaq DNA Polymerase (5 U/µl)	0.1
gDNA	1.5

Crossings of Reporter Line with Candidate Mutants

Positively tested reporter line plants were crossed with homozygous plants of the respective ordered T-DNA insertion Salk line (for used mutant and Salk lines see Appendix table 15). Buds of the Salk lines were opened shortly before anthesis and emasculated. These emasculated flowers were pollinated with pollen from reporter line plants. The resulting F1 seeds were sown and selected with Basta as described before. Only Basta resistant plants were allowed to self-cross and to produce seeds. F2 seedlings were selected again with Basta and surviving plants were genotyped with a multiplex genotyping PCR using three primers in one reaction (table 7).

Table 7: Master mix composition for a genotyping PCR to identify homozygote *A. thaliana* Salk line plants.

Substance	Volume per sample [µl]
H_2O	14.4
10x DreamTaq Buffer	2
10 mM dNTPs	0.5
10 µM Salk LP Primer	0.5
10 µM Salk RP Primer	0.5
10 µM LBb1.3	0.5
DreamTaq DNA Polymerase (5 U/µl)	0.1
gDNA	1.5

GUS Assays

Young inflorescences of genotyped F2 plants were harvested in ice cold 90% acetone and incubated for 20 min at room temperature. The GUS staining was performed according to Weigel and Glazebrook (2002). After the staining, the inflorescences were embedded in paraplast for sectioning according to Weigel and Glazebrook (2002). The microtome RM2125 RTS (Leica Microsystems GmbH, Wetzlar, Germany) was used to make 10 µm thick sections from the embedded tissues to analyze the GUS staining with a Leica microscope DCM5500.

CRC Binding Motif Search in Putative Target Genes

Promoter regions of putative CRC target genes were screened for the presence of the three YABBY binding motifs (Shamimuzzaman and Vodkin, 2013; Franco-Zorrilla *et al.*, 2014), using PlantPAN2.0 as described in Gross *et al.* (2018). POLYUBIQUITIN10 (UBQ10, AT4G05320), ACTIN2 (ACT2, AT3G18780), and ELONGATION FACTOR1 α (EF-1α, AT1G07920) were used as references.

Co-expression Analysis of CRC

The expression of CRC was analyzed using the online tools Expression Angler (Austin *et al.*, 2016) and PlaNet (Mutwil *et al.*, 2011). Genes, co-expressed to CRC, were identified by these programs based on Pearson correlation. In addition, PlaNet applied a highest reciprocal rank (HRR) cutoff of 10 ≤ HRR ≤ 30 to identify biological significant co-expression relationships. The identified genes were compared with the putative CRC regulators, identified in the Y1H screen. The expression values of co-expressed putative regulators of CRC were downloaded from Expression Angler and a heatmap, comparing their expression in stigma, ovary, and in complete flowers of stage 9, 10-11, 12, and 15 (according to with the CRC expression, was made using Python v3.6.8, Seaborn v0.9.0, and Pandas v0.23.4. The PlaNet co-expression network was imported into Cytoscape 3.7.1 and all non-transcription factors were removed from the network. CRC co-expression data, generated by Dr. Denise Herbert, from a RNA-seq analysis (Kivivirta *et al.*, unpublished data) was compared to the Y1H dataset. The expression values of co-occurring genes during four developmental stages (stage 5, 9, 11, and 12) were extracted and a heatmap was generated as described before.

Symplasmic Transport

Generation of Reporter Constructs

The intermediate constructs pGGM000 *proCRC:N-Dummy:mCherry:D-Dummy:Ter$_{RBCS}$:F-H*, pGGM000 *proCRC:N-Dummy:3xmCherry:D-Dummy:Ter$_{RBCS}$:F-H*, and pGGN000 *H-A:proCRC: N-Dummy:CRC:GFP:Ter$_{RBCS}$:Basta* were generated in three Greengate reactions (table 8).

Table 8: Composition of the Greengate reactions for the intermediate constructs pGGM000 *proCRC:N-Dummy:mCherry:D-Dummy:Ter$_{RBCS}$:F-H*, pGGM000 *proCRC:N-Dummy:3xmCherry:D-Dummy:Ter$_{RBCS}$:F-H, and* pGGN000 *H-A:proCRC: N-Dummy:CRC:GFP:Ter$_{RBCS}$:Basta*.

Vector designation	Insert	Amount
pGGA004	*proCRC*	150 ng
pGGB003	N-dummy	150 ng
pGGC000	CRC or mCherry or 3xmCherry	150 ng
pGGD002	Linker-GFP or C-dummy	150 ng
pGGE001	RBCS terminator	150 ng
pGGF001	pMAS:Basta:tMAS	150 ng
pGGM000 or pGGN000		100 ng
10 x CutSmart buffer		1.5 µl
10 mM ATP		1.5 µl
T4-DNA ligase (5 U/µl)		1 µl
BsaI-HF (20 U/µl)		1 µl
H_2O		Up to 15 µl

Chemocompetent *E. coli* DH5α cells were transformed with 4 µl Greengate ligation mix as described before. Validated intermediate plasmids were then subjected to a second Greengate reaction in which either pGGM000 *proCRC:N-Dummy:mCherry:D-Dummy:TerRBCS:F-H* and pGGN000 *H-A:proCRC:N-Dummy:CRC:GFP:TerRBCS:Basta* or pGGM000 *proCRC:N-Dummy:3xmCherry:D-Dummy:TerRBCS:F-H* and pGGN000 *H-A:proCRC: N-Dummy:CRC:GFP:TerRBCS:Basta* were ligated into pGGZ003 (for vector maps see Appendix figures 37 and 38). The resulting plasmids were transformed into *E. coli* DH5α as described before and verified by sequencing. Verified plasmids were transformed into *A. tumefaciens* GV3101 pSOUP^{+} as described before and the floral dip method was used to transform *A. thaliana* Col-0 *crc* (SALK_007052C) plants as before.

Phenotypic Analysis of Transgenic *A. thaliana* Plants

In order to determine the effect of CRC-GFP expression in *A. thaliana crc* plants, 10 flowers at stage 14 were randomly picked from each line. The flowers were manually dissected under a Leica M165C stereoscope (Leica Microsystems GmbH, Wetzlar, Germany) and photographed. ImageJ 1.50 (Schneider *et al.*, 2012) was used to measure the photographed gynoecia and the data was analyzed using MS Excel 2010 (Microsoft, Redmond, USA) and the Excel add-in "Daniel's XL Toolbox" (Kraus, 2014). Mean values and standard deviations were calculated and Student's t-test was used to identify significant differences.

CLSM Analysis of Developing Gynoecia

Flower buds of different stages were embedded in 7 % low melt agarose and cut into thin cross sections under a stereo microscope using a micro scalpel. The sections were transferred to a microscope slide and were analyzed with the Leica TCS SP8 confocal laser scanning microscope. For GFP, an excitation at 488 nm, and a detection range of 496-556 nm was used. The RED FLUORESCENT PROTEIN derivative mCherry, was excited at 561 nm, and a detection range of 571-651 nm was used. Chlorophyll was excited at 488 nm and its fluorescence was detected at 670-764 nm. Hybrid detectors were used for these three detection channels. Additionally, a transmission image was made with a photomultiplier detector. The pinhole was kept constant at 1 Airy unit.

Expression Analysis of miRNA 165/166

RNA Isolation for miRNA qRT-PCR

Total RNA from buds and from young leaves of Ler-0 wild type, *crc-1*, and CRC over expression plants (Gross *et al.*, 2018) was isolated using the NucleoSpin® miRNA Kit (Macherey-Nagel) according to the manufacturer's instructions. The quantity of RNA was measured spectrophotometrically and the quality was determined with an agarose gel electrophoresis. To eliminate remaining gDNA, the RNA samples were treated a second time with a DNase. For this, 5 µg of each RNA sample was digested with TURBO™ DNase (Thermo Fisher Scientific) in a 50 µl reaction with 1 µl TURBO DNase 2 U/µl and 5 µl TURBO DNase buffer. The reactions were incubated for 30 min at 37 °C and terminated using the DNase inactivation reagent according to the manufacturer's instructions. As the inactivation reagent contains EDTA which might interfere with later experimental steps, the DNase treated RNA was purified using a NaOAc precipitation. To 50 µl DNase treated RNA, 5 µl RNase free 3 M NaOAc pH 4,5 and 125 µl 100 % ethanol were added. Afterwards, the tubes were kept for 5 min in liquid nitrogen and centrifuged at 13.300 rpm and 4 °C for 20 min. The supernatant was discarded and the precipitated RNA dissolved in RNase free water after washing it with 75 % ethanol and centrifugation at the same settings as before.

cDNA Synthesis

First strand cDNA synthesis was performed using the RevertAid H Minus Reverse Transcriptase (Thermo Fisher Scientific Inc., Schwerte, Germany) with random hexamer primer according to the manufacturer's instructions with 1 µg of DNase treated RNA.

Expression Analysis via qRT-PCR

Quantitative reverse transcription PCR was performed to determine the expression levels of two miR165 (A and B), seven miR166 (A-G), five HD-ZIP III (CNA, REV, PHB, PHV, ATHB8), KAN1-3, WOX1, PRS and their *E. californica* orthologues on a Lightcycler II (Roche Diagnostics Deutschland GmbH, Mannheim, Germany) using the Luna® Universal qPCR Master Mix (NEB). At first a dilution series of the cDNA from 1:10 to 1:10,000 was performed to determine the amplification efficiencies of the qRT-PCR primers. Amplification efficiencies were calculated in Excel 2010 (Microsoft, Redmond, USA). Only primer pairs with amplification efficiencies ~2 were used for further analysis. The qRT-PCR run (95 °C for 60 s, 95 °C for 10 s, 60 °C for 10 s, 72 °C for 10 s and 45 cycles) was followed by a melting curve analysis to detect off target amplifications. Two technical replicates and three biological replicates were performed. The obtained data was analyzed using the Pfaffl method (Pfaffl, 2001).

Results

Multiple Putative Candidates Revealed for CRC Expression Regulation

CRCs expression is tightly regulated in a spatial and temporal manner being first restricted to two lateral stripes in the young gynoecium, then CRC expression is expanding throughout the circumference and commences in four internal stripes, only to recede in these internal stripes and in the replum region in later developmental stages. This order of different expression domains has to be coordinated by different transcription factors. To elucidate this regulatory network, a Yeast-1-hybrid (Y1H) screen of the CRC promoter was performed in which the full length promoter and 13 500 bp promoter fragments (for sequences see electronic appendix) were used. Of the 14 tested bait strains, four (*proCRC A*, *proCRC F2*, *proCRC F5*, *proCRC F8*) showed autoactivation with resistance to 1000 ng/ml AbA and were discarded. The remaining ten strains were transformed with the three different libraries of prey transcription factors (see for composition of library 1 Mitsuda *et al.* (2010), for libraries 2 and 3 Appendix table 14 and 15) and grown on selective SD-Leu or SD-Trp medium for up to ten days at room temperature. The resulting colonies were further selected and the respective prey proteins were identified by Sanger sequencing and blasting the sequences against the NCBI *A. thaliana* nucleotide collection. Further analyzes for selection have been conducted for 147 proteins using PlantPAN 2.0 (Chow *et al.*, 2016) and in addition plant transcription factor databases like PlnTFDB .

The identified 147 proteins (table 9) were imported into the plant promoter database PlantPAN 2.0 to identify their binding sites in the CRC promoter *in silico*. 33 % of the 147 proteins (48 proteins) (figure 11) were present in PlantPAN 2.0 (PP) and exhibited a DNA binding motif in the CRC promoter.

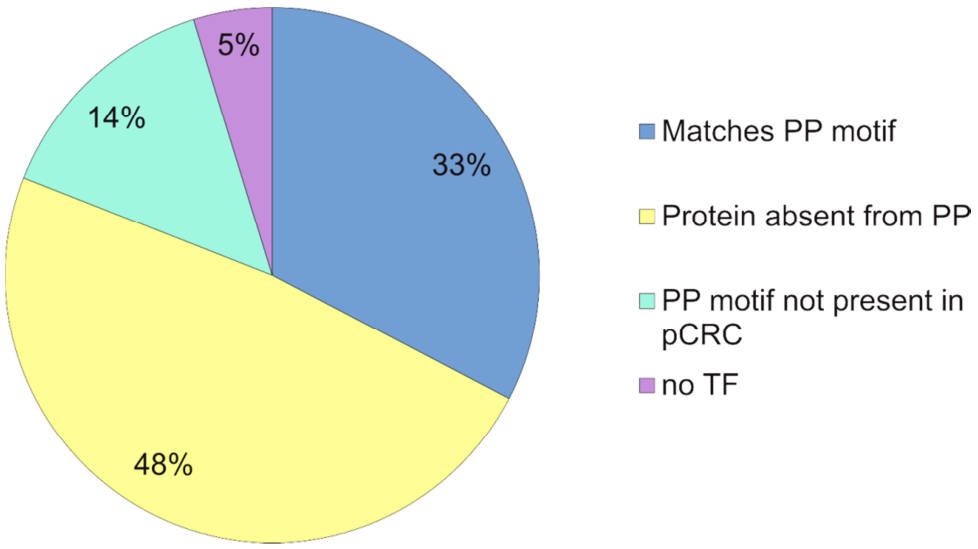

Figure 11: Percentage distribution of the identified transcription factors. Identified proteins were grouped according to the available information in PlantPAN 2.0 (PP) (Chow *et al.*, 2016). Proteins with *in silico* binding sites in *proCRC* were placed in "matches PP motif", proteins without an entry or no motif in PP were marked as "absent", proteins with known motifs which were not present according to PP were marked as "PP motif not present in *proCRC*", and all proteins with no known DNA binding capability were marked as "no TF".

The remaining 99 prey proteins could be separated into three different categories: 1) 71 proteins (48 %) were not included in PP, 2) binding motifs of 21 proteins (14 %) were included in PP but after evaluation not present in the CRC promoter, and 3) seven identified prey proteins (5 %) from the Mitsuda *et al.* library were not transcription factors (TF) at all and were excluded from further analyses. Proteins in category 2 were more complicated to treat. Either these 21 proteins have additional binding motifs that were not identified yet, or they have indeed no binding site in *proCRC* and can be seen as false positive signals. Therefore, these proteins were excluded from further analyses after the functional categorization.

Table 9: Prey proteins from the three different libraries identified by multiple Y1H analyzes. Shown are Tair locus, the gene name and the respective protein family. The identified proteins were color coded according to their category.

Locus	Name	Family
AT1G10120	CIB4	bHLH
AT1G23420	INO	C2C2-YABBY
AT1G24260	SEP3	MADS

AT1G25330	HAF	bHLH
AT1G26310	CAL	MADS
AT1G47655		C2C2-Dof
AT1G50680		AP2-EREBP
AT1G54160	NF-YA5	CCAAT
AT1G54830	NF-YC3	CCAAT
AT1G59750	ARF1	ARF
AT1G67260	TCP1	TCP
AT1G68670	HHO2	G2-like
AT1G68920	CIL1	bHLH
AT1G76420	CUC3	NAC
AT1G76580		SBP
AT2G03710	SEP4	MADS
AT2G26580	YAB5	C2C2-YABBY
AT2G33860	ETT	ARF
AT2G38880	NF-YB1	CCAAT
AT2G41690	HSFB3	HSF
AT2G42400	VOZ2	VOZ
AT3G06740	GATA15	C2C2-GATA
AT3G07340	CIB3	bHLH
AT3G16870	GATA17	C2C2-GATA
AT3G20910	NF-YA9	CCAAT
AT3G24050	GATA1	C2C2-GATA
AT3G25730	EDF3	AP2-EREBP
AT3G27010	TCP20	TCP
AT3G28910	MYB30	MYB
AT3G30260	AGL79	MADS
AT3G50870	HAN	C2C2-GATA
AT3G51080	GATA6	C2C2-GATA
AT3G60390	HAT3	HB
AT3G60530	GATA4	C2C2-GATA
AT4G02670	IDD12	C2H2
AT4G08150	KNAT1/BP	HB
AT4G11070	WRKY41	WRKY
AT4G16780	HAT4	HB
AT4G28790	bHLH23	bHLH
AT4G36900	DEAR4	AP2-EREBP
AT4G40060	ATHB16	HB
AT5G02840	RVE4	MYB-related
AT5G04340	ZAT6	C2H2
AT5G37020	ARF8	ARF
AT5G50915	bHLH137	bHLH
AT5G60910	FUL	MADS
AT5G63790	NAC102	NAC
AT5G65310	ATHB5	HB
AT1G02220	NAC003	NAC
AT1G13880	ELM2	MYB-related

AT1G14685	BPC2	BBR/BPC
AT1G16490	MYB58	MYB
AT1G20900	ESC	AT-Hook
AT1G43850	SEU	ABI3VP1
AT1G46408	AGL97	MADS
AT1G65360	AGL23	MADS
AT1G68480	JAG	C2H2
AT1G69580		G2-like
AT1G75710		C2H2
AT1G76510		ARID
AT2G14760		bHLH
AT2G16770	BZIP23	bZIP
AT2G17770	BZIP27	bZIP
AT2G24840	AGL61	MADS
AT2G28540		unknown
AT2G31380	STH	Orphans
AT2G35270	GIK	AT-Hook
AT2G35430		C3H
AT2G37060	NF-YB8	CCAAT
AT2G39880	MYB25	MYB
AT2G42300	BHLH48	bHLH
AT2G45160	HAM	GRAS
AT3G01530	MYB57	MYB
AT3G08500	MYB83	MYB
AT3G11100	VFP3	Trihelix
AT3G16500	PAP1	AUX/IAA
AT3G18650	AGL103	MADS
AT3G19360		C3H
AT3G20640		CCAAT
AT3G24140	FAMA	bHLH
AT3G25710	TMO5	bHLH
AT3G26640	LWD2	WD40
AT3G45260	BIB	C2H2
AT3G55560	AHL15	AT-Hook
AT3G57180	BPG2	unknown
AT3G58630		Trihelix
AT3G58680	MBF1B	MBF1
AT3G61950	bHLH67	bHLH
AT3G61970	NGA2	ABI3VP1
AT4G24440		C2C2-GATA
AT4G28190	ULT1	ULT
AT4G30180		unknown
AT4G31420	REIL1	C2H2
AT4G32551	LUG	LUG
AT4G35700	DAZ3	C2H2
AT4G36740	ATHB40	HB
AT4G38960	BBX19	Orphans

AT5G01200		MYB
AT5G02030	PNY	HB
AT5G05830		PHD
AT5G06160	ATO	C2H2
AT5G08190	NF-YB12	CCAAT
AT5G09460	SACL1	bHLH
AT5G09780	REM25	ABI3VP1
AT5G11270	OCP3	HD
AT5G14000	NAC084	NAC
AT5G18090		ABI3VP1
AT5G22290	NAC089	NAC
AT5G25890	IAA28	AUX/IAA
AT5G39750	AGL81	MADS
AT5G45580		G2-like
AT5G49420		MADS
AT5G49490	AGL83	MADS
AT5G49700	AHL17	AT-Hook
AT5G53660	GRF7	GRF
AT5G56840		MYB-related
AT5G56900		C3H
AT5G57660	COL5	C2C2-CO-like
AT5G61470		C2H2
AT1G01030	NGA3	ABI3VP1
AT1G08010	GATA11	C2C2-GATA
AT1G12630		AP2-EREBP
AT1G53170	ERF8	AP2-EREBP
AT1G54060	ASIL1	Trihelix
AT1G68800	TCP12	TCP
AT1G69010	BIM2	bHLH
AT1G72360	ERF73	AP2-EREBP
AT2G18380	HANL1	C2C2-GATA
AT2G40220	ABI4	AP2-EREBP
AT2G40970	MYBC1	G2-like
AT2G41940	ZFP8	C2H2
AT3G23240	ERF1	AP2-EREBP
AT3G61630	CRF6	AP2-EREBP
AT4G13620		AP2-EREBP
AT4G28140		AP2-EREBP
AT4G32040	KNAT5	HB
AT5G13790	AGL15	MADS
AT5G13910	LEP	AP2-EREBP
AT5G52020		AP2-EREBP
AT5G61890	ERF114	AP2-EREBP
AT1G76710	ASHH1	Methyltransferase
AT2G20760	CLC1	Clathrin light chain protein
AT2G30410	KIESEL	Tubulin binding cofactor A
AT3G05155		Major facilitator superfamily protein

AT4G30860	ASHR3	SET
AT4G33540		Metallo b-lactamase
AT5G63730	ARI14	E3 Ligase

Three Transcription Factor Families Are Mainly Involved in CRC Regulation

140 transcription factors were compared to the Plant Transcription Factor Database (PlnTFDB, Pérez-Rodríguez *et al.* (2010)) to identify their respective protein families (figure 12). The three largest families have at least 13 members from the 140 protein list: AP2-EREBP, bHLH, and MADS. While most members of the AP2-EREBP family show no motif in *proCRC* (11 proteins), both in bHLH and MADS families are multiple proteins with matching DNA binding motifs and also important floral developmental regulators like HALF FILLED, SEP3, CAULIFLOWER, and FRUITFULL. In addition, multiple zinc finger domain containing proteins, in the families C2C2-CO-like, C2C2-Dof, C2C2-GATA, C2C2-YABBY, C2H2, C3H, and VOZ bind to the CRC promoter in this Y1H analysis. The most prominent proteins in these groups are INO (C2C2-YABBY), YAB5 (C2C2-YABBY), HANABA TANARU (C2C2-GATA), and JAGGED (C2H2). Another family with multiple transcription factors with matching DNA binding motifs is the family of homeodomain containing proteins (HD), with members like KNOTTED-LIKE FROM ARABIDOPSIS THALIANA 1 or BREVIPEDICELLUS (KNAT1 or BP) and RPL/PNY. Moreover, auxin response factors, typically involved in multiple developmental steps, are present with the three members ARF1, ARF3/ETTIN, and ARF8.

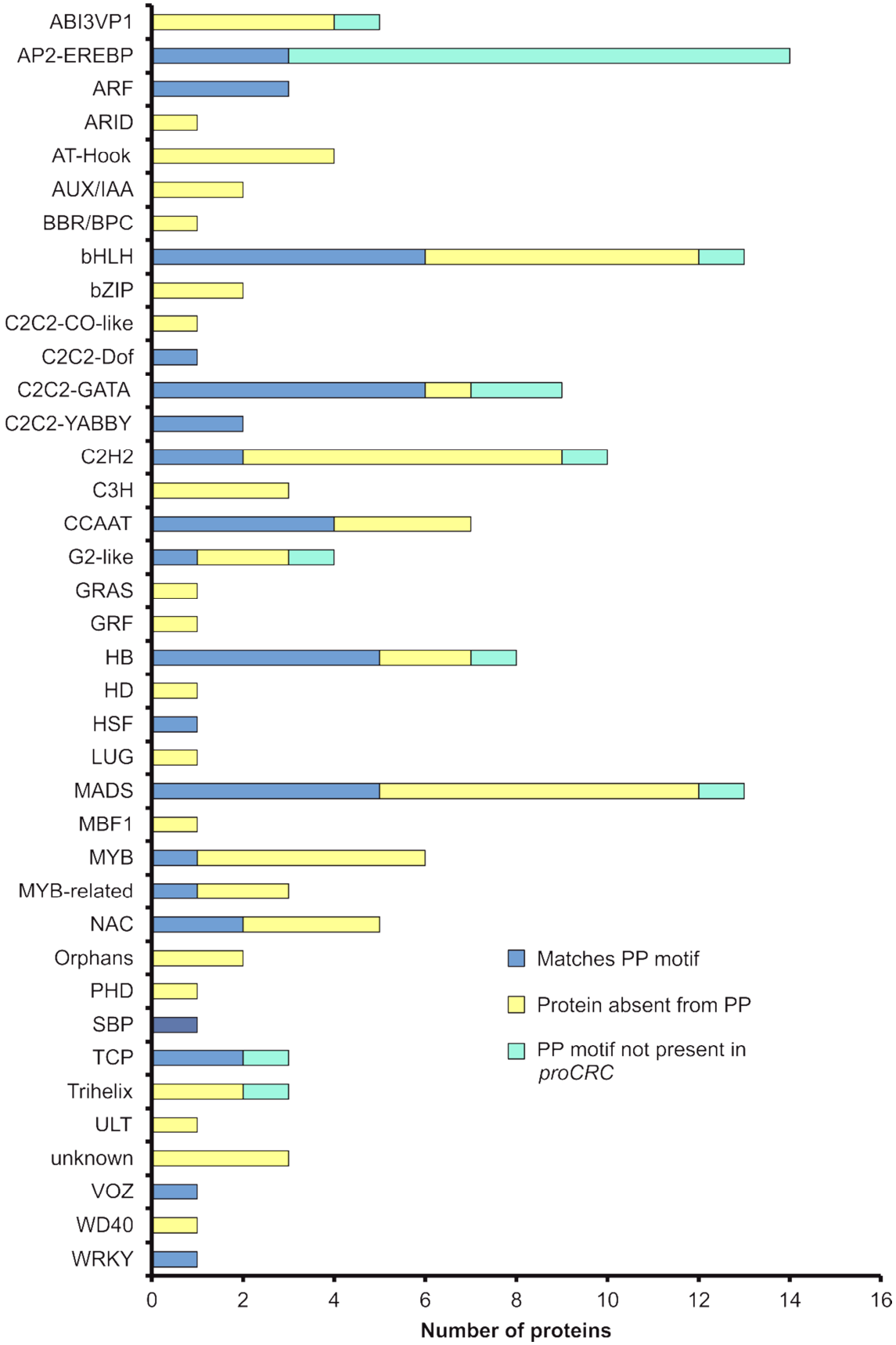

Figure 12: Family distribution of the identified proteins. All transcription factors were compared with the PlnTFDB and their respective protein family was identified.

Most Functional Annotated Regulators Are Involved in Flower Development

The 140 identified putative regulators were sorted into functional categories based on publications and gene ontology predictions to identify promising candidate genes for further expression studies. Eight categories (circadian clock, embryo development, flower development, vegetative growth, metabolism, senescence, stress, and unknown function) were defined (figure 13). Up to three genes were present in the categories “circadian clock”, “metabolism”, and “senescence”. The categories “embryo development” and “stress” contain nine and 12 proteins, respectively. The majority (34 proteins) of the identified and functional annotated regulators is involved in flower development. Flower developmental proteins are especially involved either in flower initialization and floral organ formation (CAULIFLOWER, SEP3, ETT, and FRUITFULL) or in “fine tuning” the floral development like regulating the development of the transmitting tract (HALF FILLED). The second largest group of proteins (28 proteins) with an annotated function is involved in vegetative growth. Proteins like FAMA regulate the development of the leaf lamina and of stomata (Ohashi-Ito and Bergmann, 2006), or ARABIDOPSIS THALIANA HOMEOBOX PROTEIN 2 which is restricting cell proliferation in the SAM and in developing lateral organs (Carabelli *et al.*, 2018). However, the largest group (50 proteins) has no functional annotation.

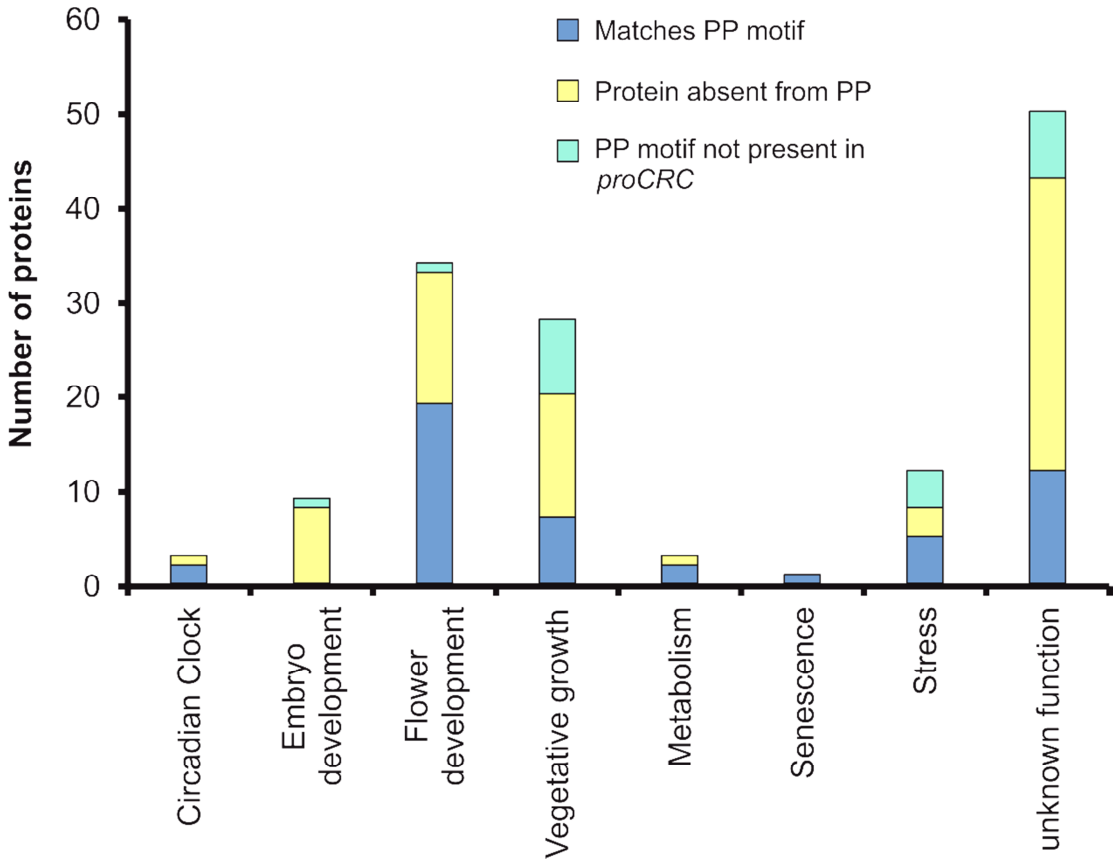

Figure 13: Functional categories in which the identified proteins have been grouped. Categorization was based on either described functions or predictions.

All further analyses were performed with the 48 proteins whose DNA binding motif were present in *proCRC* and the 71 proteins whose DNA binding motifs are still unknown, as both groups are more likely regulators of CRC expression than the 21 proteins whose known DNA binding motif did not match to *proCRC*. Furthermore, only proteins identified as transcription factors by the PlnTFDB were retained in the following analyses.

Binding Sites in *proCRC* Are Unevenly Distributed

An *in silico* analysis of the spatial distribution of the different binding motifs in *proCRC* (figure 14) showed that the binding motifs of the 140 different identified regulators are unevenly distributed over the CRC promoter with its five conserved regions (A - E) and the five not conserved regions. Two maxima are at both ends, distal and proximal to the start codon in regions End-E, E, and A with 27 - 31 binding regulators. The least binding sites according to

PlantPAN are in region E-D, D, and B-A with 16 - 18 binding regulators. Almost an identical number of regulators bind to regions C-D, C, C-B, and B (21-23 regulators). Comparing these numbers with the distribution identified by the screen itself (figure 15), the most transcription factors bound to region C, followed by region E. Regions D, B, and A could not be tested due to autoactivation, similar to F2, F5, and F8. Interestingly, 26 transcription factors bound to fragment 6 which is partially overlapping with the C region of *proCRC*.

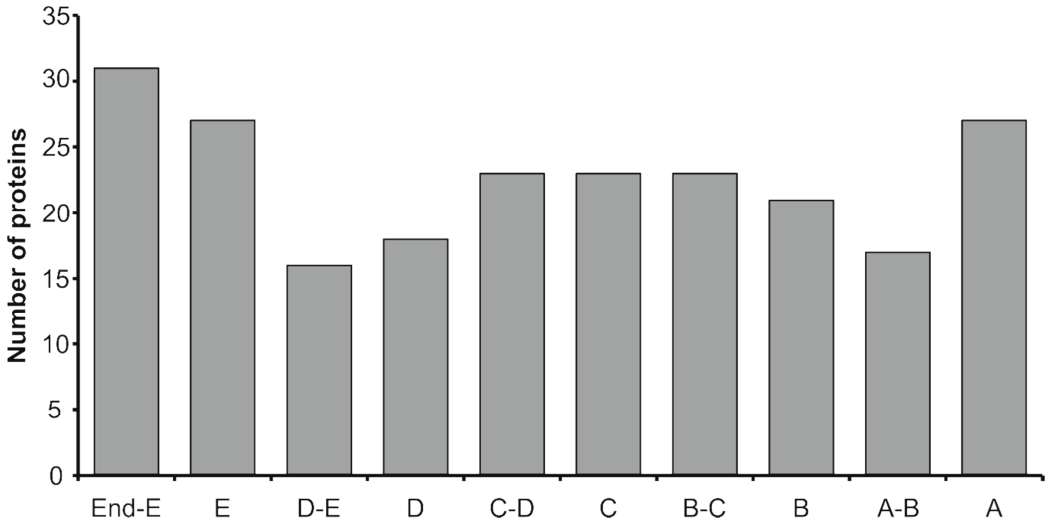

Figure 14: Distribution of binding transcription factors in the different regions of *proCRC*. Binding sites were identified with PlantPAN2.0.

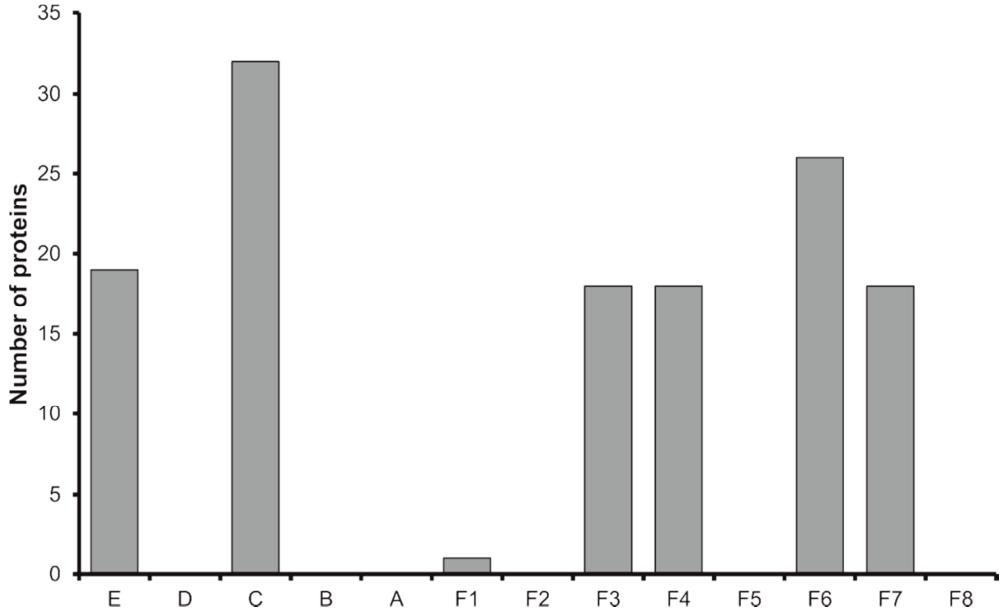

Figure 15: Number of binding transcription factors in the different fragments of *proCRC* used in the Y1H screen.

When displaying the actual distribution of the transcription factor binding motifs (figure 16), one can find that multiple regulators, such as GATA1, GATA15, HANABA TARANU, NUCLEAR FACTOR (NF) –YA5, NF-YA9, NF-YB1, and NF-YC3 are present with numerous binding sites throughout the CRC promoter (not shown in figure 16). Most other identified regulators were absent from at least one region of the CRC promoter, whereas ARABIDOPSIS THALIANA HOMEOBOX PROTEIN 16 (ATHB16), CUP SHAPED COTYLEDON 3 (CUC3), DREB AND EAR MOTIF PROTEIN 4 (DEAR4), ETT, INDETERMINATE-DOMAIN 12 (IDD12), MYB30, NAC102, SEP4, TCP1, and TCP20 have only one binding site in *proCRC*.

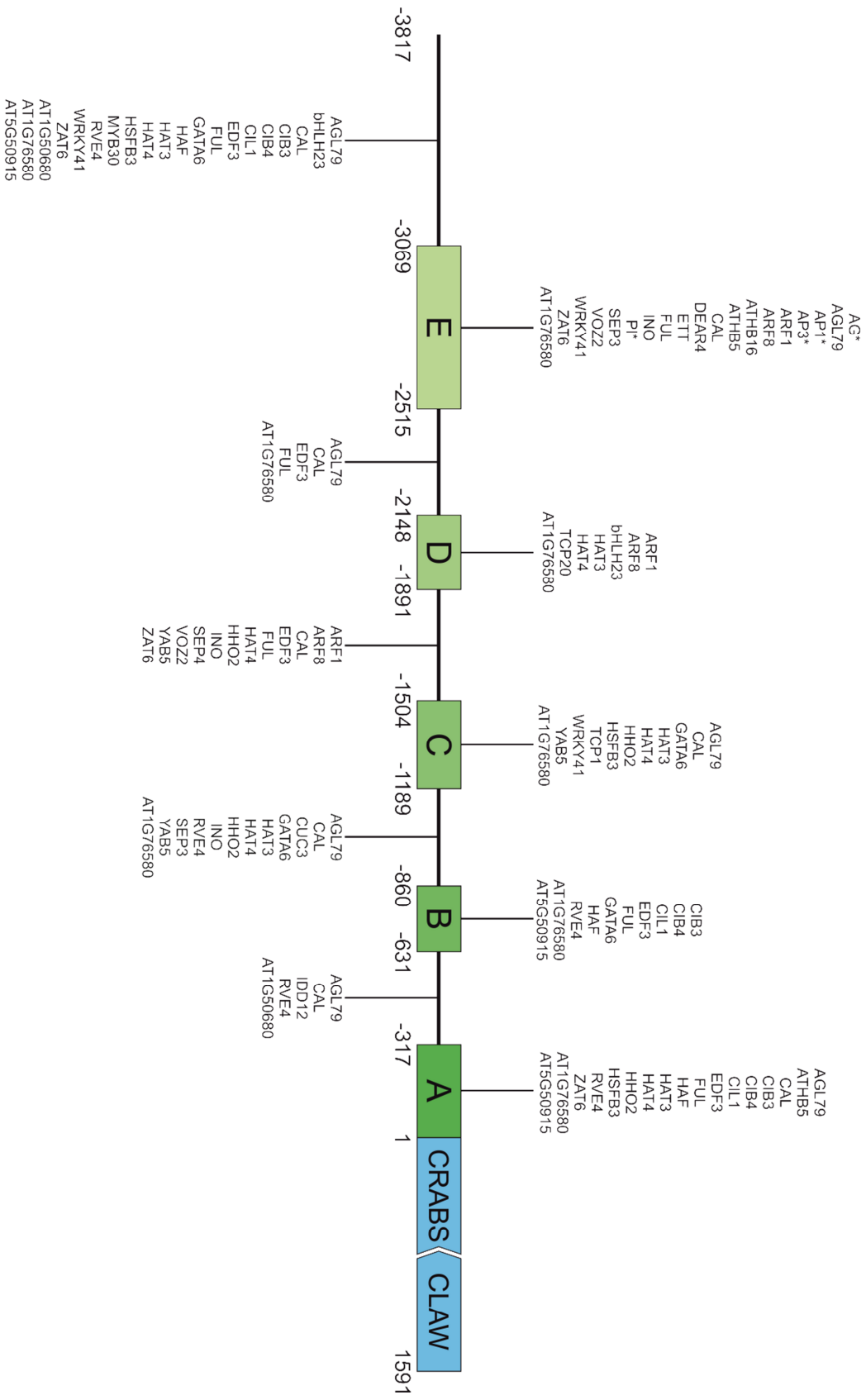

Figure 16: PlantPAN 2.0 based spatial distribution of transcription factor binding sites in *proCRC*. Putative binding sites were identified with PlantPAN2.0. Shown are only transcription factors with a known motif in PlantPAN2.0 and which do not bind in every region of *proCRC*.

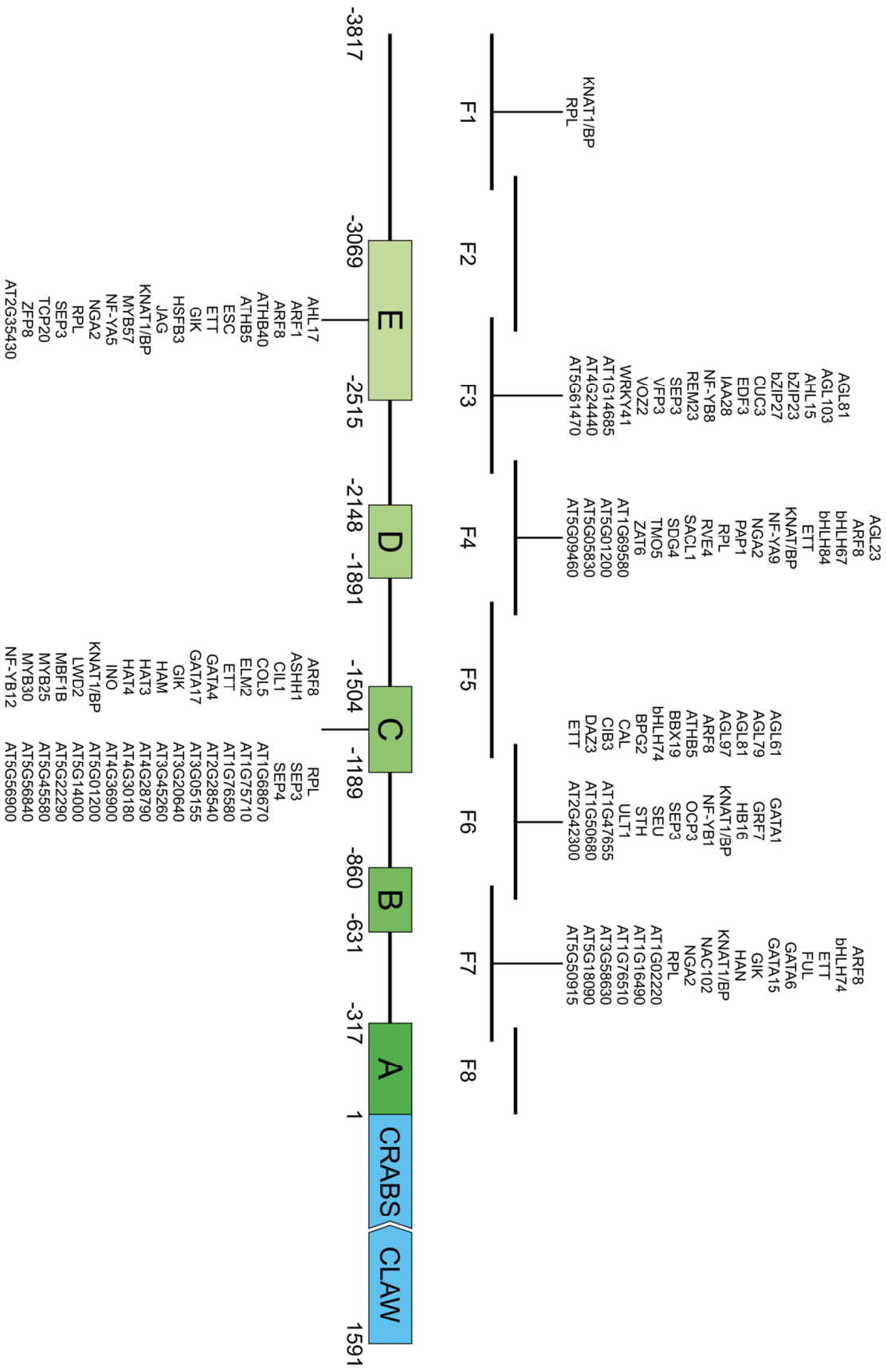

Figure 17: Y1H based spatial distribution of transcription factor binding sites in *proCRC*. Putative binding sites were identified according to the bound fragment in the Y1H screen. Shown are all identified transcription factors except those which do not bind in *proCRC* according to PlantPAN2.0.

Interestingly, the spatial distribution of the binding sites in *proCRC* of the *in silico* analysis in PlantPAN2.0 differs from the spatial distribution based on the actual data from the Y1H screen (figure 17). Except for the regions E and C it is difficult to identify regulators that bind in the conserved regions due to the division of *proCRC* into eight overlapping fragments (*proCRC* F 1-8). Nevertheless, most identified regulators can be found in region C and fragment 6, which contains part of regions C and B and the intermediate region C-B. Additionally, the regulators AGAMOUS LIKE 83 (AGL83), ATROPOS (ATO), HAF, IDD12, INO, LEUNIG (LUG), MYB83, REI1-LIKE 1 (REIL1), SEP3, TCP1, and YAB5 cannot be assigned to any region or fragment as they were identified in a screen with the full length promoter.

Regulators of CRC Expression Are Co-expressed During Flower Development

As activators of CRC expression are likely to be similarly expressed during flower development in *A. thaliana*, 1567 similarly expressed genes were identified with Expression Angler based on Pearson correlation (Austin *et al.*, 2016) in the AtGenExpress developmental data set (Schmid *et al.*, 2005) and in the carpel and stigma datasets from Swanson *et al.* (2005). Of these 1567 co-expressed genes, 12 were present in the Y1H dataset (figure 18). Almost all genes (except for *SEP3*) are higher expressed in the ovary than in the stigma in stage 8 flowers. In later flower stages, CRC expression is declining and so is the expression of most of the co-expressed genes.

More recent data obtained from RNA sequencing (RNA-seq) allows detailed following of the CRC expression inside the carpel (figure 19). Carpel tissue from four different developmental stages was collected via laser microbeam microdissection (Kivivirta *et al.*, unpublished data), followed by RNA-seq. Genes, co-expressed to CRC were identified and were compared to the results of the Y1H analysis. When the CRC expression was followed over its temporal course through the transcriptomes, 7577 co-expressed genes were identified based on Pearson correlation. Of those, 5167 genes were positively correlated with CRC expression and 2410 negatively. In total, 34 genes identical to the Y1H analysis, were found in the 7577 co-expressed genes. 22 genes show a similar expression pattern as CRC (positive correlation)

with high expression in early developmental stages of carpel development and a lower expression in later stages (figure 19). The remaining 12 genes are expressed in an opposite manner to CRC and were highly expressed in the late carpel development.

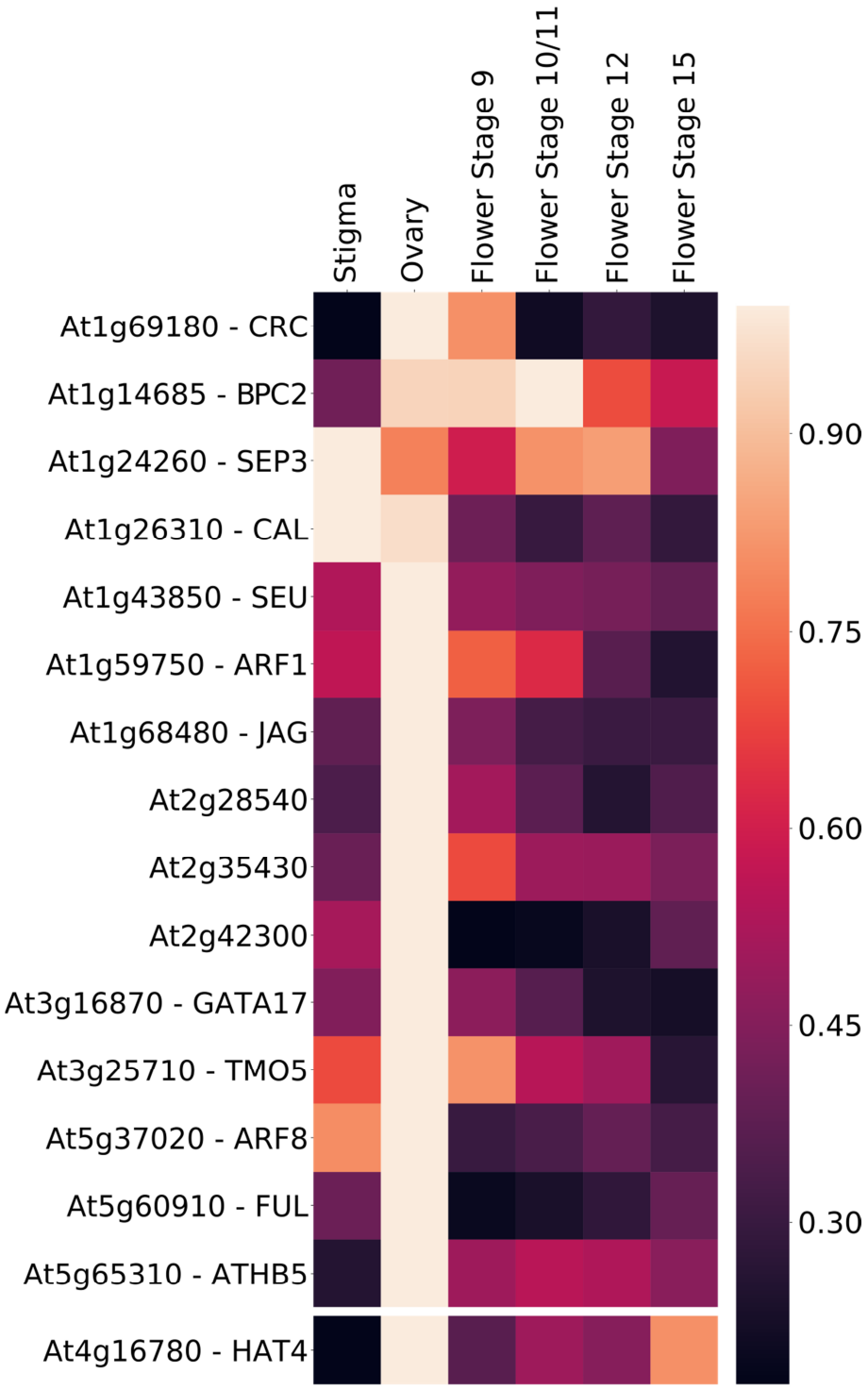

Figure 18: Heatmap of CRC and its co-expressed genes in different parts of the gynoecium and flower stages. The different rows are not correlated with each other. Color intensity represents expression level. A light color represents high expression and a dark color low expression. Data was exported from Expression Angler and the heatmap was made using Python v3.6.8, Seaborn v0.9.0, and Pandas v0.23.4.

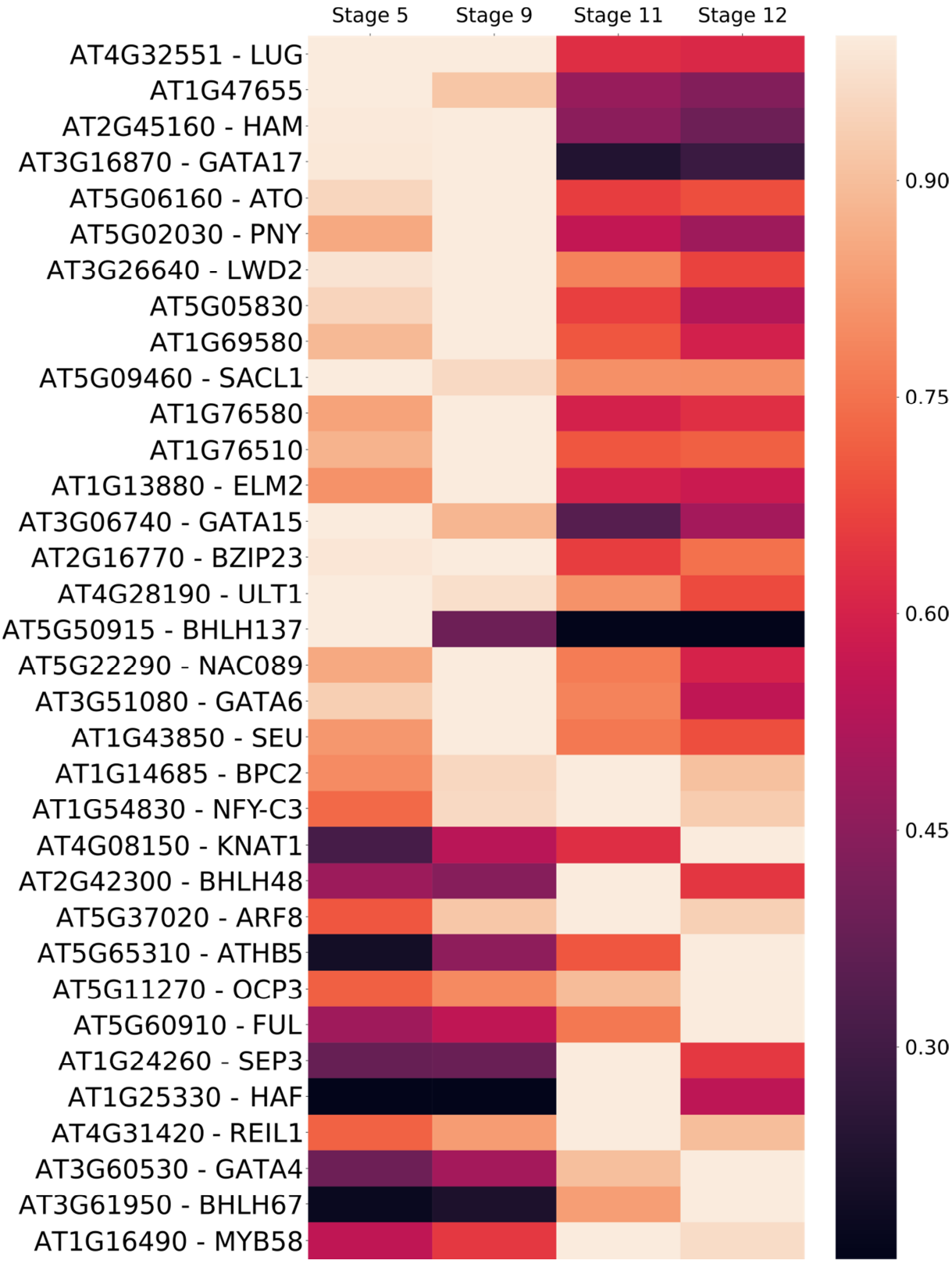

Figure 19: Heatmap of CRC and its co-expressed genes in the carpel at different developmental stages. The different rows are not correlated with each other. Color intensity represents expression level. A light color represents high expression and a dark color low expression. Data was exported from the RNA-seq analysis of *A. thaliana* carpel tissue and the heatmap was made using Python v3.6.8, Seaborn v0.9.0, and Pandas v0.23.4.

Additionally, PlaNet, a web tool for visualization of co-functioning gene networks was applied (Mutwil *et al.*, 2011), using *A. thaliana* expression data deposited at TAIR (arabidopsis.org), to construct a co-expression network of CRC (figure 20). 87 co-expressed genes were identified via Pearson correlation and applying a highest reciprocal rank (HRR) cutoff of 10 ≤ HRR ≤ 30 to identify biological significant relationships (Mutwil *et al.*, 2011). Only co-expressed transcription factors are displayed as first or second neighbors with first neighbors show a higher correlation to CRC than second neighbors. Three (CUC3, FUL, and HAF) out of the 26 identified co-expressed transcription factors appear also in the Y1H dataset. Of these 26 transcription factors, 12 are shared with the Expression Angler data set (Appendix table 11) and 11 genes with the RNA-seq data set (Appendix table 12). Additionally, AP1 and PI are first (red ring) and second neighbors of CRC and bind to the E region of *proCRC*. The different neighbors of CRC can be grouped into different functional modules, based on published functions of the neighbors or predictions. CRC is connected to modules of carpel development (encircled with a dark purple line) via its first neighbor SQUAMOSA PROMOTER BINDING PROTEIN-LIKE 9 (SPL9) and a small nectary development module (green line), consisting out of the first neighbor BLADE ON PETIOLE 1 (BOP1) and BOP2. An even smaller wax biosynthesis module (orange line) is represented by SHINE1 (SHN1). The remaining co-expressed factors are involved in the regulation of the activity of the floral meristem (red line) such as AP1, SHOOT MERISTEMLESS (STM), CUC1, and CUC3.

These co-expression analyses show the tight integration of CRC into different aspects of carpel development and give rise to a better understanding of CRC's functions.

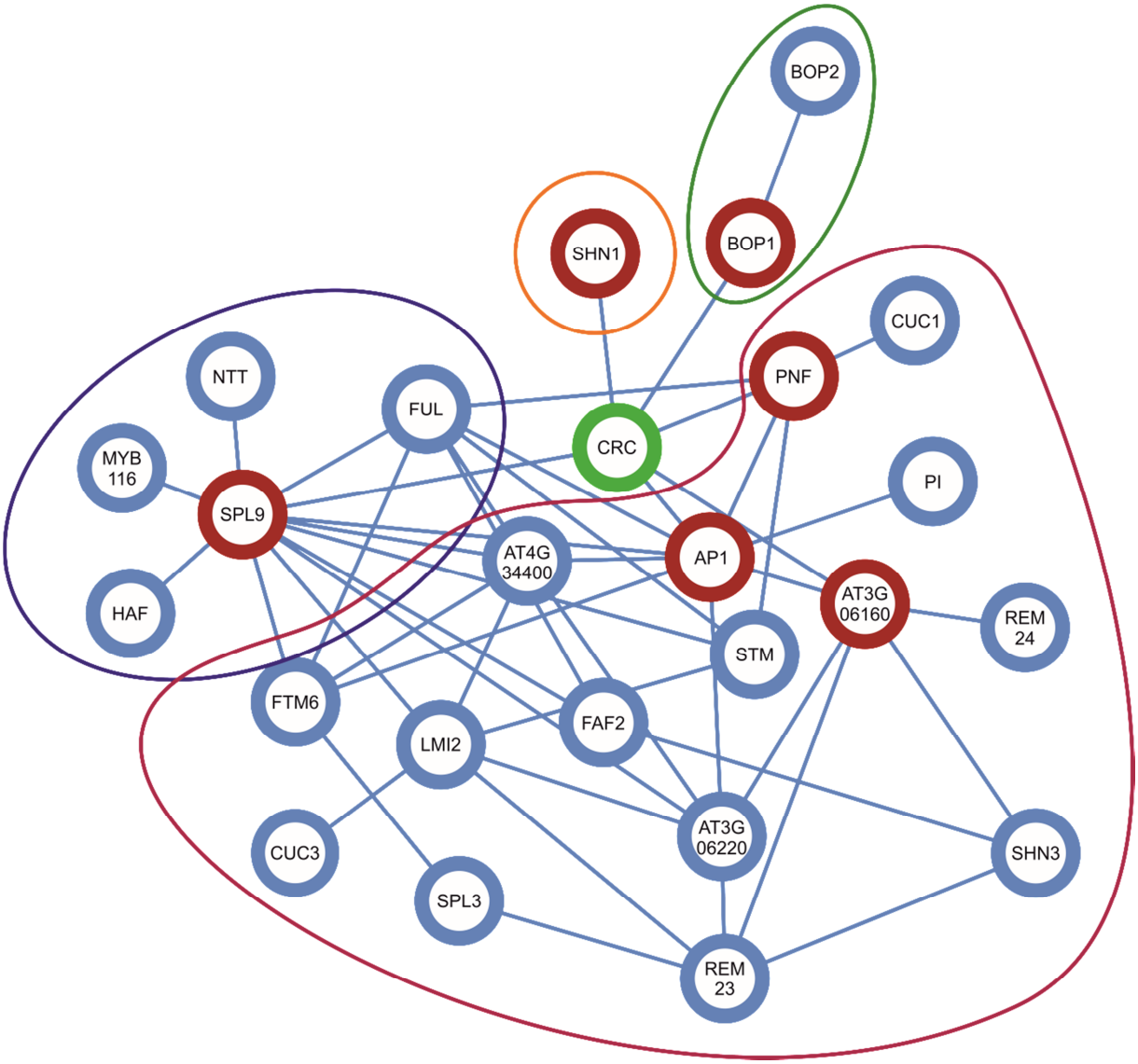

Figure 20: Co-expression network of CRC with other transcription factors based on PlaNet data. Cytoscape version 3.7.1 (Shannon *et al.*, 2003) was used to visualize the network. Nodes represent the transcription factors and edges indicate co-expression relationships between genes. The colored lines represent the different modules: dark purple, carpel development; green, nectary development module; orange, wax biosynthesis module; red, regulation of the floral meristem.

CRC Regulates Adaxial-Abaxial Factors

Specific Members of the mir165/166 Family Are Regulated by CRC

Previous studies have identified YABBY proteins, especially FIL and YAB3, to be involved in the regulation of the two micro RNA families mir165/166 (Tatematsu *et al.*, 2015). These miRNAs negatively regulate adaxial specifying transcription factors, members of HD-ZIP III protein family and thus are necessary to establish the adaxial-abaxial polarity in leaves. To identify the position of CRC in this regulatory network, multiple qRT-PCRs were performed.

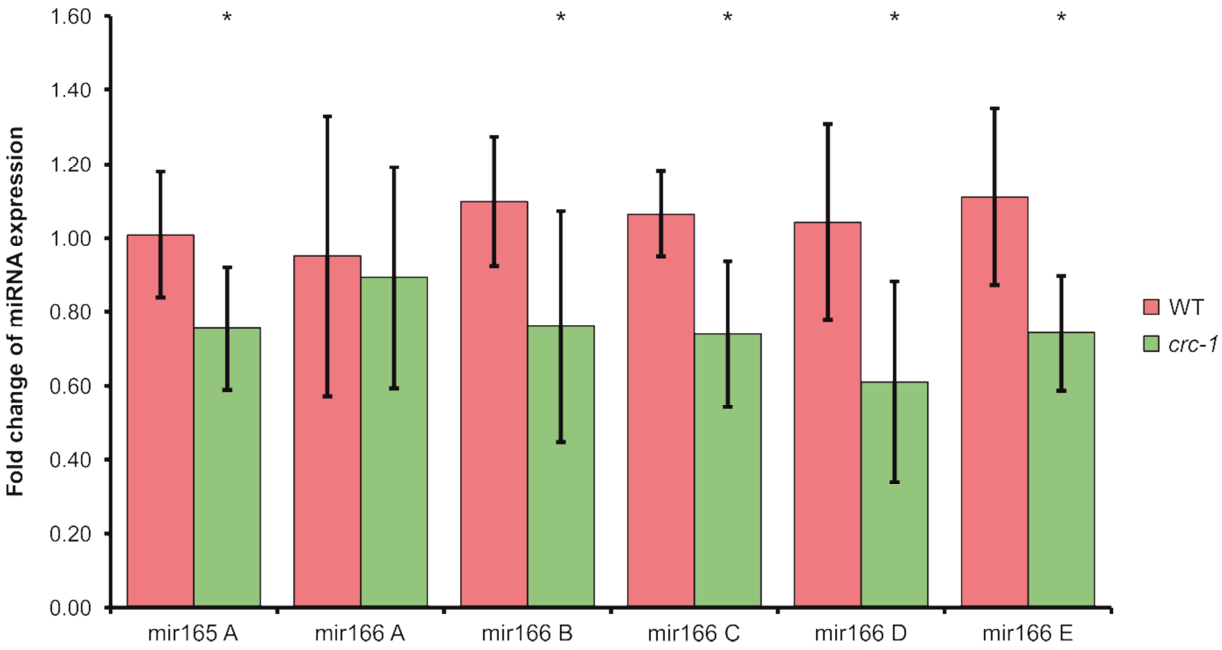

Figure 21: Expression analysis of mir165/166 members in buds of *A. thaliana* in wild type and *crc-1* plants. The fold changes of expression were calculated using the ΔΔCt method according to Pfaffl (2001) and error bars represent the standard deviation of the mean. Asterisks indicate significant ($p < 0.05$) differences compared to the wild type.

Out of the nine members of mir165/166 (mir165 with two members and mir166 with seven members), six members were chosen (mir165 A, mir166 A, mir166 B, mir166 C, mir166 D, and mir166 E), as already established primers were present (Carlsbecker *et al.*, 2010). Primer establishment for the remaining miRNAs (mir165 B, mir166 F, and mir166 G) was not successful. The miRNA expression was tested in inflorescences of wild type *A. thaliana* Ler-0 plants and in *crc-1* plants (figure 21). The majority of the tested miRNAs (mir165 A, mir166 B,

mir166 C, mir166 D, and mir166 E) were significantly downregulated in a *crc-1* background and the expression of mir165 A, mir166 B, mir166 C, and mir166 E declined by about 25 % with 0.75 ± 0.17, 0.76 ± 0.31, 0.74 ± 0.20, and 0.74 ± 0.15, respectively. With a decline of 39 % (0.61 ± 0.27), mir166 D showed the highest reduction. The expression of mir166 A was not changed in *crc-1* mutants (0.89 ± 0.30) and remained at wild type level (0.95 ± 0.38).

CRC Activates the Expression of HD-ZIP III Genes

As most of the analyzed miRNAs showed a reduction of expression in a *crc-1* background, the responses of the mir165/166 targeted HD ZIP III genes *CNA*, *REV*, *PHV*, *ATHB8*, and *PHB* were of special interest. *PHB* did only show a very weak expression and was excluded from the analysis.

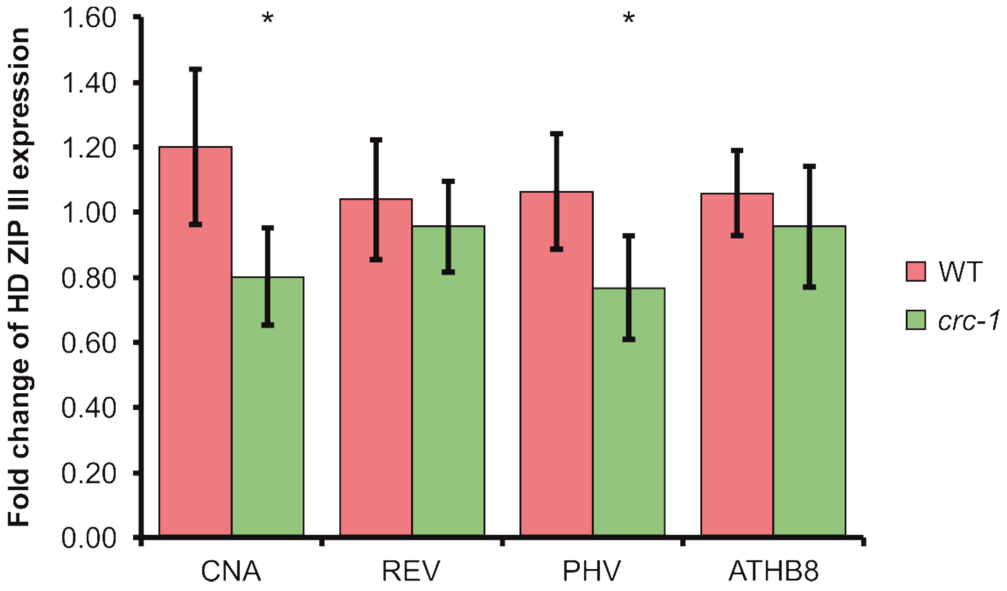

Figure 22: Expression analysis of HD ZIP III members in buds of *A. thaliana* in wild type and *crc-1* plants. The fold changes of expression were calculated using the ΔΔCt method according to Pfaffl (2001) and error bars represent the standard deviation of the mean. Asterisks indicate significant ($p < 0.05$) differences compared to the wild type.

Two of the four analyzed HD ZIP III members were, similar to members of mir165/166, negatively affected by a *crc* mutation (figure 22). The expression level of *CNA* and *PHV* were

significantly reduced to 0.80 ± 0.15 and 0.77 ± 0.16, respectively. In contrast to this, *REV* and *ATHB8* showed no significant differences in their expression compared to the wild type.

Expression of Abaxial and Middle Domain Regulators Is Controlled by CRC

The surprising effect of a *crc* mutation negatively affecting both, abaxial (miRNA 165/166) and adaxial (HD ZIP III) regulators, led to the question if CRC influences also the expression of the major abaxial regulators, the *KAN* genes (*KAN1*, *KAN2*, *KAN3*, and *KAN4*) and also of the middle domain specifying WOX genes (*WOX1* and *WOX3*/*PRS*). *KAN4* is mainly expressed in developing ovules and was excluded from the qRT PCR analyszes. Additionally, *PRS* was removed due to weak expression.

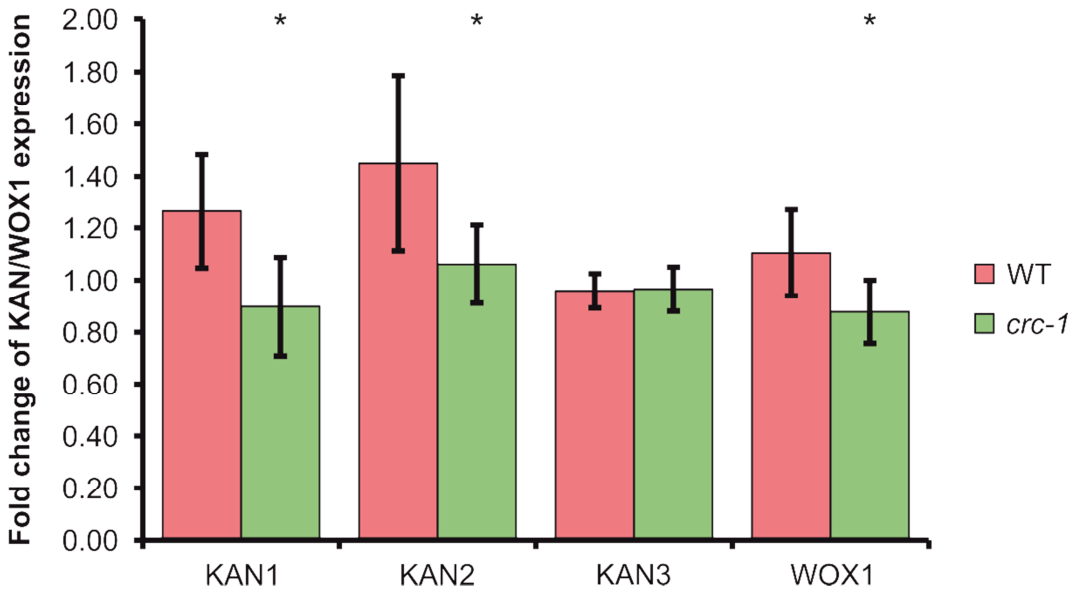

Figure 23: Expression analysis of KANADI members and WOX1 in buds of *A. thaliana* in wild type and *crc-1* plants. The fold changes of expression were calculated using the ΔΔCt method according to Pfaffl (2001) and error bars represent the standard deviation of the mean. Asterisks indicate significant ($p < 0.05$) differences compared to the wild type.

The same expression pattern as in mir165/166 and HD ZIP III expression can be observed (figure 23). Both, *KAN1* and *KAN2* expression levels are reduced in the *crc-1* background (0.90 ± 0.19 and 1.06 ± 0.15, respectively) compared to KAN1/2 expression in wild type plants (1.26 ± 0.22 and 1.45 ± 0.34, respectively), whereas *KAN3* expression is identical in *crc-1* and in wild type plants (0.96 ± 0.07 and 0.97 ± 0.09, respectively). *WOX1* expression is

also significantly decreased in *crc-1* mutants (0.88 ± 0.12) compared to the wild type (1.10 ± 0.17).

YABBY Binding Motifs Are Present in Target Gene Promoters

Different YABBY binding motifs (YBMs) have been identified so far (Shamimuzzaman and Vodkin, 2013; Franco-Zorrilla *et al.*, 2014). However, until now only the motifs, identified by Shamimuzzaman and Vodkin (2013), have been shown to influence the expression of CRC target genes like *TRN2* (Yamaguchi *et al.*, 2017). Thus the binding site analysis will only address the three motifs identified by Shamimuzzaman and Vodkin (2013). Promoter regions of the different adaxial-abaxial regulators were analyzed as described in Gross *et al.* (2018). Reference genes, commonly used in qRT-PCR analyzes, were chosen as comparison to rule out random occurrence of the respective motifs in typical promoter regions. Of all YBMs, YBM2 (GARAGAAA) is more abundant than YBM1 (CCMYCWWC) or YBM3 (GTGGGG). Many of the involved adaxial–abaxial regulators exhibit YBMs in their promoter regions (figure 24). Five members of mir165/166 exhibited at least one YBM, with mir165 A and mir166 A having up to 7 YBMs in their respective promoter. Interestingly, there are no YBMs in the promoter regions of mir166 C, mir166 D, mir166 E, and mir166 G, even though, the first three showed a reduced expression in *crc-1* mutants. In contrast to these few YBMs in mir165/166, promoter regions of the five HD ZIP III genes contain at least 2 YBMs, with the exception of PHB. The two HD ZIP III genes, CNA and PHV, which were significantly less expressed in *crc-1* mutants, exhibited the most YBMs in their promoter regions (5 and 6, respectively). Also the abaxial acting *KAN* genes exhibit YBMs. Interestingly, there are 2 YBMs in *proKAN3* but the *KAN3* expression was identical in wild type and *crc-1* plants. Additionally, the middle domain factor WOX1 has 3 YBMs in its promoter present.

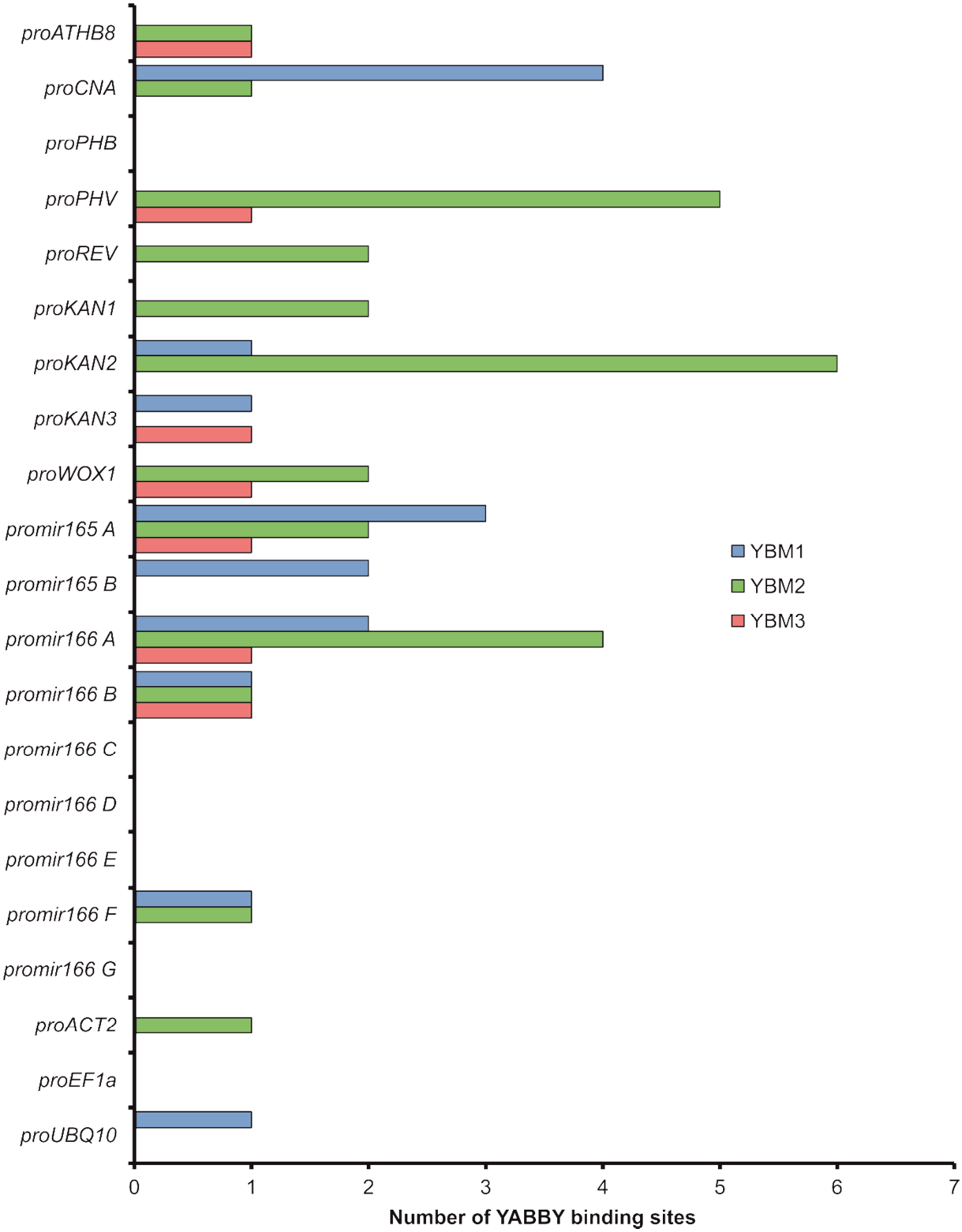

Figure 24: Analysis of the presence of three putative YABBY binding motifs (identified by Shamimuzzaman and Vodkin (2013) and confirmed by Yamaguchi *et al.* (2017)) in the promoter regions of putative CRC target genes. Promoter regions of three commonly used qRT-PCR reference genes (Czechowski *et al.*, 2005) were used as comparison. The number of each binding site in the respective promoter was determined using PlantPAN2.0 (Chow *et al.*, 2016).

Effects of CRC Depletion Are Not Conserved Between *A. thaliana* and *E. californica*

To further investigate CRCs position in the adaxial-abaxial regulatory network, orthologues of adaxial-abaxial regulators were identified in *Eschscholzia californica* (a basal eudicot plant from the order Ranunculales) with an *E. californica* carpel transcriptome (personal communication Kimmo Kivivirta) and with the newly published *E. californica* genome (Hori *et al.*, 2018). The *E. californica* orthologues EcCNA1, EcCNA2, EcPHX, EcWOX1, EcKAN1, Ecmir166 A were identified and their expression was analyzed via qRT-PCR. As there is no *crc* knock-out line in *E. californica*, wild type *E. californica* plants were subjected to viral induced gene silencing (VIGS) through which the endogenous EcCRC mRNA was post-transcriptionally degraded and by this a *crc* phenotype was induced in these knock-down plants (the sample material was a kind gift of Anna Barbara Dommes).

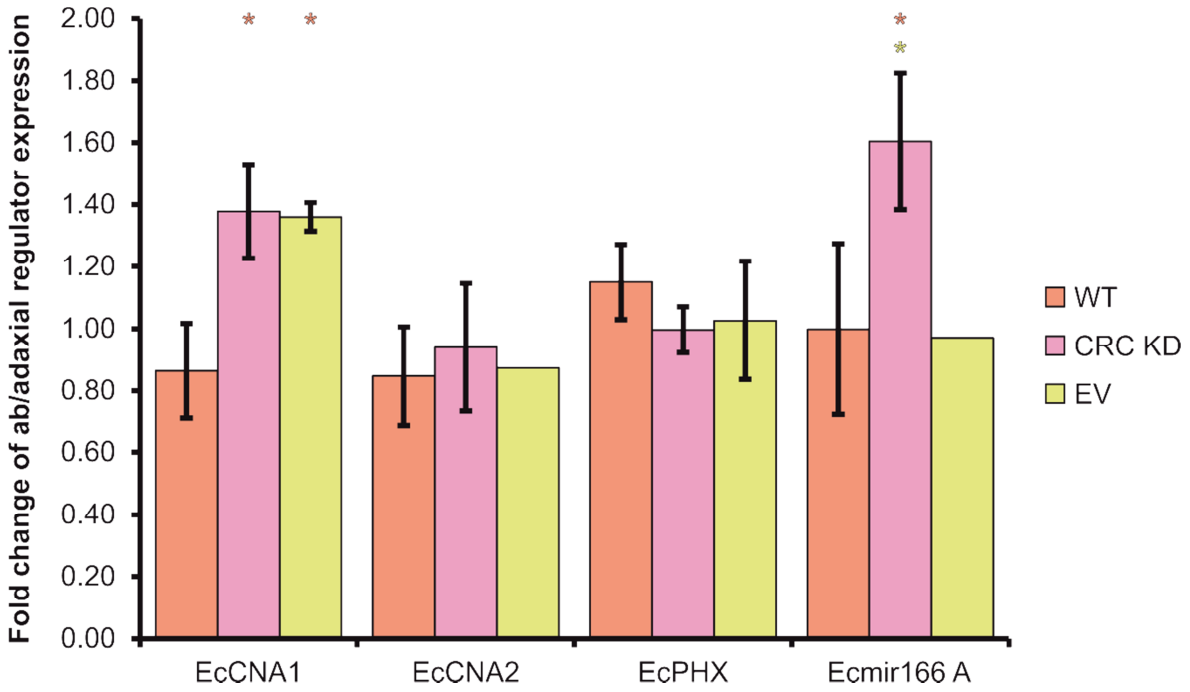

Figure 25: Expression analysis of HD ZIP III members and Ecmir166 A in buds of *E. californica* in wild type, CRC knock down plants, and empty vector control plants. The fold changes of expression were calculated using the ΔΔCt method according to Pfaffl (2001) and error bars represent the standard deviation of the mean (calculated if possible). Asterisks indicate significant differences ($p < 0.05$) compared to the wild type (orange asterisks) or to the empty vector control (yellow asterisks).

In contrast to *A. thaliana*, one of the analyzed HD ZIP III genes (EcCNA1) in *E. californica* showed an increased expression in CRC knock down (CRC KD) plants (1.38 ± 0.15) compared to wild type plants (0.86 ± 0.15) (figure 25). However, the expression level of EcCNA1 is identical in CRC KD and in the empty vector (EV) control (1.36 ± 0.05), this increase is probably not caused by the knock down of EcCRC, but by the general change in mRNA expression upon the viral infection. No significant differences were observed in EcCNA2 expression (0.85 ± 0.16, 0.94 ± 0.21, and 0.87, respectively) and in EcPHX expression (1.15 ± 0.12, 1.00 ± 0.07, and 1.03 ± 0.19, respectively). Additionally, the expression of Ecmir166 A is severely enhanced in the CRC KD samples (1.60 ± 0.22) compared to wild type plants (1.00 ± 0.27) and EV control (0.97) and by this, showing the exact opposite of Atmir166 A expression in *crc-1*.

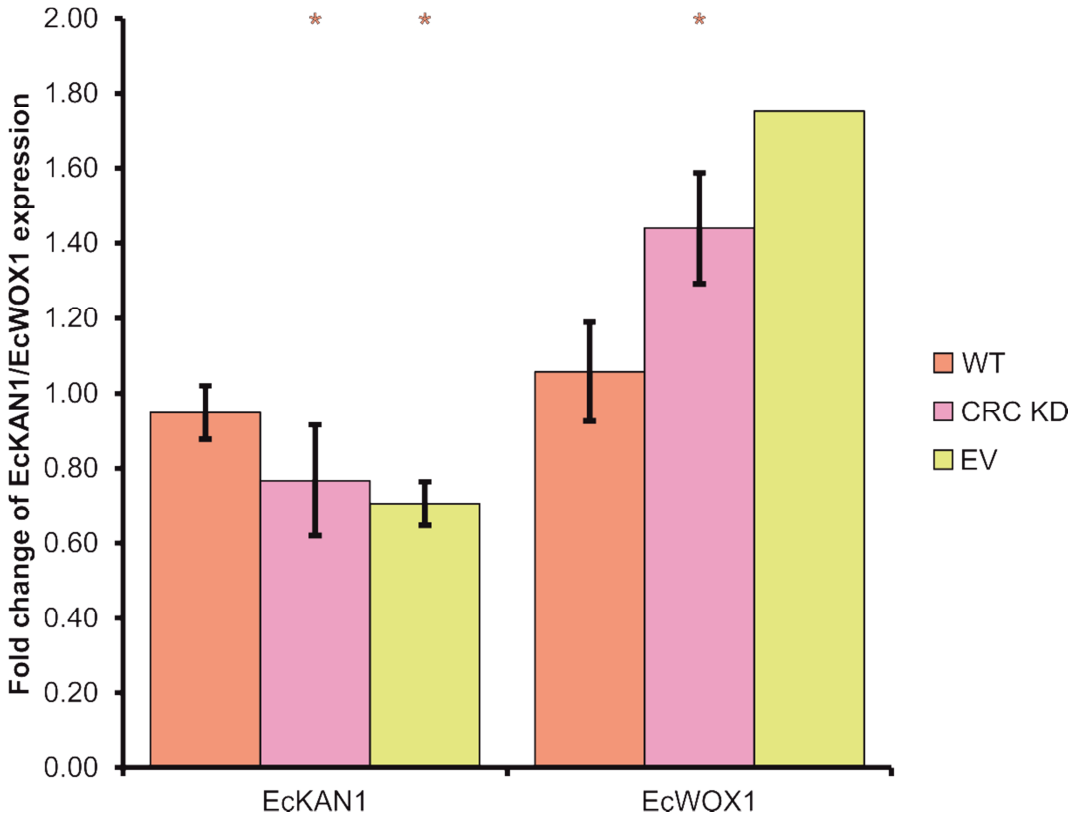

Figure 26: Expression analysis of HD ZIP III members and Ecmir166 A in buds of *E. californica* in wild type, CRC knock down plants, and empty vector control plants. The fold changes of expression were calculated using the ΔΔCt method according to Pfaffl (2001) and error bars represent the standard deviation of the mean (calculated if possible). Asterisks indicate significant ($p < 0.05$) differences compared to the wild type (orange asterisks) or to the empty vector control (yellow asterisks).

The expression of the adaxial regulator EcKAN1 and the middle domain specifying factor EcWOX1 are both changed in the CRC KD lines (figure 26). Whereas, EcKAN1 expression

decreases in CRC KD (0.77 ± 0.15) and in the EV control (0.71 ± 0.06) compared to the wild type (0.95 ± 0.07), the expression of EcWOX1 increases in both CRC KD (1.44 ± 0.15) samples and in the EV control (1.75) compared to the wild type (1.06 ± 0.13).

CRC Has a Second Mode of Non-Cell-Autonomous Action

Rescue of *crc* Mutants by Expression of GFP Tagged CRC

CRC has been shown to regulate the expression of the non-cell-autonomous miRNAs mir165/166. Nevertheless, there might be a second mode of non-cell-autonomous-action. To validate the hypothesis, of a transport of the CRC protein itself, multiple constructs (*proCRC:CRC-GFP*; *proCRC:3xmCherry* and *proCRC:CRC-GFP*; *proCRC:mCherry*) with fluorescent proteins (GFP, mCherry, and 3xmCherry) were generated and introduced into *A. thaliana* Col-0 *crc* plants. Transformed plants were phenotyped to ensure the functionality and the correct expression of the GFP tagged CRC protein (CRC-GFP). Only if the expressed CRC-GFP protein is able to substitute the non-functional endogenous CRC protein, a rescue of the mutant phenotype can be observed. Seven independent Basta resistant transgenic lines of *proCRC:CRC-GFP; proCRC:3xmCherry* (G3mC in the following) but no Basta resistant transgenic lines of *proCRC:CRC-GFP*; *proCRC:mCherry* were generated. In six out of seven lines of G3mC a phenotypical rescue of the *crc* phenotype was observed (figure 27 A).

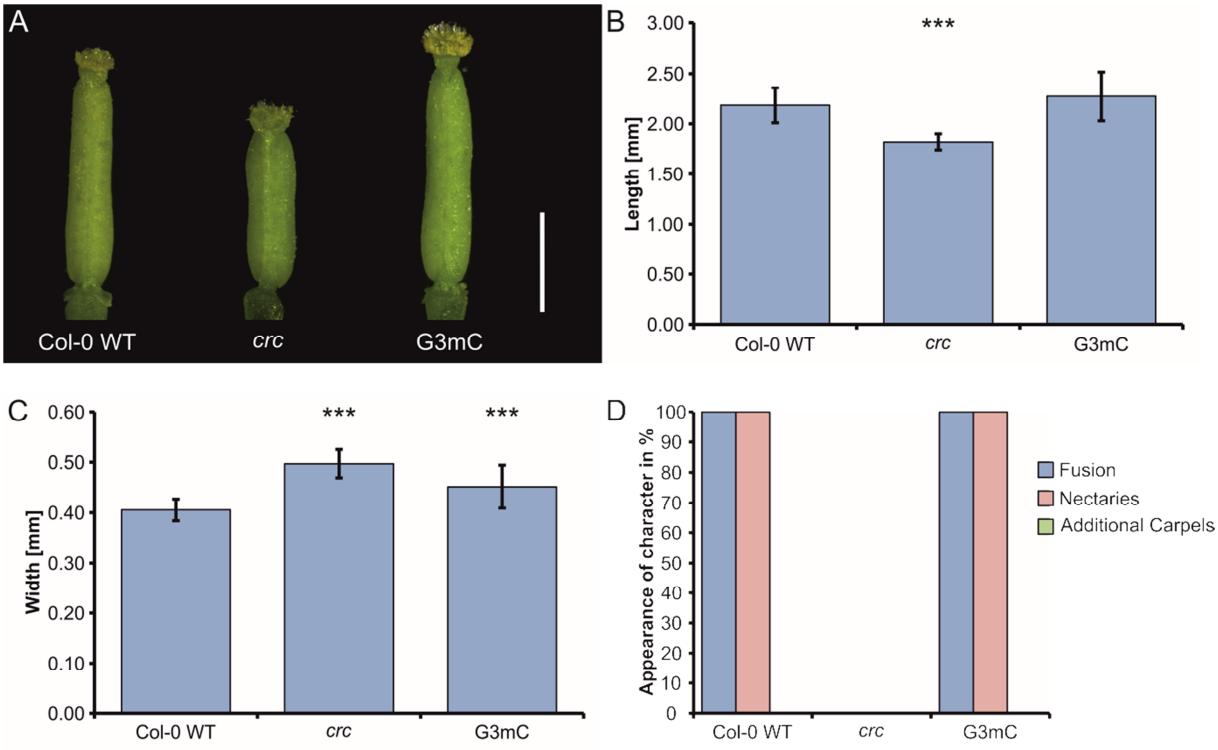

Figure 27: Phenotypic analysis of G3mC expressing *A. thaliana* Col-0 plants. A: Representative gynoecia of Col-0 wild type, *crc*, and G3mC plants. Scale bar represents 1 mm. Statistical analysis of gynoecium length (B), width (C), a summary of other described defects of the *crc* phenotype (D), and the number of carpels in the analyzed gynoecia of the three plant lines. Both, length and width comparisons are mean values with their respective standard deviation. Percent values are shown in D. Student's t-test was applied to compare the wild type gynoecia with the other lines and significant differences were marked with up to three asterisks (* p<0.05, ** p<0.01, *** p<0.001).

Gynoecia of complemented plants showed no significant differences in length (2.27 mm ± 0.24) compared to wild type gynoecia (2.18 mm ± 0.17) and were significantly longer than *crc* gynoecia (1.82 mm ± 0.08) (figure 27 B). While the length of the gynoecia was identical to the wild type, the complemented gynoecia were significantly wider (0.45 mm ± 0.04) than wild type gynoecia (0.41 mm ± 0.02) but thinner than *crc* gynoecia (0.50 mm ± 0.03) (figure 27 C). Gynoecia of complemented plants exhibited also no other typical *crc* characters like split carpels or missing nectaries (figure 27 D). Additional carpels, a *crc* phenotype appearing only in a low frequency, were not observed in any of the analyzed plant lines (figure 27 D).

CRC is Localized Throughout the Developing Gynoecium

In order to analyze the CRC distribution in the gynoecium, whole inflorescences were mounted in agarose and dissected with a micro scalpel. The sections were then analyzed using a confocal laser scanning microscope (CLSM). The distribution of CRC-GFP and 3xmCherry in the developing gynoecia was observed in gynoecia of different floral stages to establish a timeline of CRC localization. Even though, 3xmCherry was not expressed and thus was not detectable with the CLSM, the localization of CRC-GFP was possible. In the youngest observed gynoecia (stage 7-8), CRC-GFP is present in the nuclei of all abaxial cells with the strongest staining in the abaxial epidermis (figure 28 A-E). Additionally, CRC-GFP is localized to nuclei in adaxial cell layers (figure 28 A). Only in the inner most cells, which give rise to the carpel margin meristems (CMMs), almost no CRC-GFP is present. In addition both CMMs are still separated as indicated by the distribution of chloroplasts and the transmission image (figure 28 C and D). The presence of CRC-GFP is then restricted to purely abaxial cell layers around the circumference of the gynoecium in stage 9 (figure 28 F-J); while the two adaxial CMMs fuse and form the septum in the middle of the gynoecium. CRC-GFP fluorescence persists through stage 10 – 11 (figure 28 K-O), as it can be still observed in the abaxial epidermis and the two cell layers below the epidermis. Additionally, it is present in the future valves, valve margins, and replum (figure 28 K). Only after this stage, CRC-GFP is not detectable in the abaxial epidermis anymore and only chlorophyll fluorescence is detectable while ovule and replum development is nearly finished shortly before anthesis (stage 11-12, Appendix figure 36).

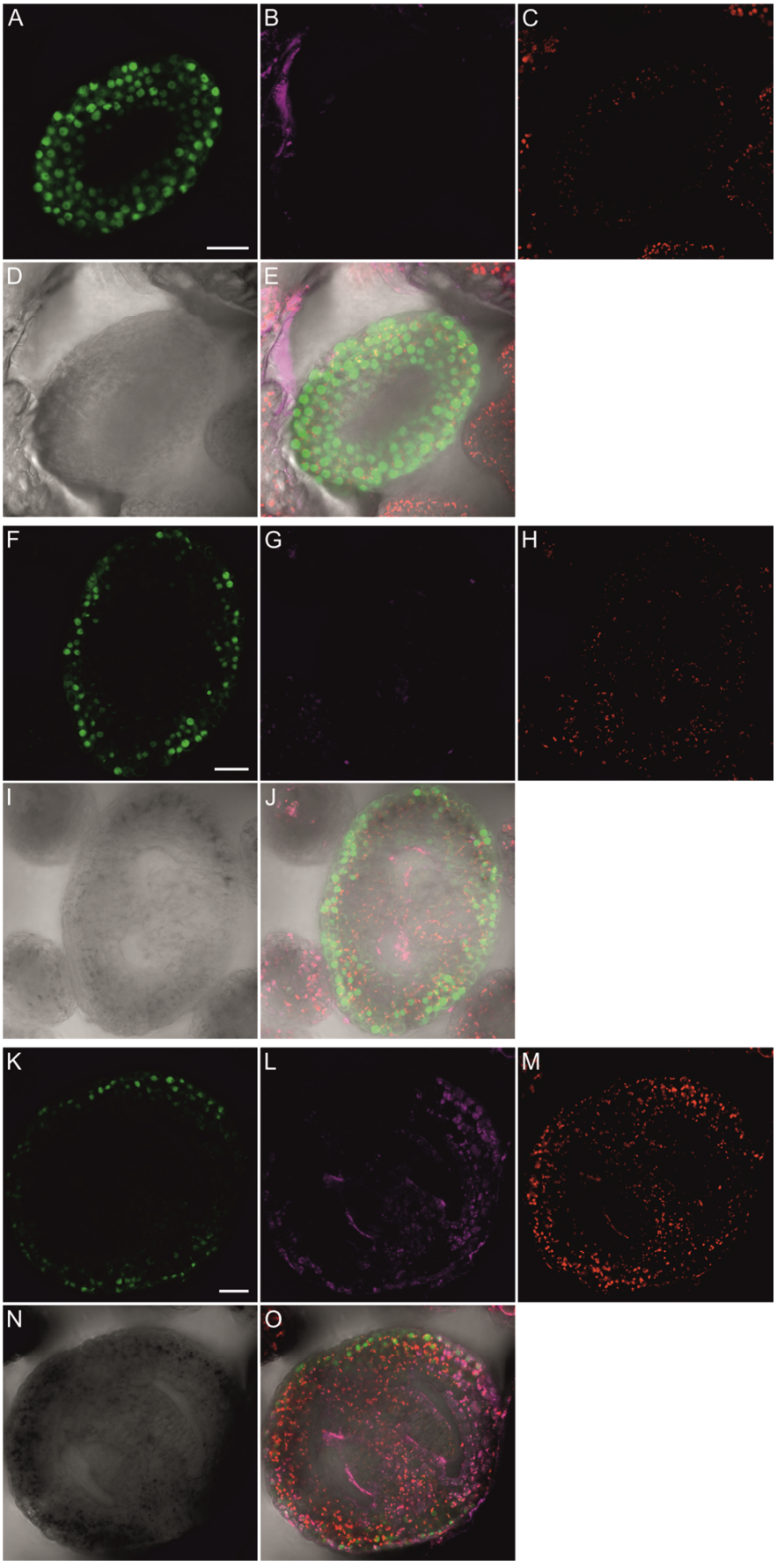
A
B
C
D
E
F
G
H
I
J
K
L
M
N
O

Figure 28: Distribution of CRC-GFP in developing gynoecia. CRC-GFP, 3xmCherry, and chlorophyll were detected by CLSM. In addition a transmission image was taken and an overlay was made out of the different individual images. False colors were assigned to GFP (green), 3xmCherry (magenta), chlorophyll (red), and transmission (grey). Gynoecia in three different stages are shown: A-E, stage 7-8; F-J, stage 9; K-O, stage 10-11. Scale bars represent 20 µm.

Discussion

CRC Expression Is Tightly Regulated

CRC is expressed in a complex spatial and temporal manner. In early floral developmental stages it is expressed in two lateral stripes in the two valves, then after carpel fusion, around the circumference of the gynoecium and in four internal stripes. Only in later stages, CRC expression ceases, first in the four stripes and in the future replum and then in the circumference (Bowman and Smyth, 1999). This expression pattern cannot solely rely on MADS box transcription factors and LEAFY, which have already been shown to bind to specific regions in the CRC promoter (Lee *et al.*, 2005a). The Y1H analysis in this study revealed 119 additional putative regulators of CRC expression. Multiple of those regulators have numerous binding sites in the CRC promoter and bind in every region (A-E) and between (figures 16 and 17). As the different conserved regions of the CRC promoter have different functions (Lee *et al.*, 2005a), the distribution of the identified transcription factor binding sites might help to discriminate between activators or repressors of CRC expression. The A region of *proCRC* is containing general transcription start motifs like the TATA box and has been shown to be essential for the transcription of *CRC* (Lee *et al.*, 2005a), thus transcription factors binding in the A region might recruit the necessary factors for transcription. Especially the NF-Y family, a group of trimeric or heterodimeric acting pioneer transcription factors is known to recruit other transcription factors to promoter regions (Oldfield *et al.*, 2014), and might form the scaffold for recruiting further transcription factors. The remaining regions are specifying the exact position of CRC expression. Regions C and E are necessary for proper expression in the carpel but allow CRC expression in other floral tissues, whereas regions B and D negatively regulate CRC expression and restrict CRC expression to parts of the gynoecium and exclude CRC expression from other floral organs (Lee *et al.*, 2005a).

Activation and Repression of CRC Expression by Flower Developmental Regulators

As not all 119 transcription factors can be discussed in detail, the discussion will be limited to the most promising and best described regulators, which were chosen based on information in literature and temporal and spatial expression in the carpel. The auxin response factor ETT has been shown to activate the expression of YABBY genes like FIL in leaves (Garcia *et al.*, 2006). This fits to the Y1H screen data as ETT binding sites can be found in region E (*in silico*) and in regions E and C (screen distribution) with both regions supporting CRC expression (figures 16 and 17). Additional ETT binding sites in fragments F4, F6, F7 overlap with the repressing regions D and B but an exact position cannot be given and thus they might be in the non-conserved regions. Similar to this, the zinc finger protein JAGGED (JAG) binds to region E and might also activate CRC expression. Previous studies have shown that JAG acts together with FIL and YAB3 to activate the expression of FUL in the valves (Ohno *et al.*, 2004; Dinneny *et al.*, 2005), antagonistically to REPLUMLESS (RPL or PENNYWISE/PNY) and KNAT1/BP which suppress FUL expression and also JAG and FIL expression in the future replum (Dinneny *et al.*, 2005; González-Reig *et al.*, 2012). Interestingly, this repression effect is delayed for CRC. Whereas, FIL is expressed in two horse shoe like domains in the lateral regions of the gynoecium, which become later the valves (Siegfried *et al.*, 1999), CRC is expressed around the circumference of the developing gynoecium and its expression ceases in the replum in stage 10, shortly before the visual differentiation of valves and replum in stage 12 (Bowman and Smyth, 1999). However, BP and RPL/PNY cannot be clearly assigned to be activators or repressors, as both bind throughout *proCRC* (figures 16 and 17). The antagonistic to RPL acting FUL is present throughout the development of the gynoecium and determines valve identity but it is also necessary for the post fertilization elongation of the gynoecium/developing fruit (Gu *et al.*, 1998; Ferrandiz *et al.*, 2000). Thus, FUL could be an activator of CRC expression in the valves but similar to RPL, there are binding sites not only in region E but also in B. In addition, a recent ChIP-SEQ analysis of FUL targets did not identify CRC among them (Bemer *et al.*, 2017), thus the FUL binding sites in *proCRC* are either a random occurrence or chromatin remodelers have turned the FUL binding sites inaccessible for the FUL protein. Especially the last option seems likely; as gynoecia and fruits after stage 12 were analyzed in which CRC expression is only present in the not

collected nectaries and as heterochromatin regions are underrepresented in ChIP-SEQ analyzes (Teytelman *et al.*, 2009; Chen *et al.*, 2012). HAF is likely a negative regulator of CRC expression as its appearance in the adaxial carpel tissues (septum and placenta) commences with the decline of CRC expression in the four interior stripes during stages 9-10. According to PlantPAN, there are HAF binding sites in regions A and B but there is no comparison to the Y1H screen possible as HAF was detected using the full length promoter (figure 16).

Table 10: Summary of the classification of some identified putative CRC regulators into activators of CRC expression and repressors of CRC expression. Transcription factors marked with "unclear" showed binding sites in both activating regions of proCRC and repressing regions.

Gene identifier	Gene name	Putative role
AT1G23420	INO	Activator
AT1G24260	SEP3	Activator
AT1G68480	JAG	Activator
AT2G03710	SEP4	Activator
AT2G26580	YAB5	Activator
AT2G33860	ETT	Activator
AT2G35270	GIK	Activator
AT4G11070	WRKY41	Activator
AT4G36900	DEAR4	Activator
AT4G40060	ATHB16	Activator
AT5G04340	ZAT6	Activator
AT5G65310	ATHB5	Activator
AT1G10120	CIB4	Repressor
AT1G25330	HAF	Repressor
AT1G68920	CIL1	Repressor
AT3G07340	CIB3	Repressor
AT3G25710	TMO5	Repressor
AT3G25730	EDF3	Repressor
AT4G28790	bHLH23	Repressor
AT1G26310	CAL	unclear
AT1G59750	ARF1	unclear
AT3G27010	TCP20	unclear
AT3G60390	HAT3	unclear
AT3G61970	NGA2	unclear
AT4G08150	KNAT1/BP	unclear
AT4G16780	HAT4	unclear
AT4G38960	BBX19	unclear
AT5G02030	RPL/PNY	unclear
AT5G37020	ARF8	unclear
AT5G60910	FUL	unclear

Taken together, the assumption that activators or repressors of CRC expression can solely be discriminated based on their binding site in *proCRC* cannot universally be confirmed. Even though, the discrimination of the bound transcription factors into activators or repressors is possible for a few transcription factors (see table 10), it needs to be supported by other experimental data like qRT-PCR expression data, GUS staining's of reporter lines crossed with mutants of the identified transcription factors, or RNA *in situ* hybridization. Preliminary data about the *proCRC* activity in *bbx19* and *cil1* mutants was obtained via GUS stainings (Appendix figure 33), but so far no differences were observed compared to wild type plants. However, the GUS staining intensity need to be adjusted for further expression analyzes. Only then it is possible to get an overall better view of CRC regulation.

Nevertheless, a general description is still possible. Many of the identified proteins are functionally annotated (figure 13) and take part in important developmental steps during plant development. The most obvious category is "floral development" as CRC is only expressed in the gynoecium. Lee *et al.* (2005a) and Ó'Maoiléidigh *et al.* (2013) identified MADS box transcription factor binding sites in the E region of *proCRC*. The here performed Y1H screen was able to identify a SEP3 binding site in region E, but also a SEP3 and a SEP4 binding site in region C. As SEP proteins act as a "molecular glue" in the MADS box protein tetrads (Immink *et al.*, 2009), these binding sites can be seen as hubs for other MADS box proteins. Interestingly, MADS tetrads, once bound to DNA, are likely to act as histone substitutes, form nucleosome like complexes, and recruit chromatin remodelers to their binding site (Theißen *et al.*, 2016). Additionally, the protein ULTRAPETALA 1 (ULT1) binds to *proCRC*. ULT1 probably binds to DNA with its SAND (Sp100, AIRE-1, NucP41/75, DEAF-1) domain but it is not a transcription factor per se (Bottomley *et al.*, 2001), as it exhibits also a trithorax group (Carles and Fletcher, 2009). Thus, it can mediate the removal of repressive histone H3 lysine methylation marks (H3K27me3) or hinder their newly positioning and by this activating the expression of its target genes like AG (Carles and Fletcher, 2009). By this pathway, ULT1 could not just activate AG expression but also CRC expression, partially through direct interaction with the CRC promoter, as indicated by the Y1H screen, and also by activing AG expression which then leads to the expression of CRC (Bowman and Smyth, 1999; Lee *et al.*, 2005a; Ó'Maoiléidigh *et al.*, 2013). Interestingly, CRC and ULT1 act redundantly to terminate the floral meristem (Prunet *et al.*, 2008). Counteracting the ULT1 activity is GIANT KILLER (GIK), a AT-hook type DNA binding protein (Ng *et al.*, 2009). GIK

expression is regulated by AG and it is regulating different genes involved in carpel development like ETT and CRC. The expression of both of them is repressed by GIK (Ng *et al.*, 2009) and in addition GIK, like ULT1, influences the posttranslational modification of histones and it is regulating the placement of the repressing histone mark H3K9me2 in the ETT promoter (Ng *et al.*, 2009).

CRC Expression Is Regulated by Developmental and Growth Related Genes

A combination of floral developmental and of growth related genes could also control CRC expression (figure 13). Both NGATHA2 (NGA2) and TEOSINTE-LIKE1, CYCLOIDEA, PROLIFERATING CELL FACTOR1 (TCP) 1 bind in activating regions of *proCRC* (region E and C, respectively) and both are involved in the length growth of lateral organs (Ballester *et al.*, 2015; Lee *et al.*, 2015), with NGA2 having special functions in the formation of style and stigma (Alvarez *et al.*, 2009; Trigueros *et al.*, 2009). As *crc-1* gynoecia are typically shorter than wild type gynoecia, CRC has to be involved in the regulation of longitudinal growth of the gynoecium. Thus, both genes might act through CRC to control this longitudinal growth. Similar to TCP1/NGA2, the growth associated GROWTH FACTOR 7 (GRF7) is a member of the small GRF family which positively influences growth of leaves and flowers in *A. thaliana (JH Kim et al., 2003)*. Thus, beside TCP1/NGA2, also GRF7 could have an influence on the length of the developing gynoecium by regulating the expression of CRC. While these members of the growth category influence cell division/cell elongation after the formation of the lateral organ, BASIC PENTACYSTEINE 2 (BPC2) is directly influencing cell divisions in the SAM, inflorescence meristem, and floral meristem by regulating the expression of the KNOX I transcription factor STM (Santi *et al.*, 2003; Simonini and Kater, 2014). Triple mutants of *bpc1*, *bpc2*, and *bpc3* exhibit extra floral organs and their gynoecia consist out of up to three carpels (Simonini and Kater, 2014), showing a delayed termination of the floral meristem as seen in some *crc-1* flowers. Interestingly, a link between BPCs and YABBY genes had been established previously as BPCs bind also to the promoter of INO (Meister *et al.*, 2004). Another direct influence on meristem activity is HAIRY MERISTEM (HAM). HAM confines the expression of CLAVATA 3 (CLV3), a repressor of WUSCHEL (WUS) expression, to the

uppermost cell layers of the SAM, whereas HAM itself is expressed in the basal part of the SAM (Zhou *et al.*, 2018). By this confinement, HAM allows WUS expression in the central zone of the SAM and further formation of stem cells. As CRC terminates the floral meristem by repressing WUS expression, HAM could delay CRC expression until the carpel primordium is formed, thus preventing a premature meristem termination.

In the same Y1H screen of *proINO* (Meister *et al.*, 2004), ZINC FINGER OF ARABIDOPSIS THALIANA 6 (ZAT6), a cold induced gene which modulates responses to stresses like heavy metal uptake, biotic stress, and cold stress (Shi and Chan, 2014; Shi *et al.*, 2014; Chen *et al.*, 2016), was identified. As ZAT6 appears also in the Y1H screen of *proCRC*, it seems that ZAT6 is regulating the expression of YABBY genes, at least the floral expressed ones. Yet, there is no link between ZAT6 and flower development which might explain its role in flower development.

The Y1H analysis has identified many putative regulators of CRC expression, exceeding the limited numbers of MADS box transcription factors and LFY which have been previously described to regulate CRC expression. However, fine tuning of the CRC expression is not possible with these few regulators but with the newly identified more than 100 putative regulators the proper temporal and spatial regulation of CRC expression is possible in the developing gynoecium.

The Co-expression of Co-functional Genes Reveals High Connectivity of CRC to Important Aspects of Flower Development

CRC is integrated in different regulatory pathways during flower development like the termination of the floral meristem (Bowman and Smyth, 1999; Prunet *et al.*, 2008; Sun and Ito, 2015). Members of these pathways or in general in co-functional networks are often co-expressed and thus co-expression analysis can help to predict the function of a gene (Usadel *et al.*, 2009). Even though, co-expressed genes are not necessarily co-functional (Usadel *et al.*, 2009), by using a functional annotated “guide-gene” like CRC in a well-studied model organism this problem can be bypassed. Three co-expression data sets (figures 18, 19, and

20) were obtained in this work but a network analysis was only possible with the data retrieved from PlaNet, as Expression Angler and the RNA-seq analysis did not construct co-expression networks. However, in all three co-expression databases, CRC was co-expressed to putative regulators that were identified in the Y1H analysis of *proCRC*. The co-expression analysis with Expression Angler identified 1567 co-expressed genes to CRC with 161 of those being transcription factors. Compared to this, PlaNet identified, with stricter criteria and a different dataset of microarrays (Schmid *et al.*, 2005; Mutwil *et al.*, 2011), 87 co-expressed genes, including 26 transcription factors. Of these 26 transcription factors, 12 are shared between the two data sets (Appendix table 11). The more thorough RNA-seq analysis was able to identify 34 putative regulators of CRC to be co-expressed to CRC out of the 7577 co-expressed genes with 2 being shared between the RNA-seq and the co-expression network.

When using the co-expression network as starting point, many co-expressed putative CRC regulators and co-expressed transcription factors can be grouped into different functional modules. The first module is the carpel module (figure 20) with its hub node SPL9. Interestingly, SPL9 has no described effect on carpel development but on the regulation of flowering time in *A. thaliana* (Schwarz *et al.*, 2008). Nevertheless, the other nodes in this module, except for MYB116, have important functions during carpel development. NO TRANSMITTING TRACT, a C2H2 zinc finger protein, and the bHLH protein HALF FILLED, are both necessary for the development of the transmitting tract (Crawford *et al.*, 2007; Crawford and Yanofsky, 2011), a special region of the false septum that allows the pollen tubes to grow easily through and reach the ovules. Mutations in these genes disable partially or completely the development of the transmitting tract and thus are reducing the number of fertilized ovules. This is similar to *crc-1* mutants in which the septum is “patchy” as random parts of it are not developed (Alvarez and Smyth, 1999; Bowman and Smyth, 1999; Alvarez and Smyth, 2002). HAF is also present in the two other co-expression analyzes, even though it is positively correlated to CRC in the Expression Angler analysis and negatively in the RNA-seq analysis (figure 18 and 19). Interestingly, FUL and KNAT1/BP, two other putative regulators, are negatively correlated to CRC expression in the RNA-seq analysis. Both proteins showed indications of activation and repression of CRC expression and combined with the negative correlation of CRC expression, a role as repressors of CRC expression might be fitting.

The second module, the wax module, consists only of SHINE 1 (SHN1), an AP2/EREBP family member. SHN1 influences the cuticular wax biosynthesis by activating 3-KETOACYL-COA SYNTHASE 1 (Broun *et al.*, 2004). Similar to this, CRC is regulating members of the 3-KETOACYL-COA SYNTHASE family. Several KCS are weaker expressed in a *crc-1* background (Han *et al.*, 2012) and CRC physically interacts with the promoter regions of KCS7 and KCS15 and activates their expression (Han *et al.*, 2012; Gross *et al.*, 2018). The same study showed that AP1 is regulating the same KCS as CRC, allowing the addition of AP1 to the wax module.

CRC is a general regulator of floral and extra floral nectary development in the core eudicots (Lee *et al.*, 2005b). Additional to CRC, BLADE ON PETIOLE 1 (BOP1) and BOP2 are also involved in nectary development in *A. thaliana* (McKim *et al.*, 2008). Plants with mutations in both genes do not develop nectaries but small protrusions at the base of the stamens. Similar to AP1, BOP1 and BOP2 can also be assigned to a second module: floral meristem regulation. BOP1/2 are specifying organ boundaries in lateral organs and inhibit the action of PNY and POUND-FOLISH (PNF) in the SAM, and thus preventing the transition of the SAM into an inflorescence meristem (Khan *et al.*, 2015).

The last and biggest module, which has a connection to CRC, is the floral meristem regulatory module. One of the first neighbors of CRC in this module is AP1. During floral induction, FT is activating AP1 and LFY expression in the SAM which leads to the transformation of the SAM into an inflorescence meristem (Wigge *et al.*, 2005; Abe *et al.*, 2005). Additionally, AP1 strengthens the action of STM and together they promote the activity of the floral meristem and maintain its identity (Smith *et al.*, 2011; Roth *et al.*, 2018). Parts of this interaction are the BEL1-like HOMEODOMAIN (BELL) proteins RPL/PNY and PNF (Byrne *et al.*, 2003; Kanrar *et al.*, 2008), with the latter one being another direct neighbor of CRC in the co-expression network. Even though, these two proteins dimerize with STM, only PNY is mandatory for the correct function of STM (Kanrar *et al.*, 2008). However, PNF is restricting the action of different organ boundary genes like BOP1/2, and ARABIDOPSIS THALIANA HOMEOBOX PROTEIN1 (ATH1), to promote the meristematic activity of the IM/FM (Khan *et al.*, 2015). Additionally, PNY and PNF negatively regulate mir156 which post-transcriptionally regulates three members of the SPL family: SPL3, FTM6/SPL4, and SPL5 (Lal *et al.*, 2011). The remaining first neighbor, REM18, is part of the REPRODUCTIVE MERISTEM family, a group of highly redundant B3 transcription factors, to which also REM23 and

REM24 belong (Romanel *et al.*, 2009). In contrast to REM23 and REM24, REM18 is regulated by LFY and also co-expressed with LFY (Mantegazza *et al.*, 2014). However, LFY is neither appearing in the PlaNet generated co-expression network, nor in the co-expression data retrieved from Expression Angler and the RNA-seq. This is either based on stricter criteria, as additional to a Pearson correlation coefficient a highest rank cut off was applied in PlaNet or based on using microarray data from different developmental stages. Interestingly, LATE MERISTEM IDENTITY2 is part of the co-expression network. LMI2 is regulated by LFY and it activates by interacting with LFY the expression of AP1 (Pastore *et al.*, 2011). Remaining transcription factors like CUP-SHAPED COTYLEDON1 and CUC3 are NAC transcription factors that regulate the formation of lateral organ boundaries, by restricting the proliferation and the differentiation in these regions (Vroemen, 2003). Furthermore, both genes are upregulated by STM (Spinelli *et al.*, 2011). In addition with being co-expressed to CRC, CUC3 binds in *proCRC* and probably regulates CRC expression. FANTASTIC FOUR 2 (FAF2), a putative transcription factor, is repressing WUS action in the floral meristem and supports the termination of the floral meristem (Wahl *et al.*, 2010). Thus, it works in concert with CRC which acts redundantly to RBL, SQN, and ULT1, which is also co-expressed to CRC (figure 19), to terminate the activity of the floral meristem via WUS down regulation. Antagonistically to CRC could act the transcriptional co-repressors SEUSS and LEUNIG (Franks *et al.*, 2002). Both proteins are putative regulators of CRC expression and are known to interact with YABBY proteins in leaves (Stahle *et al.*, 2009). They typically restrict AG expression in the outer floral whorls but also prevents meristem termination by sustaining STM expression (Bao *et al.*, 2010).

All in all, CRC and many of its transcriptional regulators are part of the same co-expression network, which resembles multiple important developmental modules during flower development and especially during the development of the gynoecium. Additionally, each module resembles a part of CRC action and relates to all phenotypes appearing in a *crc-1* mutant. Even though, there are differences in the different co-expression analyzes through different experimental setups all three analyzes have CRC's co-expression with its putative regulators in common.

CRC Is Tightly Integrated in Two Major Regulatory Networks

Leaves and flowers are both lateral plant organs and the different floral organs (sepals, petals, stamens, and carpels) have probably evolved from leaves (Goethe, 1790), as one can observe in *sep1/2/3/4* quadruple mutants in which all floral organs are transformed into leaf like structures (Ditta *et al.*, 2004). Thus, regulatory circuits determining such fundamental principles as adaxial-abaxial polarity should be at least similar in both leaves and floral organs. Even though, leaves and especially carpels are quite different organs, the key elements of the adaxial-abaxial polarity regulation (*KAN* genes and HD ZIP III genes) are present in the developing carpel (Kerstetter *et al.*, 2001; Prigge *et al.*, 2005; Jung and Park, 2007). Nevertheless, certain regulators have additional functions and additional regulators like CRC are involved (figure 29, stages 7-9). The vegetative YABBY proteins FIL, YAB2, YAB3, and YAB5 are involved in establishing the abaxial side of leaves. In carpels, CRC is acting in concert with them. As shown by expression studies of putative CRC target genes involved in adaxial-abaxial polarity and supported by the presence of YBMs in their respective promoter regions (figures 21-24), CRC is activating the expression of WOX1 and mir165/166 in the developing carpels, similar to FIL/YAB3 in leaves (Nakata *et al.*, 2012; Tatematsu *et al.*, 2015). By integrating the expression data with previous analyzes of *crc-1 kan2* double mutants, which exhibit an increased activity range of HD ZIP III genes and phenotypic changes like ectopic ovules (Eshed *et al.*, 1999), it becomes obvious that CRC supports KAN function by activating the expression of *KAN1* and *KAN2* and, additionally, by physically interacting with both proteins in Y2H analyzes, similar to FIL and INO (Trigg *et al.*, 2017; Herrera-Ubaldo *et al.*, 2018). A controversial result is the reduced expression of the HD ZIP III genes *CNA* and *PHV* in *crc-1* mutants (figure 22). As the degree of *mir165/166*, *KAN1/2* and *WOX1* expression is reduced in *crc-1* plants, the expression of HD ZIP III genes should increase instead of decrease. An increase in HD ZIP III activity would ultimately lead to an adaxialization of carpel tissue. However, if the expression of the most important regulators (*KAN* genes, mir165/166, HD ZIP III's) is identically reduced, the complete network might retain its equilibrium and fulfil its function and none or only minor phenotypes will arise as seen in the *crc-1* mutant. This argues for a minor or supportive role of CRC in the adaxial-abaxial network. Nevertheless, the magnitude of CRC's role in this network does not explain the reduced expression of the HD ZIP III genes. *CNA* and *PHV* expression is significantly

reduced in *crc-1* plants and *ATHB8* and *REV* expression is also slightly, yet not significantly, reduced. In contrast to the leaf regulatory network in which there is no direct regulatory connection between e.g. FIL and HD ZIP III genes (Bonaccorso *et al.*, 2012), there has to be a direct or indirect regulation of the HD ZIP III genes by CRC, independent of mir165/166, WOX1, and KAN1-3. The direct regulation is supported by the presence of multiple YBMs in the promoters of the HD ZIP III proteins (figure 24). Shamimuzzaman and Vodkin (2013) identified three putative binding motifs of YABBY proteins in *Glycine max* (soy) and Franco-Zorrilla *et al.* (2014) identified a fourth binding motif through protein-binding microarrays. Yet, only the first three motifs (YBM1-3) have been shown to effect gene expression in *O. sativa* and *A. thaliana* (Yang *et al.*, 2016; Yamaguchi *et al.*, 2017; Yamaguchi *et al.*, 2018). Four out of five HD ZIP III genes exhibit these YBMs in their respective promoter and the two with the highest number of YBMs (*CNA* and *PHV*) are the ones with the most drastic changes in expression in *crc-1* plants. Taken together, these results indicate a direct regulation of HD ZIP III genes by CRC, parallel to the regulation through mir165/166, KAN1-3, and WOX1.

During leaf development, the expression of *KAN1* is restricted to the abaxial side, in contrast to this, the *KAN1* expression first takes place in the abaxial side of carpels (figure 29, stage 7-8) and in later developmental stages (figure 29, stage 9), the *KAN1* expression domain switches to the adaxial side (Kerstetter *et al.*, 2001). As *KAN1* expression moves from the abaxial side to the adaxial side, KAN1 interacts with its former repressor ULT1 to establish the apical – basal polarity of the developing carpel (Pires *et al.*, 2014). This change of expression sides follows the appearance of the four internal stripes of CRC expression during stage 7-8 (Bowman and Smyth, 1999). Hence, CRC could activate *KAN1* expression in adaxial tissues, restarting the self-sustaining feedback loop of *KAN1* expression; this incorporates CRC into the apical-basal regulatory network. This network controls the structuring of the developing carpel into stigma, style, ovary, and gynophore and there are overlaps, other than KAN1 and ULT1, with the adaxial-abaxial network. The auxin response factor ETT and the bHLH protein SPATULA (Sessions *et al.*, 1997; Heisler *et al.*, 2001).

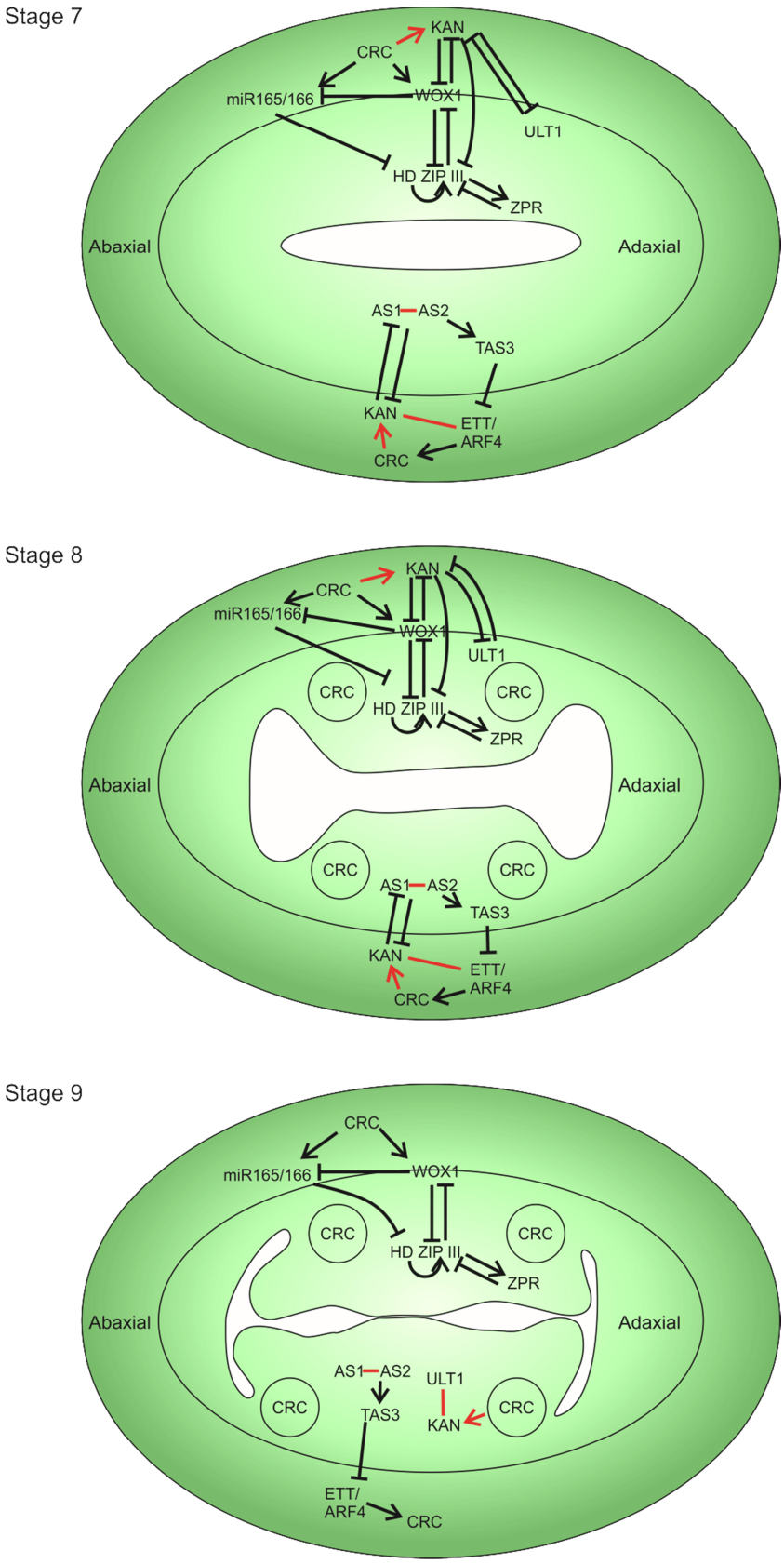

Figure 29: Putative determination of adaxial–abaxial identity in the developing gynoecium. Three stages (7-9) of development are shown. Red lines represent a physical interaction. Pointed arrows indicate enhancing the action of the target, by activation of transcription. Blunt arrows indicate repression of the target either by repressing its transcription or by enhancing its post-transcriptional degradation. Based on Merelo *et al.*

(2017), Reinhart *et al.* (2013), Tatematsu *et al.* (2015), Garcia *et al.* (2006), Moubayidin and Ostergaard (2014), and updated with the here presented results.

Whereas, SPATULA is necessary for style and stigma development (Heisler *et al.*, 2001), ETT controls the formation of the ovary by repressing SPT expression in this region (Sessions *et al.*, 1997; Alvarez and Smyth, 1998). Both genes are also connected to CRC by multiple means. ETT has been previously shown to induce the expression of YABBY genes in leaves (Garcia *et al.*, 2006), and it also binds in the CRC promoter as the Y1H analysis has shown (figures 16 and 17). SPT in contrast, did not appear in the Y1H screen, but previous studies have shown a genetic interaction between both genes (Alvarez and Smyth, 1999, 2002). Alvarez and Smyth (1999) demonstrated that, *crc-1 spt* double mutants show an almost complete separation of the two carpels; whereas both single mutants show only apical splits.

In order to explain the pattering of the gynoecium, Nemhauser *et al.* (2000) hypothesized that auxin acts as a morphogen through an apical-basal auxin gradient. And soon the YUCCA proteins were found. YUCCAs are flavin monooxygenases, involved in auxin biosynthesis, and thus are able to increase the amount of synthesized auxin, causing an auxin maximum at the apex of the gynoecium (Zhao *et al.*, 2001; Cheng *et al.*, 2006). Polar auxin transport by PIN proteins creates an apical-basal auxin gradient then, which leads to the differentiation of carpel tissue into stigma, style, ovary and gynophore. However, different approaches to visualize this gradient with auxin sensors (e.g. DR5 or DII sensors) failed (reviewed in Larsson *et al.* (2013)).

Even though, there is probably no apical-basal auxin gradient, auxin is still a major morphogen during carpel development and newer findings suggest not one, but multiple local auxin maxima (as reviewed in Larsson *et al.* (2013)). These local auxin maxima are in the style, the lateral regions of the valves and the gynophore (Larsson *et al.*, 2014). CRCs connection to auxin was established with the discovery of the rescue of *crc-1* mutants by the application of ectopic auxin by Ståldal *et al.* (2008). Recent studies identified two additional links of CRC to auxin mediated gynoecium differentiation. The expression of *TRN2*, a plasma membrane located tetraspannin regulating auxin homeostasis, is repressed by CRC and at the same time CRC activates the expression of *YUC4* (Yamaguchi *et al.*, 2017; Yamaguchi *et al.*, 2018). Additionally, CRC interacts with ARABIDOPSIS RESPONSE REGULATOR12 (ARR12),

a part of the cytokinin signaling pathway and inducer of *WUS* expression, acting antagonistic to auxin by repressing the expression of *YUC4*, other YUCCAs, and other auxin biosynthesis genes (Meng *et al.*, 2017; Zhang *et al.*, 2017; Yan *et al.*, 2017; Dai *et al.*, 2017; Herrera-Ubaldo *et al.*, 2018). As CRC is activating the expression of *YUC4*, it can be assumed that CRC counteracts the action of ARR12 by interacting with it, with the result of an increasing auxin concentration in the young gynoecium and inhibited cytokinin response. This concludes in a lower WUS activity and ends with the termination of the floral meristem.

CRC is a supporting member of the adaxial-abaxial regulatory network, enhancing the expression of the major abaxial regulators, the *KAN* genes, and regulates other abaxial and also adaxial regulators. It is also connected to the apical-basal regulatory network through ETT, KAN1, ULT1, and SPT and modulates auxin concentration and distribution. By this it intertwines the two regulatory networks further. The change of *KAN1* expression from abaxial to adaxial and the presence of CRC in the same regions – the presence of two abaxial factors in adaxial tissues – are highly different to leaves. Hence, a model of gynoecium development with gynoecium development divided into two phases can be proposed: An early leaf like phase and a late derived carpel specific phase. The early leaf like phase starts with carpel initiation in stage 5. In this phase the basic structure of the two carpels is formed. Also auxin distribution during the beginning of this phase is similar to leaves (Larsson *et al.*, 2014). The early phase ends with the start of CRC expression in the four adaxial stripes and the activation of the carpel margin meristem (CMM), which is a WUS independent meristem (reviewed in Reyes-Olalde *et al.* (2013)), during stages 7-8. In the second phase, the CMM forms other carpel specific structures like the transmitting tract and most importantly ovules. Additionally, the establishment of the three dimensional structure of the gynoecium finishes with the formation of style and stigma. The formation of style and stigma is another carpel specific process, as the gynoecium loses its bilateral symmetry in these tissues and establishes, based on a circular auxin distribution that is established in stage 9, a radial symmetry (Moubayidin and Ostergaard, 2014).

CRC plays a supporting role in the adaxial-abaxial network but it is also involved in the apical-basal patterning and interconnects both important regulatory systems during carpel development and thus earns the title “major carpel developmental regulator”.

CRC's Function in the Adaxial-Abaxial Network Is Not Conserved in *E. californica*

The aforementioned adaxial-abaxial regulatory network model is mostly based on work with *A. thaliana* and already other models like the ABCE model needed to be adapted to basal eudicot species (as reviewed in Soltis *et al.* (2007)) and to monocot species (Wu *et al.*, 2017).

E. californica is a basal eudicot plant from the order of Ranunculales and as such it is used as a model plant between eudicots and monocots. Furthermore, it is easy to cultivate, diploid, and transcriptomic and genomic sequence data are available (Becker *et al.*, 2005; Hori *et al.*, 2018). The gynoecium of *E. californica* consists out of two fused carpels, similar to *A. thaliana*, but it does not develop a false septum. Even though, there is a growing amount of functional data about genes in *E. californica*, little is known about the adaxial–abaxial/apical-basal networks, compared to *A. thaliana*. As there are only few mutants of *E. californica* available (Lange *et al.*, 2013) and stable transformation is possible but laborious (Tekleyohans, 2014), functional analysis via gene knock-down through VIGS is commonly used (Wege *et al.*, 2007). CRC knock-down plants show similar phenotypes as *crc-1* mutants in *A. thaliana*. Their gynoecia are sometimes slightly split in the apical part and the termination of the floral meristem is impaired (Orashakova *et al.*, 2009). Hence, CRCs position in the adaxial-abaxial network might be similar. However, the qRT-PCR analysis revealed important differences between both organisms (figures 25 and 26).

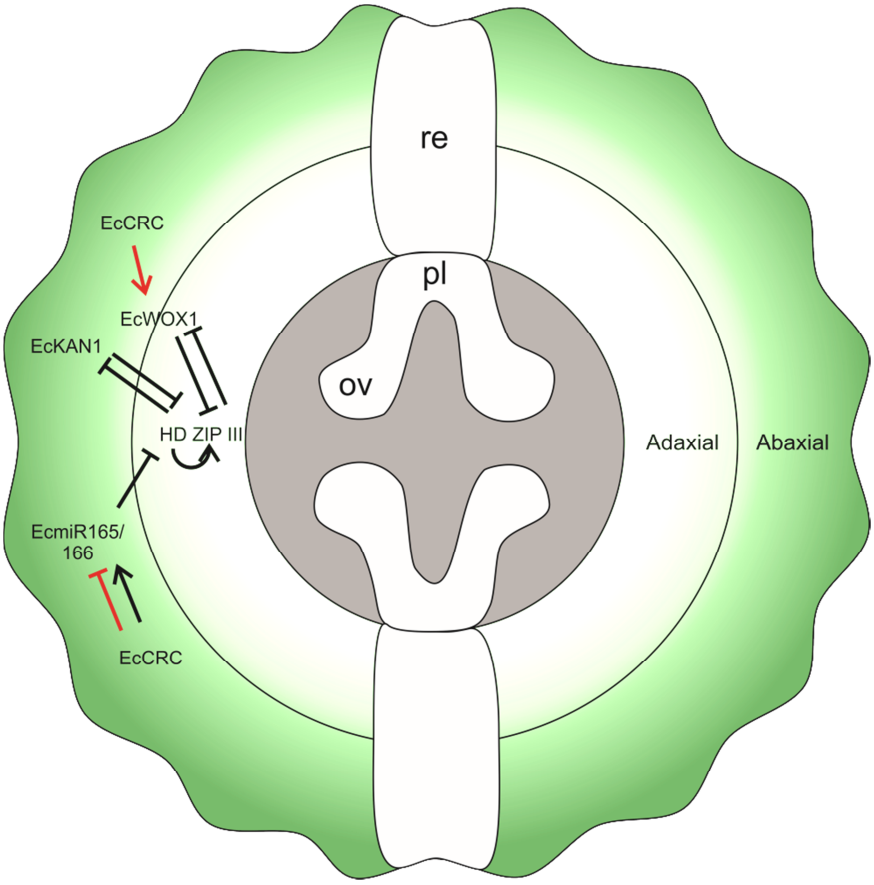

Figure 30: Putative regulation of adaxial–abaxial polarity in the gynoecium of *E. californica*. Shown are the relationships between the *E. californica* homologs of known adaxial -abaxial regulators. Red lines are based on the qRT-PCR results, black lines on *A. thaliana* homology. EcCRC expression takes place in the green abaxial region, whereas EcCRC expression is missing from the white parts of the gynoecium. Re, replum; pl, placenta; ov, ovule.

In contrast to AtCRC in *A. thaliana*, EcCRC is neither activating the expression of the HD ZIP III genes *EcCNA1*, *EcCNA2*, and *EcPHX*, nor of the *AtKAN1* orthologue *EcKAN1*. Thus, EcCRC plays only a small role in the *E. californica* adaxial-abaxial network (figure 30). The core regulators HD ZIP III genes and *KAN* genes act without CRC involvement. Maybe the AtKAN1/AtCRC protein-protein interaction is conserved in *E. californica* and EcKAN1 interacts with EcCRC. Similar to *A. thaliana*, EcCRC is a positive regulator of the middle domain specifying EcWOX1. Interestingly, EcCRC knock-down has an opposite effect on the expression of *Ecmir166 A* than a *crc-1* mutation in *A. thaliana*. While the expression of *miRNA165/166* decreases in *A. thaliana*, it increases in *E. californica*.

There is more than one model how mir165/166 could be affected like this by a knock-down of EcCRC. EcCRC could be restricting the expression of mir165/166 at a certain time point during flower development in *E. californica*. Overexpression of these miRNAs leads to a loss of floral meristem termination in *A. thaliana* (Zhou *et al.*, 2007). Thus, EcCRC might downregulate EcmiRNAs to keep the HD ZIP III levels high enough to act together with EcCRC to terminate the floral meristem. As there are no changes in expression of *EcCNA1*, *EcCNA2*, and *EcPHX*, other members of the HD ZIP III family might be the target of the EcCRC regulated mir165/166. In a second model, EcCRC accumulated mutations in the YABBY domain. These mutations resulted in changes in protein-protein interactions of EcCRC and as discussed in Gross *et al.* (2018), after which the effect of CRC is dependent on its interaction partners, this might lead to functional changes. Either by losing interactions with transcriptional activators or by recruiting new interactors like strong transcriptional repressors.

EcCRC shares some functions with AtCRC. Both terminate the floral meristem and are involved in the regulation of adaxial-abaxial polarity. However, the differences in regulation of adaxial and abaxial factors suggest the evolution of species specific regulatory traits, likely by changes of protein protein interactions or by general changes of the developing program.

CRC Has Multiple Routes to Confer Its Non-Cell-Autonomous Action

Non-cell-autonomous regulation of development is a common factor in animals and plants (see reviews Gallagher *et al.* (2014) and Perrimon *et al.* (2012). In contrast to gap junctions in animals, plants have evolved special cell connections, the plasmodesmata, which allow not only cell-cell communication with small molecules but also the transport of metabolites, nucleic acids, and proteins (reviewed in Ehlers and Westerloh (2013). These transport processes can stop in the neighboring cells but also long distance transport, once the phloem is reached, is possible. More than 2000 different long distance mobile mRNAs and 41 mobile proteins have been identified in *A. thaliana* (Thieme *et al.*, 2015) but recent estimations are much higher with almost 20 % of all protein coding transcripts being mobile

(reviewed in Winter and Kragler (2018)). Thus, cell to cell transport of mRNA and proteins is an elementary part of plant development. Different studies have observed a non-cell-autonomous effect of YABBY proteins in *A. thaliana*, *P. sativum*, *E. californica*, and in other species so far (Bowman and Smyth, 1999; Goldshmidt *et al.*, 2008; Orashakova *et al.*, 2009; Fourquin *et al.*, 2014; Toriba and Hirano, 2014; Strable and Vollbrecht, 2019). The question is how this non-cell-autonomous effect is conferred. Is the mRNA, the protein, or a derived signal transported? The derived signal could be a mobile product of a target gene or any other kind of secondary messenger.

Analyzes in leaves have shown that the non-cell-autonomous effect of FIL does not rely on the transport of the FIL protein but on a derived signal (Goldshmidt *et al.*, 2008). This signal was later identified as the members of the micro RNA family mir165/166 (Tatematsu *et al.*, 2015). According to the here presented qRT-PCR expression analysis (figure 21), CRC activates the expression of members of mir165/166. Members of this miRNA family are typically abaxially expressed and are able to move through the plasmodesmata into the adaxial domain of the plant organ (Miyashima *et al.*, 2011). Thereby they form a gradient from abaxial to adaxial and post-transcriptional silence the expression of the adaxial acting HD ZIP III genes in the abaxial domain. This miRNA gradient is an important aspect of correct patterning of every plant organ. In roots, miRNA 165/166 expression is regulated by the two GRAS transcription factors SHORT ROOT (SHR) and SCARECROW (SCR) (reviewed in Rybel *et al.* (2016) and Di Mambro *et al.* (2019)). SHR is expressed in the stele but migrates to the endodermis via plasmodesmata, while further transport into cortex cells is blocked. It activates the expression of *mir165/166* together with SCR which then move through plasmodesmata in the opposite direction of SHR and downregulate the activity of HD ZIP III genes. Through these three gradients, the xylem in the stele is correctly patterned into metaxylem (high HD ZIP III concentration) and protoxylem (low HD ZIP III concentration) (reviewed in Rybel *et al.* (2016) and Di Mambro *et al.* (2019)). CRC, similar to SHR and SCR, activates the expression of mir165/166 in the abaxial domain of the carpel which then migrate through the plasmodesmata. However, the miRNA transport can only explain the abaxial developmental defects in *crc-1* mutants. Other phenotypes like the unfused carpels are probably independent of mir165/166.

In addition to the non-cell-autonomous action through miRNAs, a recent study in maize (*Zea mays*) links the CRC orthologues ZmDL1 and ZmDL2 with the regulation of *CLE* genes (Strable and Vollbrecht, 2019). CLE peptides, like CLV3, are short secreted polypeptides of less than 15 kDa which need to be proteolytically processed to a dodecapeptide to be functional (reviewed in Yamaguchi *et al.* (2016)). Even though, the WUS/CLV3 feedback loop which limits the size of the SAM is a well-studied system, there is only little functional data available about most of the other CLE peptides. Interestingly, many CLE peptides are functionally redundant and regulate related genes to WUS like WOX5 (reviewed in Yamaguchi *et al.* (2016)). Expression studies of FIL showed no change of CLE expression upon FIL activation (Bonaccorso *et al.*, 2012). The two microarray based co-expression analyzes cannot be used to find a link between CRC and CLE genes, as both analyzes are based on microarray data which does not include most of the CLE genes. However, the recent RNA-seq analysis of *A. thaliana* carpel tissue (Kivivirta *et al.*, unpublished data), found CLE42 to be co-expressed with CRC throughout gynoecium development. CLE42 is involved in the outgrowth of axillary buds and organ size determination as over expression lines are bushy with no sign of apical dominance and remain dwarfed (Strabala *et al.*, 2006; Yaginuma *et al.*, 2011). Yet, a promoter analysis showed only one YBM in *proCLE42*. Thus, it seems unlikely that CRC influences the expression of CLE peptides and by this influences non-cell-autonomously the activity of WUS or WUS relatives.

Goldshmidt *et al.* (2008) concluded that not the YABBY proteins but a derived signal is transported into neighboring cells in leaves. Even though, carpels and leaves share some morphological characters, carpels are more complex than leaves. In addition, the regulation of HD ZIP III genes through YABBY proteins is different in leaves and in carpels, thus it is questionable if CRC is identical to FIL in terms of cell to cell mobility. Two combinations of fluorescent proteins with the native CRC promoter were introduced in *A. thaliana* Col-0 *crc* plants: CRC-GFP/mCherry and CRC-GFP/3xmCherry. The size exclusion limit of plasmodesmata changes during development and shrinks with progressing development but typically proteins to bigger than 80 kDa are not able to pass through plasmodesmata (Crawford and Zambryski, 2001). Therefore, 3xmCherry was intended to be the non-mobile promoter activity control, and mCherry the mobile diffusion control. By comparing the distribution of CRC-GFP with the two mCherry distributions, CRC could be distinguished as non-mobile, mobile via diffusion, or mobile via transport.

However, it was not possible to identify transgenic *A. thaliana* plants expressing CRC-GFP/mCherry and the transgenic G3mC plants did not express 3xmCherry. Hence, the comparison of the (possibly) mobile CRC-GFP and the not mobile 3xmCherry was not possible. Nevertheless, the distribution of CRC-GFP can be compared with previously published CRC mRNA *in situ* hybridizations to circumvent the problem of a missing promoter activity control. The phenotypical analysis of *A. thaliana* Col-0 wild type plants, *crc* plants, and G3mC plants revealed an almost perfect complementation of the *crc* phenotype in G3mC plants (figure 27). Thus, the addition of a C-terminal GFP tag does not affect the activity and function of CRC by e.g. conformational changes and the native promoter is active in the correct tissues.

The CRC mRNA localization by Bowman and Smyth (1999) revealed two expression domains in the gynoecium. An external expression around the circumference of the gynoecium and four internal stripes are present in the gynoecium during stage 8. Compared to the distribution of CRC-GFP in the same stage, CRC-GFP is present almost throughout the complete gynoecium (figure 31), maybe even forming a gradient from abaxial to adaxial. Only the most adaxial part, the future adaxial CMM, is free of CRC-GFP (figure 28 A-E). In later stages, CRC-GFP is restricted to the abaxial domain (stage 10-11) but still present in the replum (figure 31). However, the CRC expression is decreasing in the replum and stops during stage 10-11. Thus, even though there is no CRC mRNA present in the future replum, the CRC-GFP fusion protein is either transported or diffuses into the future replum. Hypothesizing the presence of a CRC gradient, carpel cells without CRC could form the adaxial CMM, while cells with a low amount differentiate into medial tissue and the tissue between middle domain and CMM. And last, cells with a high CRC concentration develop into abaxial cells of the valves and the replum.

Interestingly, the four internal stripes, visible in mRNA *in situ* hybridiations, cannot be identified in any of the analyzed gynoecia. Either the expressed CRC-GFP fusion protein moves from these four stripes into adjacent cells to form one giant domain of CRC presence or the CRC promoter used in this study is lacking the relevant regulatory elements to allow CRC expression in the form of four stripes. Already Lee *et al.* (2005a) were not able to visualize the four stripes when GUS stainings were used to identify the minimal promoter of CRC. If the 3.8 kB fragment used as *proCRC* is missing these regulatory elements, but is still

able to complement the *crc* phenotype, these four stripes might be not relevant for the function of CRC.

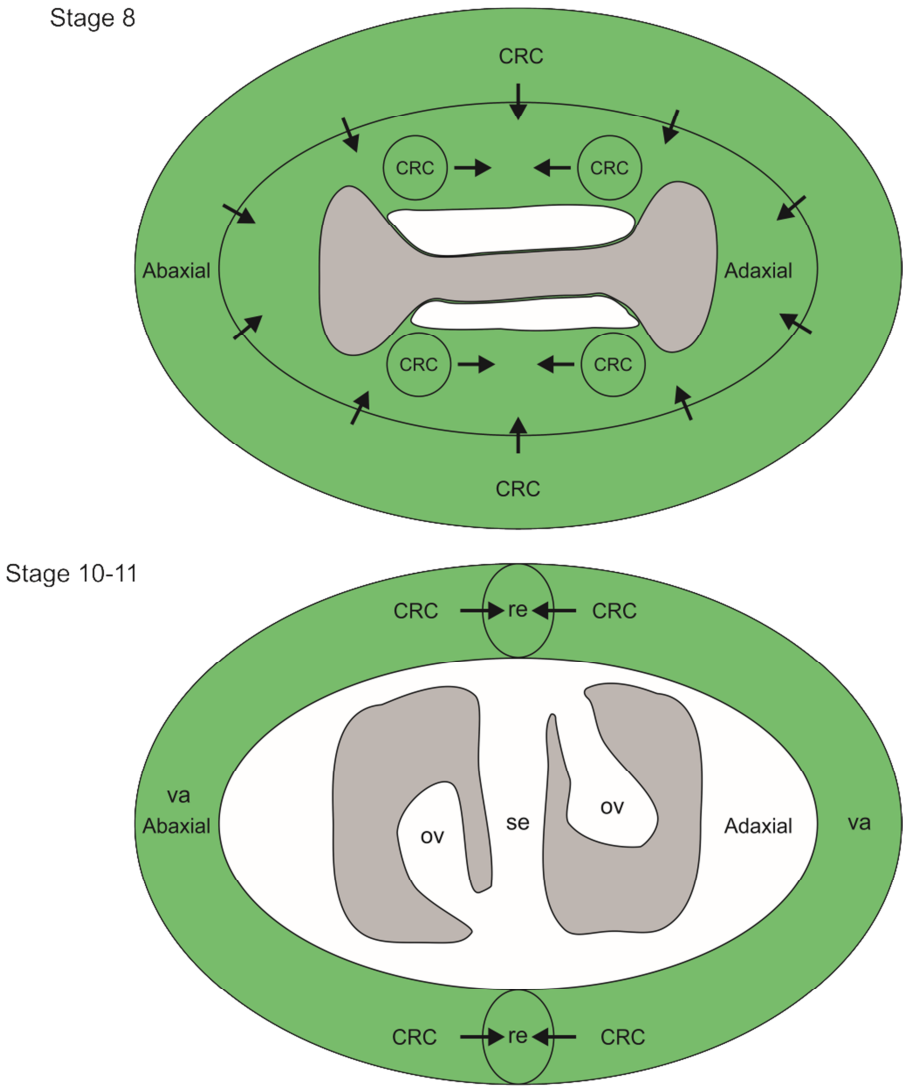

Figure 31: Possible distribution and symplasmic transport routes of CRC in the *A. thaliana* gynoecium in two stages of development. CRC is present in green areas and absent from white areas. Arrows symbolize possible routes of CRC transport. Re, replum; ov, ovule; se, septum; va, valve.

Gradients of transcription factors are present throughout the plant. In roots, PLETHORA 1-4 are regulating the longitudinal differentiation of roots cells into different tissue types, depending on their concentration (Galinha *et al.*, 2007; Santuari *et al.*, 2016). A high PLE concentration sustains the stem cell niche in the root apical meristem and prevents premature differentiation. The PLE concentration decreases then in a rootward gradient which is formed by short range cell to cell migration (Mähönen *et al.*, 2014). The elongation

zone and the differentiation zone of the root mark the point when PLE is diluted enough to allow differentiation.

At the opposite end of the plant, *WUS* is expressed in the organizing center of the SAM (Mayer *et al.*, 1998), directly below the stem cells. The high concentration of WUS inhibits the expression of CLV3 in the organizing center (Busch *et al.*, 2010). WUS moves via plasmodesmata into the stem cells, where most of the protein is proteolytically cleaved (Yadav *et al.*, 2011; Daum *et al.*, 2014; Rodriguez *et al.*, 2016). The lower WUS concentration leads to a change in the regulation of CLV3, as WUS activates the expression of CLV3 now (Busch *et al.*, 2010). CLV3 is, as mentioned before, a short secreted peptide, which then leads to the repression of WUS expression in the stem cells and retains the WUS expression to the organizing center of the SAM (Brand *et al.*, 2000).

The different actions of PLE and WUS proteins are possible due to the presence of high affinity DNA binding sites and low affinity DNA binding sites in the promoter regions of their respective target genes (reviewed in Hofhuis and Heidstra (2018)). Typically, PLE and WUS proteins bind first to their high affinity binding sites and only if the concentration of the respective protein is high enough, low affinity binding sites can be bound. In some target genes, the repressive signal of the low affinity binding sites overrules the activating high affinity binding sites and expression of the target gene cannot take place. As CRC and the other YABBY proteins exhibit multiple binding motifs, they could exploit this mechanism to regulate the expression of their target genes. Switching between activation and repression of transcription would then be independent of interaction partners as discussed in Gross *et al.* (2018). The three binding motifs identified by Shamimuzzaman and Vodkin (2013) have been proven to be functional and relevant for the repression of *TRN2* and the activation of *YUC4* by CRC. However, the same binding motif (YBM2, GARAGAAA) is present in the promoter of both genes. Therefore, it is unlikely, that these to genes are regulated by CRC in a different manner through high affinity and low affinity binding sites and more likely, CRC is depending on interaction partners.

An active transport or a passive diffusion cannot be distinguished from each other, as the necessary control construct CRC-GFP/mCherry is missing. Nevertheless, the absence of CRC from the adaxial domain in later stages indicates at least a regulated exclusion from the adaxial domain. During plant development, plasmodesmatal transport is highly regulated

and sometimes even the shutdown of transport is necessary to complete differentiation. During the development of stomata, the future guard cells seal their plasmodesmata to isolate themselves from the remaining epidermis cells (Kong *et al.*, 2012). Then, transcription factors like SPEECHLESS (SPCH), MUTE, and FAMA induce the differentiation of this progenitor cells into functional guard cells (reviewed in Simmons and Bergmann (2016)), regulating transpiration and gas exchange. If the closure of the plasmodesmata is inhibited, SPCH is able to migrate into adjacent epidermis cells and a cluster of stomata is formed (Guseman *et al.*, 2010). Thus the restriction of CRC movement into the adaxial tissue might be necessary for the correct development of septum and placenta.

In summary, CRC exhibits at least two modes of non-cell-autonomous action. Parts of its function are conferred similar to other YABBY proteins via the mobile mir165/166 but also by direct protein transport of CRC in during early carpel development.

Conclusion and Outlook

Over the last 20 years, CRC's influence on the carpel development has been studied. But many conclusions about CRC function were drawn by comparing CRC with other YABBY proteins expressed in leaves, especially FIL. However, carpels are much more complex than leaves and CRC has diverged from the other YABBY genes already before the origin of angiosperms. This indicates that there might be important differences between CRC and its family relatives.

In the here presented work, CRC has been studied in multiple previously neglected aspects (figure 32). The initially formed hypothesis that CRC expression is not just regulated by MADS box transcription factors and LFY (I) has been validated. CRC expression is regulated by a multitude of transcription factors of different families and functions, fine tuning CRC expression in the developing gynoecium into the proper temporal and spatial pattern. Even though, more detailed expression analyzes using mRNA *in situ* hybridization and GUS stainings of regulator mutant lines are necessary, it is obvious that during its expression, CRC is co-expressed with thousands of other genes and in particular with many of its own regulators such as putative activators like SEP3 and JAG, and putative repressors like HAF and KNAT1/BP.

While parts of its function are relayed by auxin synthesis and auxin distribution, the protein itself is mobile to a certain degree. In addition it activates the mobile miRNAs mir165/166. This is validating (and at the same time refuting) the initially formed hypothesis (II), as the non-cell-autonomous action does not rely on only one mode of mobility but on two, both the protein and a derived signal. The protein mobility is not just a difference to other YABBY proteins but also enhancing the complexity of the whole regulatory system by means of a necessary integration of different mobile signals into different developmental reactions. Therefore, a localization of mir165/166 in the developing gynoecium and also the proper introduction of mCherry and 3xmCherry might elucidate this further.

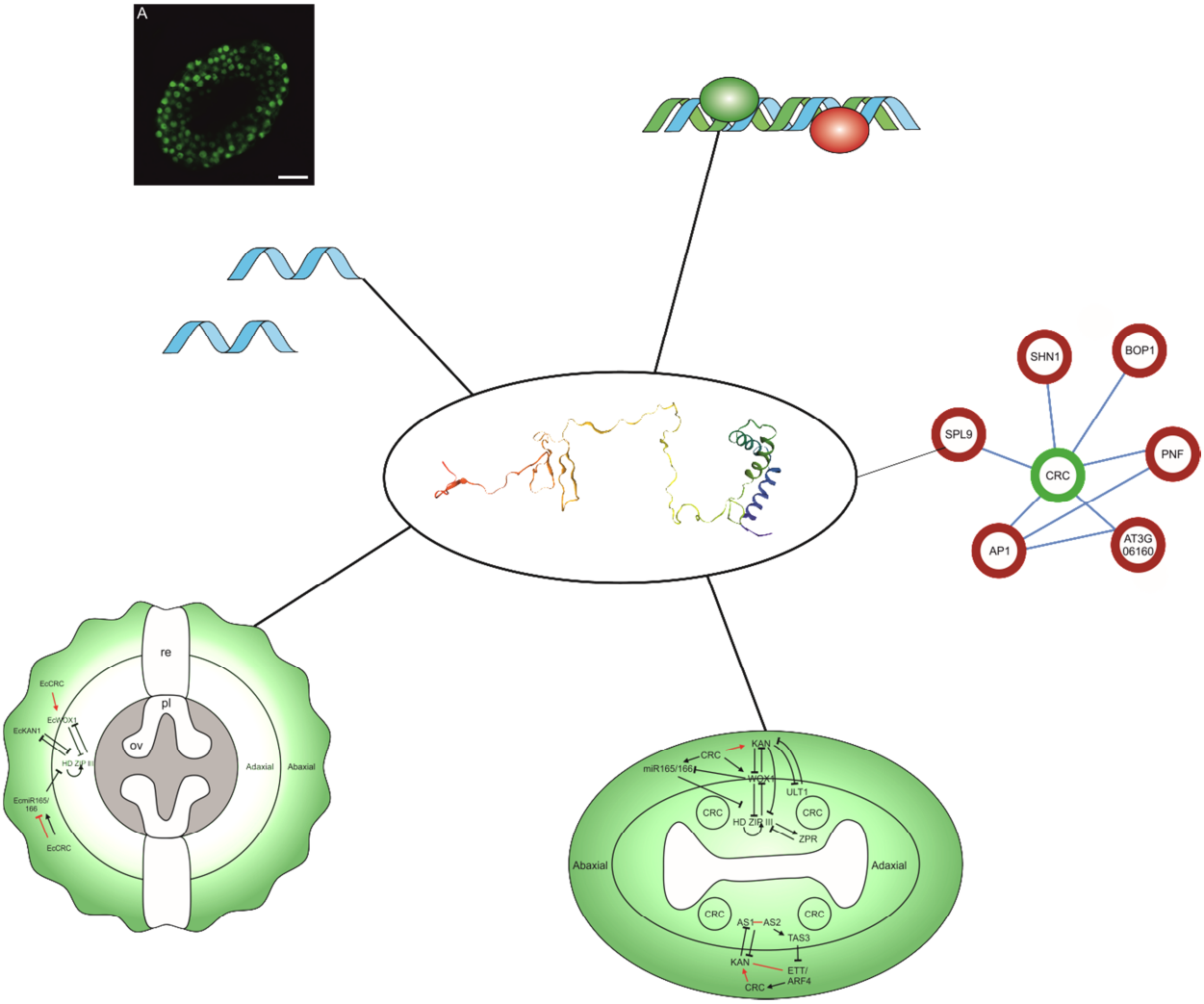

Figure 32: Aspects of CRC action, resembling the different topics of this dissertation: expression regulation, adaxial-abaxial target genes, and non-cell-autonomous effect (clockwise depicted). CRC expression is regulated by multiple newly identified transcription factors with putative activators and repressors. Multiple of these regulators are co-expressed to CRC and complex expression and functional networks are formed. CRC is regulating adaxial and abaxial factors in *A. thaliana*, but has little influence on expression of these regulators in *E. californica*. CRC's distribution indicates a transport of the CRC protein and at the same time it regulates the mobile mir165/166.

The expression analysis already shows the tight integration of CRC in the carpel developmental processes but this integration is enhanced on the protein level. CRC plays a major role in regulating the adaxial-abaxial polarity by regulating both adaxial and abaxial factors and links this regulatory network with the apical-basal regulatory network, validating the underlying hypothesis (III). Indicating the complexity of these regulatory processes but also at the same time the elegance of recruiting preexisting networks for new purposes like the complex three dimensional structure of the gynoecium. Even though aspects of CRC function, like the termination of the floral meristem, are conserved in other angiosperms,

the detailed mechanism, especially in terms of adaxial-abaxial polarity regulation, seems to be diverged, as the comparison of *A. thaliana* and *E. californica* shows drastic differences and a minimization of CRC's role in *E. californica*, thus refuting the initially formed hypothesis (IV).

All in all, this dissertation has shown that CRC is a multi-faceted regulator during carpel development with a complex transcriptional regulation, multiple important target genes, and exhibits more than one mode of non-cell-autonomous action. Thus, this dissertation highlights the importance of CRC during carpel development and terms CRC a major carpel developmental regulator. In addition, it highlightes the importance of CRCs interaction partners which are probably necessary to discriminate between activation and repression of target genes for future research.

References

Abe M, Kobayashi Y, Yamamoto S *et al.* 2005. FD, a bZIP protein mediating signals from the floral pathway integrator FT at the shoot apex. *Science* **309,** 1052–1056.

Alonso JM, Stepanova AN, Leisse TJ *et al.* 2003. Genome-wide insertional mutagenesis of *Arabidopsis thaliana*. *Science* **301,** 653–657.

Altschul SF, Gish W, Miller W, Myers EW, Lipman DJ. 1990. Basic local alignment search tool. *Journal of molecular biology* **215,** 403–410.

Alvarez J, Smyth DR. 1998. Genetic pathways controlling carpel development in *Arabidopsis thaliana*. *Journal of Plant Research* **111,** 295–298.

Alvarez J, Smyth DR. 1999. *CRABS CLAW* and *SPATULA*, two *Arabidopsis* genes that control carpel development in parallel with *AGAMOUS*. *Development* **126,** 2377–2386.

Alvarez J, Smyth DR. 2002. *CRABS CLAW* and *SPATULA* genes regulate growth and pattern formation during gynoecium development in *Arabidopsis thaliana*. *International Journal of Plant Sciences* **163,** 17–41.

Alvarez JP, Goldshmidt A, Efroni I, Bowman JL, Eshed Y. 2009. The *NGATHA* distal organ development genes are essential for style specification in *Arabidopsis*. *The Plant Cell* **21,** 1373–1393.

An H, Roussot C, Suárez-López P *et al.* 2004. CONSTANS acts in the phloem to regulate a systemic signal that induces photoperiodic flowering of *Arabidopsis*. *Development* **131,** 3615–3626.

Austin RS, Hiu S, Waese J *et al.* 2016. New BAR tools for mining expression data and exploring Cis-elements in *Arabidopsis thaliana*. *The Plant Journal* **88,** 490–504.

Ballester P, Navarrete-Gómez M, Carbonero P, Oñate-Sánchez L, Ferrándiz C. 2015. Leaf expansion in *Arabidopsis* is controlled by a TCP-NGA regulatory module likely conserved in distantly related species. *Physiologia Plantarum* **155,** 21–32.

Bao F, Azhakanandam S, Franks RG. 2010. SEUSS and SEUSS-LIKE transcriptional adaptors regulate floral and embryonic development in *Arabidopsis*. *Plant physiology* **152,** 821–836.

Becker A, Alix K, Damerval C. 2011. The evolution of flower development: Current understanding and future challenges. *Annals of botany* **107,** 1427–1431.

Becker A, Ehlers K. 2016. *Arabidopsis* flower development - of protein complexes, targets, and transport. *Protoplasma* **253,** 219–230.

Becker A, Gleissberg S, Smyth DR. 2005. Floral and vegetative morphogenesis in California Poppy (*Eschscholzia californica* Cham.). *International Journal of Plant Sciences* **166,** 537–555.

Bemer M, van Mourik H, Muiño JM, Ferrándiz C, Kaufmann K, Angenent GC. 2017. FRUITFULL controls *SAUR10* expression and regulates *Arabidopsis* growth and architecture. *Journal of experimental botany* **68,** 3391–3403.

Benitez-Alfonso Y. 2014. Symplastic intercellular transport from a developmental perspective. *Journal of Experimental Botany* **65,** 1857–1863.

Benitez-Alfonso Y, Faulkner C, Ritzenthaler C, Maule AJ. 2010. Plasmodesmata: gateways to local and systemic virus infection. *Molecular plant-microbe interactions MPMI* **23,** 1403–1412.

Bennett MD, Leitch IJ, Price HJ, Johnston JS. 2003. Comparisons with *Caenorhabditis* (100 Mb) and *Drosophila* (175 Mb) using flow cytometry show genome size in *Arabidopsis* to be 157 Mb and thus 25 % larger than the *Arabidopsis* Genome Initiative estimate of 125 Mb. *Annals of botany* **91,** 547–557.

Bonaccorso O, Lee JE, Puah L, Scutt CP, Golz JF. 2012. FILAMENTOUS FLOWER controls lateral organ development by acting as both an activator and a repressor. *BMC Plant Biology* **12**.

Bottomley MJ, Collard MW, Huggenvik JI, Liu Z, Gibson TJ, Sattler M. 2001. The SAND domain structure defines a novel DNA-binding fold in transcriptional regulation. *Nature structural biology* **8,** 626–633.

Bowman JL, Smyth DR. 1999. *CRABS CLAW*, a gene that regulates carpel and nectary development in *Arabidopsis*, encodes a novel protein with zinc finger and helix-loop-helix domains. *Development* **126,** 2387–2396.

Brand U, Fletcher J, Hobe M, Meyerowitz E, Simon R. 2000. Dependence of stem cell fate in *Arabidopsis* on a feedback loop regulated by CLV3 activity. *Science* **289,** 617–619.

Broun P, Poindexter P, Osborne E, Jiang C-Z, Riechmann JL. 2004. WIN1, a transcriptional activator of epidermal wax accumulation in *Arabidopsis*. *Proceedings of the National Academy of Sciences* **101,** 4706–4711.

Burch-Smith TM, Zambryski PC. 2012. Plasmodesmata paradigm shift: regulation from without versus within. *Annual Review of Plant Biology* **63,** 239–260.

Busch W, Miotk A, Ariel FD *et al.* 2010. Transcriptional control of a plant stem cell niche. *Developmental cell* **18,** 849–861.

Byrne ME, Groover AT, Fontana JR, Martienssen RA. 2003. Phyllotactic pattern and stem cell fate are determined by the *Arabidopsis* homeobox gene *BELLRINGER*. *Development* **130,** 3941–3950.

Carabelli M, Possenti M, Sessa G, Ruzza V, Morelli G, Ruberti I. 2018. *Arabidopsis* HD-Zip II proteins regulate the exit from proliferation during leaf development in canopy shade. *Journal of experimental botany* **69,** 5419–5431.

Carles CC, Fletcher JC. 2009. The SAND domain protein ULTRAPETALA1 acts as a trithorax group factor to regulate cell fate in plants. *Genes & development* **23,** 2723–2728.

Carlsbecker A, Lee J-Y, Roberts CJ *et al.* 2010. Cell signalling by microRNA165/6 directs gene dose-dependent root cell fate. *Nature* **465,** 316–321.

Chen J, Yang L, Yan X *et al.* 2016. Zinc-finger transcription factor ZAT6 positively regulates cadmium tolerance through the glutathione-dependent pathway in *Arabidopsis*. *Plant physiology* **171,** 707–719.

Chen Y, Negre N, Li Q *et al.* 2012. Systematic evaluation of factors influencing ChIP-seq fidelity. *Nature methods* **9,** 609–614.

Cheng Y, Dai X, Zhao Y. 2006. Auxin biosynthesis by the YUCCA flavin monooxygenases controls the formation of floral organs and vascular tissues in *Arabidopsis*. *Genes & development* **20,** 1790–1799.

Chow C-N, Zheng H-Q, Wu N-Y *et al.* 2016. PlantPAN 2.0: an update of plant promoter analysis navigator for reconstructing transcriptional regulatory networks in plants. *Nucleic Acids Research* **44,** 1154-60.

Christensen NM, Faulkner C, Oparka KJ. 2009. Evidence for unidirectional flow through plasmodesmata. *Plant Physiology* **150,** 96–104.

Collard BCY, Das A, Virk PS, Mackill DJ. 2007. Evaluation of 'quick and dirty' DNA extraction methods for marker-assisted selection in rice (*Oryza sativa* L.). *Plant Breeding* **126,** 47–50.

Corbesier L, Vincent C, Jang S *et al.* 2007. FT protein movement contributes to long-distance signaling in floral induction of *Arabidopsis*. *Science* **316,** 1030–1033.

Crawford BCW, Ditta G, Yanofsky MF. 2007. The *NTT* gene is required for transmitting-tract development in carpels of *Arabidopsis thaliana*. *Current Biology* **17,** 1101–1108.

Crawford BCW, Yanofsky MF. 2011. HALF FILLED promotes reproductive tract development and fertilization efficiency in *Arabidopsis thaliana*. *Development* **138,** 2999–3009.

Crawford KM, Zambryski PC. 2001. Non-targeted and targeted protein movement through plasmodesmata in leaves in different developmental and physiological states. *Plant Physiology* **125,** 1802–1812.

Czechowski T, Stitt M, Altmann T, Udvardi MK, Scheible W-R. 2005. Genome-wide identification and testing of superior reference genes for transcript normalization in *Arabidopsis*. *Plant Physiology* **139,** 5–17.

Dai X, Liu Z, Qiao M, Li J, Li S, Xiang F. 2017. ARR12 promotes de novo shoot regeneration in *Arabidopsis thaliana* via activation of *WUSCHEL* expression. *Journal of integrative plant biology* **59,** 747–758.

Daum G, Medzihradszky A, Suzaki T, Lohmann JU. 2014. A mechanistic framework for noncell autonomous stem cell induction in *Arabidopsis*. *Proceedings of the National Academy of Sciences* **111,** 14619–14624.

Davis AM, Hall A, Millar AJ, Darrah C, Davis SJ. 2009. Protocol: Streamlined sub-protocols for floral-dip transformation and selection of transformants in *Arabidopsis thaliana*. *Plant methods* **5**.

Di Mambro R, Sabatini S, Dello Ioio R. 2019. Patterning the Axes: A Lesson from the Root. *Plants* **8**.

Dinneny JR, Weigel D, Yanofsky MF. 2005. A genetic framework for fruit patterning in *Arabidopsis thaliana*. *Development* **132,** 4687–4696.

Ditta G, Pinyopich A, Robles P, Pelaz S, Yanofsky MF. 2004. The *SEP4* gene of *Arabidopsis thaliana* functions in floral organ and meristem identity. *Current Biology* **14,** 1935–1940.

Ehlers K, Westerloh MG. 2013. Developmental control of plasmodesmata frequency, structure, and function. In: Sokołowska K, Sowiński P, eds. *Symplasmic Transport in Vascular Plants*. New York, NY: Springer New York, 41–82.

Emery JF, Floyd SK, Alvarez J *et al.* 2003. Radial patterning of *Arabidopsis* shoots by class III HD-ZIP and *KANADI* genes. *Current Biology* **13,** 1768–1774.

Eshed Y, Baum SF, Bowman JL. 1999. Distinct mechanisms promote polarity establishment in carpels of *Arabidopsis*. *Cell* **99,** 199–209.

Fahlgren N, Montgomery TA, Howell MD *et al.* 2006. Regulation of AUXIN RESPONSE FACTOR3 by TAS3 ta-siRNA affects developmental timing and patterning in *Arabidopsis*. *Current Biology* **16,** 939–944.

Faulkner C. 2013. Receptor-mediated signaling at plasmodesmata. *Frontiers in Plant Science* **4,** 521.

Ferrandiz C, Liljegren S, Yanofsky M. 2000. Negative regulation of the *SHATTERPROOF* genes by FRUITFULL during *Arabidopsis* fruit development. *Science* **289,** 436–438.

Fourquin C, Primo A, Martínez-Fernández I, Huet-Trujillo E, Ferrándiz C. 2014. The *CRC* orthologue from *Pisum sativum* shows conserved functions in carpel morphogenesis and vascular development. *Annals of botany* **114,** 1535–1544.

Franco-Zorrilla JM, López-Vidriero I, Carrasco JL, Godoy M, Vera P, Solano R. 2014. DNA-binding specificities of plant transcription factors and their potential to define target genes. *Proceedings of the National Academy of Sciences* **111,** 2367–2372.

Franks RG, Wang C, Levin JZ, Liu Z. 2002. SEUSS, a member of a novel family of plant regulatory proteins, represses floral homeotic gene expression with LEUNIG. *Development* **129,** 253–263.

Furuta K, Lichtenberger R, Helariutta Y. 2012. The role of mobile small RNA species during root growth and development. *Current opinion in cell biology* **24,** 211–216.

Galinha C, Hofhuis H, Luijten M *et al.* 2007. PLETHORA proteins as dose-dependent master regulators of *Arabidopsis* root development. *Nature* **449,** 1053–1057.

Gallagher KL, Sozzani R, Lee C-M. 2014. Intercellular protein movement: Deciphering the language of development. *Annual review of cell and developmental biology* **30,** 207–233.

Garcia D, Collier SA, Byrne ME, Martienssen RA. 2006. Specification of leaf polarity in *Arabidopsis* via the trans-acting siRNA pathway. *Current Biology* **16,** 933–938.

Goethe JWv. 1790. *Die Metamorphose der Pflanzen*. Gotha: Ettlinger.

Goldshmidt A, Alvarez JP, Bowman JL, Eshed Y. 2008. Signals derived from YABBY gene activities in organ primordia regulate growth and partitioning of *Arabidopsis* shoot apical meristems. *The Plant Cell* **20,** 1217–1230.

Gomez-Mena C, Folter S de, **Costa MMR, Angenent GC, Sablowski R.** 2005. Transcriptional program controlled by the floral homeotic gene *AGAMOUS* during early organogenesis. *Development* **132,** 429–438.

González-Reig S, Ripoll JJ, Vera A, Yanofsky MF, Martínez-Laborda A, Qu L-J. 2012. Antagonistic gene activities determine the formation of pattern elements along the mediolateral axis of the *Arabidopsis* fruit. *PLoS Genetics* **8**.

Gross T, Broholm S, Becker A. 2018. CRABS CLAW acts as a bifunctional transcription factor in flower development. *Frontiers in Plant Science* **9**.

Gu Q, Ferrándiz C, Yanofsky MF, Martienssen R. 1998. The *FRUITFULL* MADS-box gene mediates cell differentiation during *Arabidopsis* fruit development. *Development* **125,** 1509–1517.

Guseman JM, Lee JS, Bogenschutz NL *et al.* 2010. Dysregulation of cell-to-cell connectivity and stomatal patterning by loss-of-function mutation in *Arabidopsis* chorus (glucan synthase-like 8). *Development* **137,** 1731–1741.

Han X, Hyun TK, Zhang M *et al.* 2014. Auxin-callose-mediated plasmodesmal gating is essential for tropic auxin gradient formation and signaling. *Developmental cell* **28,** 132–146.

Han X, Yin L, Xue H. 2012. Co-expression analysis identifies CRC and AP1 the regulator of *Arabidopsis* fatty acid biosynthesis. *Journal of integrative plant biology* **54,** 486–499.

Heisler MG, Atkinson A, Bylstra YH, Walsh R, Smyth DR. 2001. *SPATULA*, a gene that controls development of carpel margin tissues in *Arabidopsis*, encodes a bHLH protein. *Development* **128,** 1089–1098.

Helariutta Y, Fukaki H, Wysocka-Diller J *et al.* 2000. The *SHORT-ROOT* gene controls radial patterning of the *Arabidopsis* root through radial signaling. *Cell* **101,** 555–567.

Hemsley A, Arnheim N, Toney MD, Cortopassi G, Galas DJ. 1989. A simple method for site-directed mutagenesis using the polymerase chain reaction. *Nucleic Acids Research* **17,** 6545–6551.

Herrera-Ubaldo H, Campos SE, Luna Garcia V *et al.* 2018. An interaction map of transcription factors controlling gynoecium development in *Arabidopsis*.

Hoffman CS, Winston F. 1987. A ten-minute DNA preparation from yeast efficiently releases autonomous plasmids for transformation of *Eschericha coli*. *Gene* **57,** 267–272.

Hofhuis HF, Heidstra R. 2018. Transcription factor dosage: more or less sufficient for growth. *Current opinion in plant biology* **45,** 50–58.

Hori K, Yamada Y, Purwanto R *et al.* 2018. Mining of the uncharacterized cytochrome P450 genes involved in alkaloid biosynthesis in california poppy using a draft genome sequence. *Plant & cell physiology* **59,** 222–233.

Immink RGH, Tonaco IAN, Folter S de ***et al.*** 2009. SEPALLATA3: the 'glue' for MADS box transcription factor complex formation. *Genome biology* **10**.

Irish V. 2017. The ABC model of floral development. *Current Biology* **27,** 887-890.

Johnston JS, Pepper AE, Hall AE *et al.* 2005. Evolution of genome size in Brassicaceae. *Annals of botany* **95,** 229–235.

Joubès J, Raffaele S, Bourdenx B *et al.* 2008. The VLCFA elongase gene family in *Arabidopsis thaliana*: Phylogenetic analysis, 3D modelling and expression profiling. *Plant Molecular Biology* **67,** 547–566.

Jung J-H, Park C-M. 2007. MIR166/165 genes exhibit dynamic expression patterns in regulating shoot apical meristem and floral development in *Arabidopsis*. *Planta* **225,** 1327–1338.

Källberg M, Wang H, Wang S *et al.* 2012. Template-based protein structure modeling using the RaptorX web server. *Nature protocols* **7,** 1511–1522.

Kanrar S, Bhattacharya M, Arthur B, Courtier J, Smith HMS. 2008. Regulatory networks that function to specify flower meristems require the function of homeobox genes *PENNYWISE* and *POUND-FOOLISH* in *Arabidopsis*. *The Plant Journal* **54,** 924–937.

Kerstetter RA, Bollman K, Taylor RA, Bomblies K, Poethig RS. 2001. KANADI regulates organ polarity in *Arabidopsis*. *Nature* **411,** 706–709.

Khan M, Ragni L, Tabb P *et al.* 2015. Repression of lateral organ boundary genes by PENNYWISE and POUND-FOOLISH is essential for meristem maintenance and flowering in *Arabidopsis*. *Plant physiology* **169,** 2166–2186.

Kim JH, Choi D, Kende H. 2003. The AtGRF family of putative transcription factors is involved in leaf and cotyledon growth in *Arabidopsis*. *The Plant Journal* **36,** 94–104.

Kim J-Y, Yuan Z, Jackson D. 2003. Developmental regulation and significance of KNOX protein trafficking in Arabidopsis. *Development* **130,** 4351–4362.

Kong D, Karve R, Willet A, Chen M-K, Oden J, Shpak ED. 2012. Regulation of plasmodesmatal permeability and stomatal patterning by the glycosyltransferase-like protein KOBITO1. *Plant physiology* **159,** 156–168.

Koornneef M, Meinke D. 2010. The development of *Arabidopsis* as a model plant. *The Plant Journal* **61,** 909–921.

Koornneeff M, Dellaert LWM, van der Veen JH. 1982. EMS- and relation-induced mutation frequencies at individual loci in *Arabidopsis thaliana* (L.) Heynh. *Mutation Research/Fundamental and Molecular Mechanisms of Mutagenesis* **93,** 109–123.

Kragler F. 2013. Plasmodesmata: intercellular tunnels facilitating transport of macromolecules in plants. *Cell and tissue research* **352,** 49–58.

Kraus D. 2014. Consolidated data analysis and presentation using an open-source add-in for the Microsoft Excel ® spreadsheet software. *Medical Writing* **23,** 25–28.

Lal S, Pacis LB, Smith HMS. 2011. Regulation of the *SQUAMOSA PROMOTER-BINDING PROTEIN-LIKE* genes/microRNA156 module by the homeodomain proteins PENNYWISE and POUND-FOOLISH in *Arabidopsis*. *Molecular plant* **4,** 1123–1132.

Lamesch P, Berardini TZ, Li D *et al.* 2012. The *Arabidopsis* Information Resource (TAIR): Improved gene annotation and new tools. *Nucleic Acids Research* **40**.

Lampropoulos A, Sutikovic Z, Wenzl C, Maegele I, Lohmann JU, Forner J. 2013. GreenGate - a novel, versatile, and efficient cloning system for plant transgenesis. *PloS one* **8**.

Lange M, Orashakova S, Lange S *et al.* 2013. The *seirena* B class floral homeotic mutant of California Poppy (*Eschscholzia californica*) reveals a function of the enigmatic PI motif in the formation of specific multimeric MADS domain protein complexes. *The Plant Cell* **25,** 438–453.

Larsson E, Franks RG, Sundberg E. 2013. Auxin and the *Arabidopsis thaliana* gynoecium. *Journal of experimental botany* **64,** 2619–2627.

Larsson E, Roberts CJ, Claes AR, Franks RG, Sundberg E. 2014. Polar auxin transport is essential for medial versus lateral tissue specification and vascular-mediated valve outgrowth in *Arabidopsis* gynoecia. *Plant physiology* **166,** 1998–2012.

Lee BH, Kwon SH, Lee S-J *et al.* 2015. The *Arabidopsis thaliana* NGATHA transcription factors negatively regulate cell proliferation of lateral organs. *Plant molecular biology* **89,** 529–538.

Lee J-Y, Baum SF, Alvarez J, Patel A, Chitwood DH, Bowman JL. 2005a. Activation of *CRABS CLAW* in the nectaries and carpels of *Arabidopsis*. *The Plant Cell* **17,** 25–36.

Lee J-Y, Baum SF, Oh S-H, Jiang C-Z, Chen J-C, Bowman JL. 2005b. Recruitment of CRABS CLAW to promote nectary development within the eudicot clade. *Development* **132,** 5021–5032.

Li S, He Y, Zhao J, Zhang L, Sun M-x. 2013. Polar protein transport between apical and basal cells during tobacco early embryogenesis. *Plant cell reports* **32,** 285–291.

Lu K-J, Rybel B de, **van Mourik H, Weijers D.** 2018. Regulation of intercellular TARGET OF MONOPTEROS 7 protein transport in the *Arabidopsis* root. *Development* **145**.

Lucas WJ, Lee J-Y. 2004. Plasmodesmata as a supracellular control network in plants. *Nature Reviews Molecular Cell Biology* **5,** 712–726.

Mähönen AP, Tusscher K ten, **Siligato R *et al.*** 2014. PLETHORA gradient formation mechanism separates auxin responses. *Nature* **515,** 125–129.

Mantegazza O, Gregis V, Mendes MA *et al.* 2014. Analysis of the *Arabidopsis REM* gene family predicts functions during flower development. *Annals of botany* **114,** 1507–1515.

Mayer KFX, Schoof H, Haecker A, Lenhard M, Jürgens G, Laux T. 1998. Role of WUSCHEL in regulating stem cell fate in the *Arabidopsis* shoot meristem. *Cell* **95,** 805–815.

McKim SM, Stenvik G-E, Butenko MA *et al.* 2008. The *BLADE-ON-PETIOLE* genes are essential for abscission zone formation in *Arabidopsis*. *Development* **135,** 1537–1546.

Meister RJ, Williams LA, Monfared MM *et al.* 2004. Definition and interactions of a positive regulatory element of the *Arabidopsis INNER NO OUTER* promoter. *The Plant Journal* **37,** 426–438.

Meng WJ, Cheng ZJ, Sang YL *et al.* 2017. Type-B ARABIDOPSIS RESPONSE REGULATORs specify the shoot stem cell niche by dual regulation of WUSCHEL. *The Plant Cell* **29,** 1357–1372.

Merelo P, Paredes EB, Heisler MG, Wenkel S. 2017. The shady side of leaf development: The role of the REVOLUTA/KANADI1 module in leaf patterning and auxin-mediated growth promotion. *Current opinion in plant biology* **35,** 111–116.

Mitsuda N, Ikeda M, Takada S *et al.* 2010. Efficient yeast one-/two-hybrid screening using a library composed only of transcription factors in *Arabidopsis thaliana*. *Plant and Cell Physiology* **51,** 2145–2151.

Miyashima S, Koi S, Hashimoto T, Nakajima K. 2011. Non-cell-autonomous microRNA165 acts in a dose-dependent manner to regulate multiple differentiation status in the *Arabidopsis* root. *Development* **138,** 2303–2313.

Moubayidin L, Ostergaard L. 2014. Dynamic control of auxin distribution imposes a bilateral-to-radial symmetry switch during gynoecium development. *Current Biology* **24,** 2743–2748.

Mutwil M, Klie S, Tohge T *et al.* 2011. PlaNet: combined sequence and expression comparisons across plant networks derived from seven species. *The Plant Cell* **23,** 895–910.

Nakajima K, Sena G, Nawy T, Benfey PN. 2001. Intercellular movement of the putative transcription factor SHR in root patterning. *Nature* **413,** 307–311.

Nakata M, Matsumoto N, Tsugeki R, Rikirsch E, Laux T, Okada K. 2012. Roles of the middle domain-specific *WUSCHEL-RELATED HOMEOBOX* genes in early development of leaves in *Arabidopsis*. *The Plant Cell* **24,** 519–535.

Nemhauser JL, Feldman LJ, Zambryski PC. 2000. Auxin and ETTIN in *Arabidopsis* gynoecium morphogenesis. *Development* **127,** 3877–3888.

Ng K-H, Yu H, Ito T. 2009. AGAMOUS controls GIANT KILLER, a multifunctional chromatin modifier in reproductive organ patterning and differentiation. *PLoS biology* **7**.

Notaguchi M, Abe M, Kimura T *et al.* 2008. Long-distance, graft-transmissible action of *Arabidopsis* FLOWERING LOCUS T protein to promote flowering. *Plant & cell physiology* **49,** 1645–1658.

Ohashi-Ito K, Bergmann DC. 2006. *Arabidopsis* FAMA controls the final proliferation/differentiation switch during stomatal development. *The Plant Cell* **18,** 2493–2505.

Ohno CK, Reddy GV, Heisler MGB, Meyerowitz EM. 2004. The *Arabidopsis JAGGED* gene encodes a zinc finger protein that promotes leaf tissue development. *Development* **131,** 1111–1122.

Oldfield AJ, Yang P, Conway AE *et al.* 2014. Histone-fold domain protein NF-Y promotes chromatin accessibility for cell type-specific master transcription factors. *Molecular Cell* **55,** 708–722.

Ó'Maoiléidigh DS, Wuest SE, Rae L *et al.* 2013. Control of reproductive floral organ identity specification in *Arabidopsis* by the C function regulator AGAMOUS. *The Plant Cell* **25,** 2482–2503.

Orashakova S, Lange M, Lange S, Wege S, Becker A. 2009. The *CRABS CLAW* ortholog from California poppy (*Eschscholzia californica*, Papaveraceae), *EcCRC*, is involved in floral meristem termination, gynoecium differentiation and ovule initiation. *The Plant Journal* **58,** 682–693.

Pastore JJ, Limpuangthip A, Yamaguchi N *et al.* 2011. LATE MERISTEM IDENTITY2 acts together with LEAFY to activate APETALA1. *Development* **138,** 3189–3198.

Pérez-Rodríguez P, Riaño-Pachón DM, Corrêa LGG, Rensing SA, Kersten B, Mueller-Roeber B. 2010. PlnTFDB: Updated content and new features of the plant transcription factor database. *Nucleic Acids Research* **38**.

Perrimon N, Pitsouli C, Shilo B-Z. 2012. Signaling mechanisms controlling cell fate and embryonic patterning. *Cold Spring Harbor perspectives in biology* **4**.

Pfaffl MW. 2001. A new mathematical model for relative quantification in real-time RT-PCR. *Nucleic Acids Research* **29,** 45e-45.

Pires HR, Monfared MM, Shemyakina EA, Fletcher JC. 2014. *ULTRAPETALA* trxG genes interact with *KANADI* transcription factor genes to regulate *Arabidopsis* gynoecium patterning. *The Plant Cell* **26,** 4345–4361.

Prigge MJ, Otsuga D, Alonso JM, Ecker JR, Drews GN, Clark SE. 2005. Class III homeodomain-leucine zipper gene family members have overlapping, antagonistic, and distinct roles in *Arabidopsis* development. *The Plant Cell* **17,** 61–76.

Prunet N, Morel P, Negrutiu I, Trehin C. 2009. Time to stop: flower meristem termination. *Plant Physiology* **150,** 1764–1772.

Prunet N, Morel P, Thierry A-M *et al.* 2008. *REBELOTE*, *SQUINT*, and *ULTRAPETALA1* function redundantly in the temporal regulation of floral meristem termination in *Arabidopsis thaliana*. *The Plant Cell* **20,** 901–919.

Putterill J, Robson F, Lee K, Simon R, Coupland G. 1995. The *CONSTANS* gene of *Arabidopsis* promotes flowering and encodes a protein showing similarities to zinc finger transcription factors. *Cell* **80,** 847–857.

Reinhart BJ, Liu T, Newell NR *et al.* 2013. Establishing a framework for the ad/abaxial regulatory network of *Arabidopsis*: ascertaining targets of class III homeodomain leucine zipper and KANADI regulation. *The Plant Cell* **25,** 3228–3249.

Reyes-Olalde JI, Zuniga-Mayo VM, Chavez Montes RA, Marsch-Martinez N, Folter S de. 2013. Inside the gynoecium: at the carpel margin. *Trends in plant science* **18,** 644–655.

Rodriguez K, Perales M, Snipes S, Yadav RK, Diaz-Mendoza M, Reddy GV. 2016. DNA-dependent homodimerization, sub-cellular partitioning, and protein destabilization control WUSCHEL levels

and spatial patterning. *Proceedings of the National Academy of Sciences of the United States of America* **113,** 6307-6315.

Romanel EAC, Schrago CG, Couñago RM, Russo CAM, Alves-Ferreira M. 2009. Evolution of the B3 DNA binding superfamily: new insights into REM family gene diversification. *PloS one* **4,** e5791.

Rose AS, Hildebrand PW. 2015. NGL Viewer: a web application for molecular visualization. *Nucleic Acids Research* **43,** 576-579.

Roth O, Alvarez JP, Levy M, Bowman JL, Ori N, Shani E. 2018. The KNOXI transcription factor SHOOT MERISTEMLESS regulates floral fate in *Arabidopsis*. *The Plant Cell* **30,** 1309–1321.

Rybel B de, **Mähönen AP, Helariutta Y, Weijers D.** 2016. Plant vascular development: from early specification to differentiation. *Nature reviews. Molecular cell biology* **17,** 30–40.

Samach A, Onouchi H, Gold S *et al.* 2000. Distinct roles of CONSTANS target genes in reproductive development of *Arabidopsis*. *Science* **288,** 1613–1616.

Santi L, Wang Y, Stile MR *et al.* 2003. The GA octodinucleotide repeat binding factor BBR participates in the transcriptional regulation of the homeobox gene *Bkn3*. *The Plant Journal* **34,** 813–826.

Santuari L, Sanchez-Perez GF, Luijten M *et al.* 2016. The *PLETHORA* gene regulatory network guides growth and cell differentiation in *Arabidopsis* roots. *The Plant Cell* **28,** 2937–2951.

Schlereth A, Möller B, Liu W *et al.* 2010. MONOPTEROS controls embryonic root initiation by regulating a mobile transcription factor. *Nature* **464,** 913–916.

Schmid M, Davison TS, Henz SR *et al.* 2005. A gene expression map of *Arabidopsis thaliana* development. *Nature Genetics* **37,** 501–506.

Schneider CA, Rasband WS, Eliceiri KW. 2012. NIH Image to ImageJ: 25 years of image analysis. *Nature Methods* **9,** 671–675.

Schwarz S, Grande AV, Bujdoso N, Saedler H, Huijser P. 2008. The microRNA regulated SBP-box genes *SPL9* and *SPL15* control shoot maturation in *Arabidopsis*. *Plant Molecular Biology* **67,** 183–195.

Sessions A, Nemhauser JL, McColl A, Roe JL, Feldmann KA, Zambryski PC. 1997. ETTIN patterns the *Arabidopsis* floral meristem and reproductive organs. *Development* **124,** 4481–4491.

Sessions A, Yanofsky MF. 1999. Dorsoventral patterning in plants. *Genes & Development* **13,** 1051–1054.

Sessions A, Yanofsky MF, Weigel D. 2000. Cell-cell signaling and movement by the floral transcription factors LEAFY and APETALA1. *Science* **289,** 779–781.

Shamimuzzaman M, Vodkin L. 2013. Genome-wide identification of binding sites for NAC and YABBY transcription factors and co-regulated genes during soybean seedling development by ChIP-Seq and RNA-Seq. *BMC genomics* **14**.

Shannon P, Markiel A, Ozier O *et al.* 2003. Cytoscape: a software environment for integrated models of biomolecular interaction networks. *Genome research* **13,** 2498–2504.

Shi H, Chan Z. 2014. The cysteine2/histidine2-type transcription factor ZINC FINGER OF ARABIDOPSIS THALIANA 6-activated C-REPEAT-BINDING FACTOR pathway is essential for melatonin-mediated freezing stress resistance in *Arabidopsis*. *Journal of pineal research* **57,** 185–191.

Shi H, Wang X, Ye T *et al.* 2014. The cysteine2/histidine2-type transcription factor *ZINC FINGER OF ARABIDOPSIS THALIANA6* modulates biotic and abiotic stress responses by activating salicylic acid-related genes and *C-REPEAT-BINDING FACTOR* genes in *Arabidopsis*. *Plant physiology* **165,** 1367–1379.

Siegfried KR, Eshed Y, Baum SF, Otsuga D, Drews GN, Bowman JL. 1999. Members of the *YABBY* genes family specify abaxial cell fate in *Arabidopsis*. *Development* **126,** 4117–4128.

Simmons AR, Bergmann DC. 2016. Transcriptional control of cell fate in the stomatal lineage. *Current opinion in plant biology* **29,** 1–8.

Simonini S, Kater MM. 2014. Class I BASIC PENTACYSTEINE factors regulate HOMEOBOX genes involved in meristem size maintenance. *Journal of experimental botany* **65,** 1455–1465.

Smith HMS, Ung N, Lal S, Courtier J. 2011. Specification of reproductive meristems requires the combined function of SHOOT MERISTEMLESS and floral integrators FLOWERING LOCUS T and FD during *Arabidopsis* inflorescence development. *Journal of experimental botany* **62,** 583–593.

Smyth DR, Bowman JL, Meyerowitz EM. 1990. Early flower development in *Arabidopsis*. *The Plant Cell* **2,** 755–767.

Soltis DE, Chanderbali AS, Kim S, Buzgo M, Soltis PS. 2007. The ABC model and its applicability to basal angiosperms. *Annals of botany* **100,** 155–163.

Spinelli SV, Martin AP, Viola IL, Gonzalez DH, Palatnik JF. 2011. A mechanistic link between STM and CUC1 during *Arabidopsis* development. *Plant physiology* **156,** 1894–1904.

Stahl Y, Grabowski S, Bleckmann A *et al.* 2013. Moderation of *Arabidopsis* root stemness by CLAVATA1 and ARABIDOPSIS CRINKLY4 receptor kinase complexes. *Current Biology* **23,** 362–371.

Stahl Y, Simon R. 2013. Gated communities: apoplastic and symplastic signals converge at plasmodesmata to control cell fates. *Journal of Experimental Botany* **64,** 5237–5241.

Stahle MI, Kuehlich J, Staron L, Arnim AG von, **Golz JF.** 2009. YABBYs and the transcriptional corepressors LEUNIG and LEUNIG HOMOLOG maintain leaf polarity and meristem activity in *Arabidopsis*. *The Plant Cell* **21,** 3105–3118.

Ståldal V, Sohlberg JJ, Eklund DM, Ljung K, Sundberg E. 2008. Auxin can act independently of CRC, LUG, SEU, SPT and STY1 in style development but not apical-basal patterning of the *Arabidopsis* gynoecium. *The New phytologist* **180,** 798–808.

Strabala TJ, O'donnell PJ, Smit A-M *et al.* 2006. Gain-of-function phenotypes of many *CLAVATA3/ESR* genes, including four new family members, correlate with tandem variations in the conserved CLAVATA3/ESR domain. *Plant Physiology* **140,** 1331–1344.

Strable J, Vollbrecht E. 2019. Maize *YABBY* genes *drooping leaf1* and *drooping leaf2* regulate floret development and floral meristem determinacy. *Development* **146**.

Suárez-López P, Wheatley K, Robson F, Onouchi H, Valverde F, Coupland G. 2001. CONSTANS mediates between the circadian clock and the control of flowering in Arabidopsis. *Nature* **410,** 1116–1120.

Sun B, Ito T. 2015. Regulation of floral stem cell termination in *Arabidopsis*. *Frontiers in Plant Science* **6**.

Swanson R, Clark T, Preuss D. 2005. Expression profiling of *Arabidopsis* stigma tissue identifies stigma-specific genes. *Sexual Plant Reproduction* **18,** 163–171.

Taiz L, Zeiger E. 2010. *Plant physiology,* 5. ed. Sunderland, Mass.: Sinauer Assoc.

Tatematsu K, Toyokura K, Miyashima S, Nakajima K, Okada K. 2015. A molecular mechanism that confines the activity pattern of miR165 in *Arabidopsis* leaf primordia. *The Plant Journal* **82,** 596–608.

Tekleyohans DG. 2014. Functional and molecular characterization of B_{sister} genes in the two model species: *Arabidopsis thaliana* and *Eschscholzia californica*, Justus-Liebig-Universität Giessen, Giessen.

Teytelman L, Ozaydin B, Zill O *et al.* 2009. Impact of chromatin structures on DNA processing for genomic analyses. *PloS one* **4**.

The Arabidopsis Genome Initiative. 2000. Analysis of the genome sequence of the flowering plant *Arabidopsis thaliana*. *Nature* **408,** 796–815.

Theißen G. 2001. Development of floral organ identity: stories from the MADS house. *Current opinion in plant biology* **4,** 75–85.

Theißen G, Melzer R, Rümpler F. 2016. MADS-domain transcription factors and the floral quartet model of flower development: Linking plant development and evolution. *Development* **143,** 3259–3271.

Thieme CJ, Rojas-Triana M, Stecyk E *et al.* 2015. Endogenous *Arabidopsis* messenger RNAs transported to distant tissues. *Nature Plants* **1**.

Toriba T, Hirano H-Y. 2014. The *DROOPING LEAF* and *OsETTIN2* genes promote awn development in rice. *The Plant Journal* **77,** 616–626.

Trigg SA, Garza RM, MacWilliams A *et al.* 2017. CrY2H-seq: A massively multiplexed assay for deep-coverage interactome mapping. *Nature methods* **14,** 819–825.

Trigueros M, Navarrete-Gómez M, Sato S *et al.* 2009. The *NGATHA* genes direct style development in the *Arabidopsis* gynoecium. *The Plant Cell* **21,** 1394–1409.

Urbanus SL, Martinelli AP, Peter Dinh QD *et al.* 2010. Intercellular transport of epidermis-expressed MADS domain transcription factors and their effect on plant morphology and floral transition. *The Plant Journal,* 60–72.

Usadel B, Obayashi T, Mutwil M *et al.* 2009. Co-expression tools for plant biology: opportunities for hypothesis generation and caveats. *Plant, cell & environment* **32,** 1633–1651.

Vroemen CW. 2003. The *CUP-SHAPED COTYLEDON3* gene is required for boundary and shoot meristem formation in *Arabidopsis*. *The Plant Cell* **15,** 1563–1577.

Wada T, Kurata T, Tominaga R *et al.* 2002. Role of a positive regulator of root hair development, *CAPRICE*, in *Arabidopsis* root epidermal cell differentiation. *Development* **129,** 5409–5419.

Wahl V, Brand LH, Guo Y-L, Schmid M. 2010. The FANTASTIC FOUR proteins influence shoot meristem size in *Arabidopsis thaliana*. *BMC plant biology* **10**.

Wang H, Qi M, Cutler AJ. 1993. A simple method of preparing plant samples for PCR. *Nucleic Acids Research* **21,** 4153–4154.

Wege S, Scholz A, Gleissberg S, Becker A. 2007. Highly efficient virus-induced gene silencing (VIGS) in California poppy (*Eschscholzia californica*): an evaluation of VIGS as a strategy to obtain functional data from non-model plants. *Annals of botany* **100,** 641–649.

Weigel D, Glazebrook J. 2002. *Arabidopsis: A laboratory manual*. Cold Spring Harbor, NY: Cold Spring Harbor Laboratory Press.

Wenkel S, Emery J, Hou B-H, Evans MMS, Barton MK. 2007. A feedback regulatory module formed by LITTLE ZIPPER and HD-ZIPIII genes. *The Plant Cell* **19,** 3379–3390.

Wigge PA, Kim MC, Jaeger KE *et al.* 2005. Integration of spatial and temporal information during floral induction in *Arabidopsis*. *Science* **309,** 1056–1059.

Winter N, Kragler F. 2018. Conceptual and methodological considerations on mRNA and proteins as intercellular and long-distance signals. *Plant & cell physiology* **59,** 1700–1713.

Wu F, Shi X, Lin X *et al.* 2017. The ABCs of flower development: mutational analysis of *AP1/FUL*-like genes in rice provides evidence for a homeotic (A)-function in grasses. *The Plant Journal* **89,** 310–324.

Wu G, Lin W-C, Huang T, Poethig RS, Springer PS, Kerstetter RA. 2008. KANADI1 regulates adaxial-abaxial polarity in *Arabidopsis* by directly repressing the transcription of *ASYMMETRIC LEAVES2*. *Proceedings of the National Academy of Sciences of the United States of America* **105,** 16392–16397.

Wu X, Dinneny JR, Crawford KM *et al.* 2003. Modes of intercellular transcription factor movement in the *Arabidopsis* apex. *Development* **130,** 3735–3745.

Xu XM, Jackson D. 2010. Lights at the end of the tunnel: new views of plasmodesmal structure and function. *Current opinion in plant biology* **13,** 684–692.

Xu XM, Wang J, Xuan Z *et al.* 2011. Chaperonins facilitate KNOTTED1 cell-to-cell trafficking and stem cell function. *Science* **333,** 1141–1144.

Yadav RK, Perales M, Gruel J, Girke T, Jonsson H, Reddy GV. 2011. WUSCHEL protein movement mediates stem cell homeostasis in the *Arabidopsis* shoot apex. *Genes & Development* **25,** 2025–2030.

Yaginuma H, Hirakawa Y, Kondo Y, Ohashi-Ito K, Fukuda H. 2011. A novel function of TDIF-related peptides: promotion of axillary bud formation. *Plant & cell physiology* **52,** 1354–1364.

Yamaguchi N, Huang J, Tatsumi Y *et al.* 2018. Chromatin-mediated feed-forward auxin biosynthesis in floral meristem determinacy. *Nature communications* **9**.

Yamaguchi N, Huang J, Xu Y, Tanoi K, Ito T. 2017. Fine-tuning of auxin homeostasis governs the transition from floral stem cell maintenance to gynoecium formation. *Nature communications* **8**.

Yamaguchi YL, Ishida T, Sawa S. 2016. CLE peptides and their signaling pathways in plant development. *Journal of experimental botany* **67,** 4813–4826.

Yan Z, Liu X, Ljung K *et al.* 2017. Type B response regulators act as central integrators in transcriptional control of the auxin biosynthesis enzyme TAA1. *Plant physiology* **175,** 1438–1454.

Yang C, Ma Y, Li J. 2016. The rice *YABBY4* gene regulates plant growth and development through modulating the gibberellin pathway. *Journal of experimental botany* **67,** 5545–5556.

Zhang T-Q, Lian H, Zhou C-M, Xu L, Jiao Y, Wang J-W. 2017. A two-step model for *de novo* activation of *WUSCHEL* during plant shoot regeneration. *The Plant Cell* **29,** 1073–1087.

Zhao Y, Christensen SK, Fankhauser C *et al.* 2001. A role for flavin monooxygenase-like enzymes in auxin biosynthesis. *Science* **291,** 306–309.

Zhou G-K, Kubo M, Zhong R, Demura T, Ye Z-H. 2007. Overexpression of miR165 affects apical meristem formation, organ polarity establishment and vascular development in *Arabidopsis*. *Plant and Cell Physiology* **48,** 391–404.

Zhou Y, an Yan, Han H *et al.* 2018. HAIRY MERISTEM with WUSCHEL confines *CLAVATA3* expression to the outer apical meristem layers. *Science* **361,** 502–506.

Acknowledgements

Mein besonderer Dank gilt meiner Betreuerin Prof. Dr. Annette Becker für all ihre Unterstützung in den letzten Jahren und für ihre hin und wieder notwendigen Motivationsanschübe, damit das Ganze mal zu Ende kam.

Bei Prof. Dr. Sandra Hake möchte ich mich dafür bedanken, dass sie sich bereit erklärt hat das Zweitgutachten zu dieser Arbeit zu schreiben.

Desweiteren möchte ich mich bei Dr. Katrin Ehlers bedanken, über die ich erst in diesen Teil der Botanik gelangt bin und die sich mit Annette und mir zusammengesetzt hat, um das CRC Projekt zu planen.

Bei meinen Kollegen Denise Herbert, Anna Barbara Dommes, Dominik Lotz, Kimmo Kivivirta, Andrea Weisert und Claudia Jung-Blasini bedanke ich mich für fünf großartige Jahre.

Ganz besonders möche ich mich bei Denise, Anna Barbara und Jessica Reichert bedanken, die sich die Mühe gemacht haben diese Arbeit vor allen anderen zu lesen um schlimmeres zu verhindern und mit vielen Tips und Anregungen geholfen haben sie zu verbessern.

Außerdem möchte ich mich nochmals bei Anna und Kimmo bedanken, dass ich einen Teil ihrer Arbeiten benutzen durfte. Vielen Dank an Denise und Herman Finke, die die Geduld hatten mir Bioinformatik für Anfänger zu erklären.

Für viele lustige Stunden und vor allem für die Einführung in die Botanik möchte ich mich bei der gesamten AG Spezielle Botanik bedanken. Ohne die Unterstützung von Volker Wissemann und Birgit Gemeinholzer wäre ich nicht da, wo ich heute bin.

Ebenso möchte ich mich bei Dietmar Haffer bedanken ohne welchen die meisten meiner Pflanzen nie zur Blüte gekommen wären sowie bei den Studenten Verena, Dennis, Larissa, David, Julian, Constanze, Marie, Vanessa, Evgenia und Steffi für ihre Mithilfe am Projekt.

Meiner Familie danke ich für ihre Unterstützung, Aufmunterung, Motivation, und immer-da-sein. Und natürlich Mathieu für drei wundervolle gemeinsame Jahre.

Appendix

Detailed List of CRC Regulators

Locus	Name	Family	Function
AT1G10120	CIB4	bHLH	Flower development
AT1G23420	INO	C2C2-YABBY	Flower development
AT1G24260	SEP3	MADS	Flower development
AT1G25330	HAF	bHLH	Flower development
AT1G26310	CAL	MADS	Flower development
AT1G47655		C2C2-Dof	unknown function
AT1G50680		AP2-EREBP	Stress
AT1G54160	NF-YA5	CCAAT	Flower development
AT1G54830	NF-YC3	CCAAT	Growth
AT1G59750	ARF1	ARF	Senescence
AT1G67260	TCP1	TCP	Growth
AT1G68670	HHO2	G2-like	Metabolism
AT1G68920	CIL1	bHLH	Flower development
AT1G76420	CUC3	NAC	Growth
AT1G76580		SBP	unknown function
AT2G03710	SEP4	MADS	Flower development
AT2G26580	YAB5	C2C2-YABBY	Flower development
AT2G33860	ETT	ARF	Flower development
AT2G38880	NF-YB1	CCAAT	Stress
AT2G41690	HSFB3	HSF	unknown function
AT2G42400	VOZ2	VOZ	Flower development
AT3G06740	GATA15	C2C2-GATA	unknown function
AT3G07340	CIB3	bHLH	Flower development
AT3G16870	GATA17	C2C2-GATA	unknown function
AT3G20910	NF-YA9	CCAAT	Growth
AT3G24050	GATA1	C2C2-GATA	Circadian clock
AT3G25730	EDF3	AP2-EREBP	Flower development
AT3G27010	TCP20	TCP	Metabolism
AT3G28910	MYB30	MYB	Flower development
AT3G30260	AGL79	MADS	unknown function
AT3G50870	HAN	C2C2-GATA	Flower development
AT3G51080	GATA6	C2C2-GATA	unknown function
AT3G60390	HAT3	HB	unknown function
AT3G60530	GATA4	C2C2-GATA	unknown function
AT4G02670	IDD12	C2H2	unknown function
AT4G08150	KNAT1/BP	HB	Flower development
AT4G11070	WRKY41	WRKY	Stress
AT4G16780	HAT4	HB	Growth
AT4G28790	bHLH23	bHLH	unknown function
AT4G36900	DEAR4	AP2-EREBP	unknown function

AT4G40060	ATHB16	HB	Flower development
AT5G02840	RVE4	MYB-related	Circadian clock
AT5G04340	ZAT6	C2H2	Stress
AT5G37020	ARF8	ARF	Flower development
AT5G50915		bHLH	Growth
AT5G60910	FUL	MADS	Flower development
AT5G63790	NAC102	NAC	Stress
AT5G65310	ATHB5	HB	Growth
AT1G02220	NAC003	NAC	unknown function
AT1G13880	ELM2	MYB-related	unknown function
AT1G14685	BPC2	BBR/BPC	Growth
AT1G16490	MYB58	MYB	Growth
AT1G20900	ESC	AT-Hook	Growth
AT1G43850	SEU	ABI3VP1	Flower development
AT1G46408	AGL97	MADS	unknown function
AT1G65360	AGL23	MADS	Embryo development
AT1G68480	JAG	C2H2	Flower development
AT1G69580		G2-like	unknown function
AT1G75710		C2H2	unknown function
AT1G76510		ARID	unknown function
AT2G14760		bHLH	Flower development
AT2G16770	BZIP23	bZIP	Stress
AT2G17770	BZIP27	bZIP	Flower development
AT2G24840	AGL61	MADS	Embryo development
AT2G28540		unknown	unknown function
AT2G31380	STH	Orphans	Growth
AT2G35270	GIK	AT-Hook	Flower development
AT2G35430		C3H	unknown function
AT2G37060	NF-YB8	CCAAT	unknown function
AT2G39880	MYB25	MYB	unknown function
AT2G42300		bHLH	unknown function
AT2G45160	HAM	GRAS	Growth
AT3G01530	MYB57	MYB	Flower development
AT3G08500	MYB83	MYB	Growth
AT3G11100	VFP3	Trihelix	Growth
AT3G16500	PAP1	AUX/IAA	Metabolism
AT3G18650	AGL103	MADS	Embryo development
AT3G19360		C3H	unknown function
AT3G20640		CCAAT	unknown function
AT3G24140	FAMA	bHLH	Growth
AT3G25710	TMO5	bHLH	Embryo development
AT3G26640	LWD2	WD40	Circadian clock
AT3G45260	BIB	C2H2	Growth
AT3G55560	AHL15	AT-Hook	Growth
AT3G57180	BPG2	unknown	Stress
AT3G58630		Trihelix	unknown function
AT3G58680	MBF1B	MBF1	unknown function

AT3G61950	bHLH67	bHLH	unknown function
AT3G61970	NGA2	ABI3VP1	Flower development
AT4G24440		C2C2-GATA	unknown function
AT4G28190	ULT1	ULT	Flower development
AT4G30180		unknown	unknown function
AT4G31420	REIL1	C2H2	Growth
AT4G32551	LUG	LUG	Flower development
AT4G35700	DAZ3	C2H2	Flower development
AT4G36740	ATHB40	HB	unknown function
AT4G38960	BBX19	Orphans	Flower development
AT5G01200		MYB	unknown function
AT5G02030	RPL	HB	Flower development
AT5G05830		PHD	unknown function
AT5G06160	ATO	C2H2	Embryo development
AT5G08190	NF-YB12	CCAAT	unknown function
AT5G09460	SACL1	bHLH	unknown function
AT5G09780	REM25	ABI3VP1	unknown function
AT5G11270	OCP3	HD	Stress
AT5G14000	NAC084	NAC	unknown function
AT5G18090		ABI3VP1	unknown function
AT5G22290	ANAC089	NAC	Flower development
AT5G25890	IAA28	AUX/IAA	Growth
AT5G39750	AGL81	MADS	Embryo development
AT5G45580		G2-like	unknown function
AT5G49420		MADS	Embryo development
AT5G49490	AGL83	MADS	Embryo development
AT5G49700	AHL17	AT-Hook	unknown function
AT5G53660	GRF7	GRF	Growth
AT5G56840		MYB-related	unknown function
AT5G56900		C3H	unknown function
AT5G57660	COL5	C2C2-CO-like	Flower development
AT5G61470		C2H2	unknown function
AT1G01030	NGA3	ABI3VP1	Flower development
AT1G08010	GATA11	C2C2-GATA	unknown function
AT1G12630		AP2-EREBP	unknown function
AT1G53170	ERF8	AP2-EREBP	Growth
AT1G54060	ASIL1	Trihelix	Growth
AT1G68800	TCP12	TCP	Growth
AT1G69010	BIM2	bHLH	Growth
AT1G72360	ERF73	AP2-EREBP	Stress
AT2G18380	HANL1	C2C2-GATA	unknown function
AT2G40220	ABI4	AP2-EREBP	Stress
AT2G40970	MYBC1	G2-like	unknown function
AT2G41940	ZFP8	C2H2	Growth
AT3G23240	ERF1	AP2-EREBP	Stress
AT3G61630	CRF6	AP2-EREBP	Embryo development
AT4G13620		AP2-EREBP	unknown function

AT4G28140		AP2-EREBP	Stress
AT4G32040	KNAT5	HB	Growth
AT5G13790	AGL15	MADS	Growth
AT5G13910	LEP	AP2-EREBP	Growth
AT5G52020		AP2-EREBP	unknown function
AT5G61890	ERF114	AP2-EREBP	unknown function
AT1G76710	ASHH1	Methyltransferase	unknown function
AT2G20760	CLC1	Clathrin light chain protein	Metabolism
AT2G30410	KIESEL	Tubulin binding cofactor A	Embryo development
AT3G05155		Major facilitator superfamily protein	Metabolism
AT4G30860	ASHR3	trxG	unknown function
AT4G33540		Metallo b-lactamase	unknown function
AT5G63730	ARI14	E3 Ligase	unknown function

Activity of *proCRC* in Mutants of Putative Regulators of CRC Expression

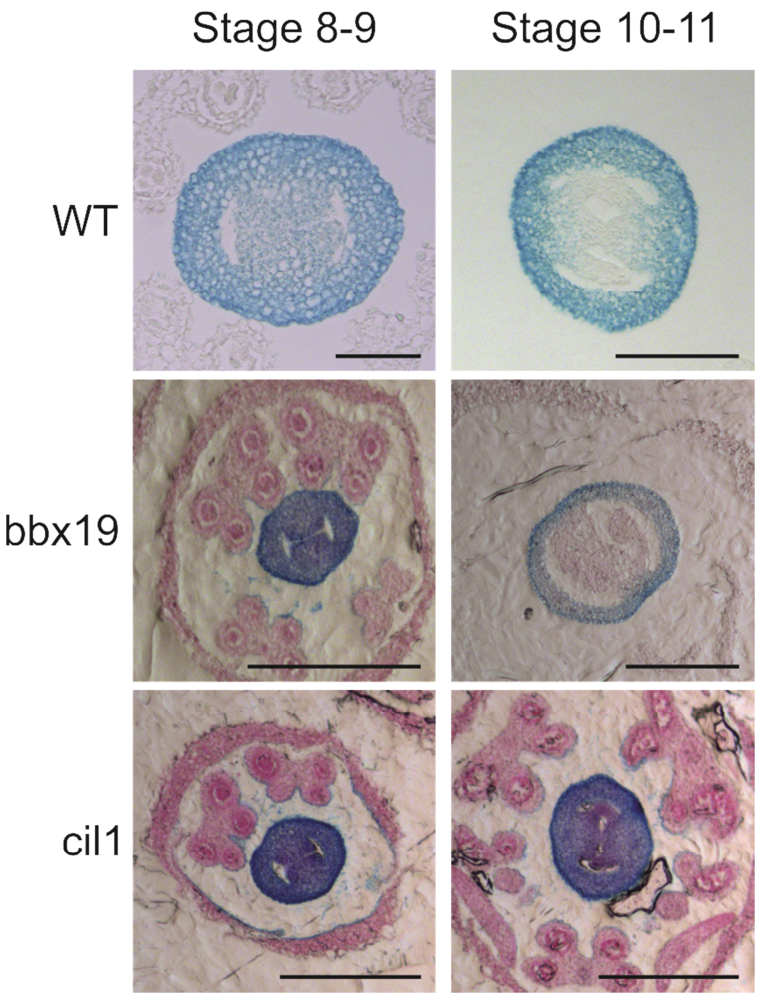

Figure 33: Activity of *proCRC* in *bbx19* and *cil1* mutants visualized by GUS stainings. Scalebars represent for WT samples 50 µm and 100 µm, for all other samples 200 µm.

Co-expression Analyzes

Table 11: Shared genes of PlaNet and Expression Angler co-expression analysis.

Locus	Name
AT1G03170	FAF2
AT1G53160	FTM6
AT1G69120	AP1
AT2G16210	REM24
AT2G33810	SPL3
AT2G35310	REM23
AT2G42200	SPL9
AT3G06160	
AT3G06220	
AT4G34400	
AT5G20240	PI
AT5G60910	FUL

Table 12: Shared genes of PlaNet and RNA-seq co-expression analysis.

Locus	Gene
AT1G25330	HAF
AT1G53160	FTM6
AT2G33810	SPL3
AT2G35310	REM23
AT2G42200	SPL9
AT3G06160	
AT3G06220	
AT3G61250	LMI2
AT4G34400	TFS1
AT5G20240	PI
AT5G60910	FUL

CRC Expression in Knock-out and Knock-down Plants

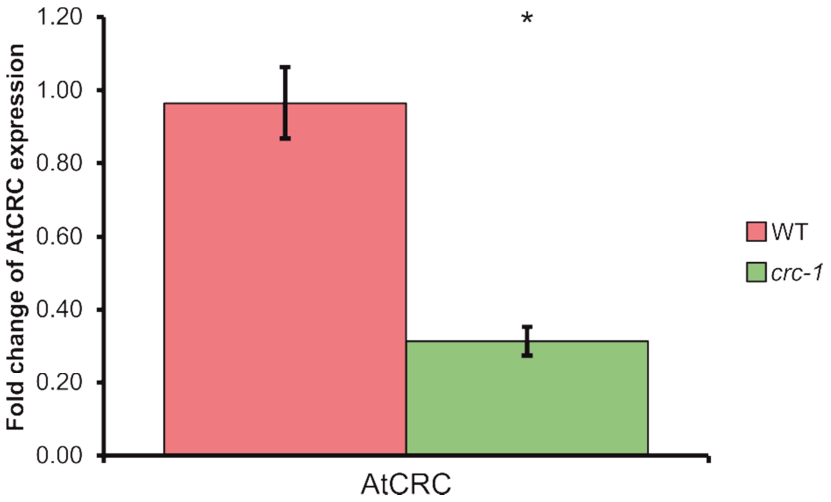

Figure 34: Expression analysis of CRC in buds of *A. thaliana* in wild type and *crc-1* plants. The fold changes of expression were calculated using the ΔΔCt method according to Pfaffl (2001) and error bars represent the standard deviation of the mean. Asterisks indicate significant ($p < 0.05$) differences compared to the wild type.

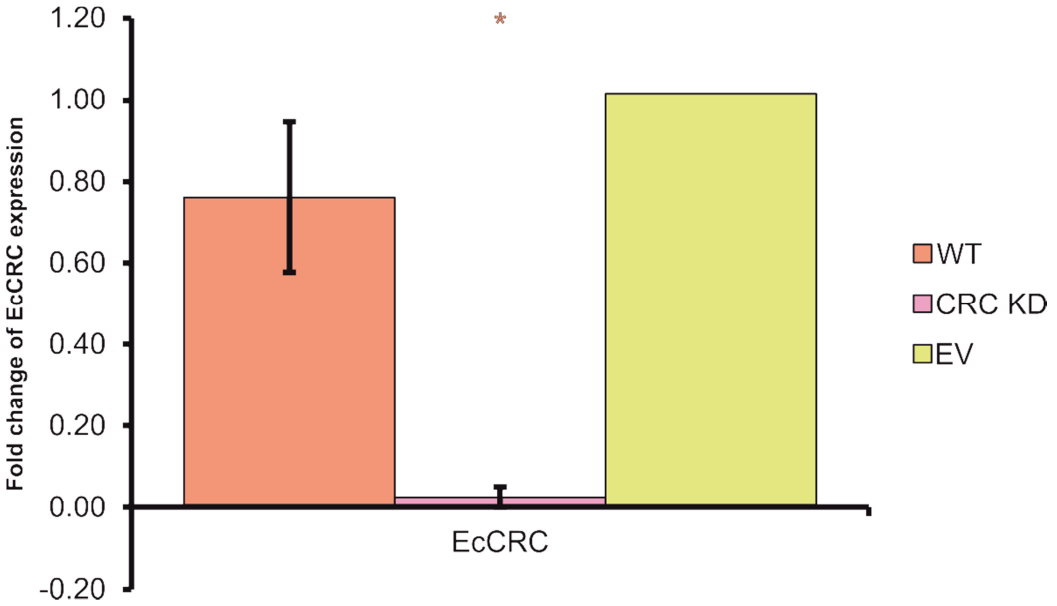

Figure 35: Expression analysis of EcCRC in buds of *E. californica* in wild type, CRC knock down plants, and empty vector control plants. The fold changes of expression were calculated using the ΔΔCt method according to Pfaffl (2001) and error bars represent the standard deviation of the mean (calculated if possible). Asterisks indicate significant differences ($p < 0.05$) compared to the wild type (orange asterisks) or to the empty vector control (yellow asterisks).

Localization of CRC During Late Carpel Development

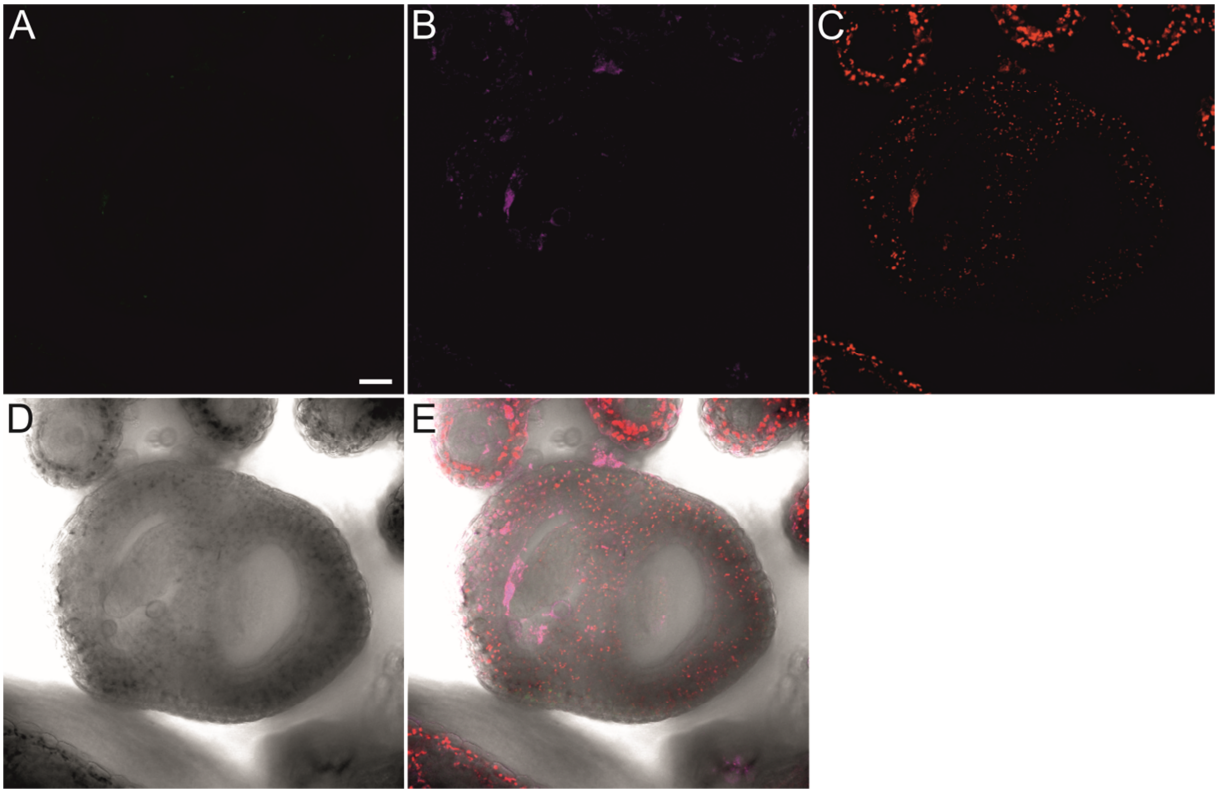

Figure 36: Absence of CRC-GFP in a stage 11-12 gynoecium. CRC-GFP, 3xmCherry, and chlorophyll were detected by CLSM. In addition a transmission image was taken and an overlay was made out of the different individual images. False colors were assigned to GFP (green), 3xmCherry (magenta), chlorophyll (red), and transmission (grey). Scale bar represent 20 µm.

List of Primers

Table 13: List of primers used in this study. If not otherwise stated, primers were made in this study.

Used in	Primer	Sequence (5' -> 3')	Published
proCRC cloning	pCRC Fw Hind	ATTAAAGCTTCCGATCGAGGTTAGGAAA	
	pCRC Rv Kpn	TCTAGGTACCGGTCTTTAGCGAATGGATTG	
	pAbAi Seq	GTTCCTTATATGTAGCTTTCGACAT	
	pCRC Seq 2	TTCTAACTTTGAGAGCAAACTTC	
	pCRC Seq 3	ATGTGTCTGAAGAAGATTCATTG	
	pCRC Seq 4	AAGATTTTGCAGAGGGAGG	
	pCRC Seq 5	GTTGTACCACTAAAACACC	

	SDM pCRC Fw	TATATATATATGTCATCGTCTCACTATGATTGTTC	
	SDM pCRC Rv	TAGAGAGAGAGAGAGAGAGCGATACAG	
	A pCRC Fw BsaI	AACAGGTCTCAACCTCCGATCGAGGTTAGGAAA	
	A pCRC Rv BsaI	AACAGGTCTCATGTTGGTCTTTAGCGAATGGATTG	
	pUBQ10 Seq Fw	TGTGATTTCTATCTAGATCTGG	
	pMAS:Basta Rv Seq	TTACGTCACGTCTTGCGCA	
	pCRC Frag 1 Rv	ACATCTCGAGTAAACTTCCCTGAGCGATCT	
	pCRC Frag 2 Fw H	ACATAAGCTTATTTCTTGTTTTTCTAATTAGGG	
	pCRC Frag 2 Rv	ACATCTCGAGGAGATGGGACGATTGCC	
	pCRC Frag 3 Fw H	ACATAAGCTTTAAACCCTAATTTCTTATTAGC	
	pCRC Frag 3 Rv	ACATCTCGAGGAAGAAAACATGAATAACTAACTA	
	pCRC Frag 4 Fw H	ACATAAGCTTGTTGATTTTGGAATTAGACTACC	
	pCRC Frag 4 Rv	ACATCTCGAGCGCTTTATTGTTGAAATTTGAGA	
	pCRC Frag 5 Fw	ACATAAGCTTCATCTTCTCTATAATTAGTATGC	
	pCRC Frag 5 Rv	ACATCTCGAGGGTCCTTTCCTGATCTTTTG	
	pCRC Frag 6 Fw	ACATAAGCTTCTCAGTTTTGCAGTGAAATC	
	pCRC Frag 6 Rv	ACATCTCGAGCTGCAAAATCTTGCAGACG	
	pCRC Frag 7 Fw	ACATAAGCTTAGTGACATTTAGGGTCTTG	
	pCRC Frag 7 Rv	ACATCTCGAGAACAACATTTAATATCATCTTATC	
	pCRC Frag 8 Fw	ACATAAGCTTCTCGTGTCTACACCAGAAT	
	pCRC E Fw Hind	ACATAAGCTTTCATTCAATAATTAAGTCGACTAAGC	
	pCRC E Rv Xho	ACATCTCGAGATCTCATCATTGGCATTAAGAGAC	
	pCRC C Fw Hind	ACATAAGCTTAATGTATGTATAGTTGGATGTGTC	
	pCRC C Rv Xho	ACATCTCGAGATGGTGTGAATATGATTACATTTAT	
	pCRC A Fw Hind	ACATAAGCTTCTCGTGTCTACACCAGAAG	
	tRBCS Rv	TTCCATTTCACAGTTCGATAGC	

	terUBQ10 Rv	TTCATCAGGGATTATACAAGGC	
Y1H library sequencing	AD Rv Mitsuda	CGTTTTAAAACCTAAGAGTCAC	Mitsuda *et al.* (2010)
	AD Fw Mitsuda	ATTCGATGATGAAGATACCCC	Mitsuda *et al.* (2010)
Salk line genotyping	LBb1.3 tDNA	ATTTTGCCGATTTCGGAAC	Alonso *et al.* (2003)
	IDD12 LP	GGTCGCATGTTCTTGTTTTTG	
	IDD12 RP	TCCTATGTCGGCGTACGATAC	
	MYB30 LP	TCCTTGTTGTGACAAAGGAGG	
	MYB30 RP	ATGATCAGGTGAAACACCAGC	
	STH LP	AGCCCAGAAAGAGAACTGAGG	
	STH RP	GCCTTTTGTTTCTTTCCCTTG	
	AGF2 LP	CAGGAAGAGAATCCGAAAACC	
	AGF2 RP	CACCACTCTCTTTGCATATAATCC	
	PAP1 LP	AATGCCTCACCCATTTCTTG	
	PAP1 RP	TTCTTGGACAACCTTCCATTG	
	NF-YA9 LP	TGGCTATTGTTGTTGTCATGC	
	NF-YA9 RP	AACTGTGAACGCATCACACTG	
	NF-YB8 LP	CTAAGCCCATTGATATCGTCG	
	NF-YB8 RP	CTGCACGTATTCTCTCTTCCG	
	TMO5 LP	TTTGCCTCTTAATACCCCCTG	
	TMO5 RP	TGAGTGCACAAGAAGTCATGG	
	FUL LP	AATTGTCCTTCTTGCTGACCC	
	FUL RP	CGATCGAGAAGTTGAGTTTGG	
	HAT4 LP	AGACCCAGATCGTCTTTCTCG	
	HAT4 RP	AAAGTAAAACTCATGCGGTCG	
	ATHB5 LP	AGAGGAAAGTGAAGCTGGCTC	
	ATHB5 RP	TGAGTAATGCATTTTCCGACC	
	ATHB16 LP	CACACATTGAATCTGAGCTGC	
	ATHB16 RP	ATTGTCTCTCGGAAAAGCTCC	
	RVE4 LP	CTGCAGAGGAAGGTCATGAAC	
	RVE4 RP	CCTGTTAACCCTAATCTCGCC	
	BBX19 LP	ATGGGGCCTTTGCATATTAAG	
	BBX19 RP	AATGAACTTCCCACACTCGTG	
	CIL1 LP	TTTCCGTCGTAACAACGAATC	
	CIL1 RP	CTAGTACCGGGTTGCAACAAG	
	AGL83 LP	GATCTGTGCATCGGAGAGAAG	
	AGL83 RP	GTCTTGTAGCGCAAACTACGC	
	AGL23 LP	TCCTTTAACCAATCATTGGTACC	
	AGL23 RP	ACCACCACTAACAGTTGCTGG	
	AGL81 LP	TTACATTTCCGCCCTAACTCC	
	AGL81 RP	TTGCTTTCTTCTCCAAGTTCG	
	VOZ2 LP	CTCTTGTCGTCTGCTGTCTCC	
	VOZ2 RP	AAGTGTGCACTATGGGATTGC	
	Haf-x8	CATCAAGCATCACTGCCATT	Crawford and Yanofsky (2011)
	DS3-2	CGATTACCGTATTTATCCCGTTC	Crawford and Yanofsky (2011)
	BEE1 Fw	CCCGGAAACTCTCCAGACAGTAGTA	Crawford and

		ACAA	Yanofsky (2011)
	BEE1 Rv	CCTTATAACATCCGGGCACCATATC TTGCA	Crawford and Yanofsky (2011)
	BEE3 Fw	CTCTACCTCTTCTGCTCAAGTTTCCA TAAA	Crawford and Yanofsky (2011)
	BEE3 Rv	AATCATAGCAAACATCACCAGTCTT ACGAG	Crawford and Yanofsky (2011)
	ETT LP	TGCATAGATGTCCCTTCCTTG	
	ETT RP	GGATGAGATTTAAAGCGAGGG	
	ARF8 LP	AACCGTTGTCACTTCCACAAG	
	ARF8 RP	CTTTGGGTCAAAAAGAAAGGG	
	RPL LP	TTGGAACCAAGTTCAAACTCG	
	RPL RP	ATGTTCACAGTTTTTGGTCGG	
	SEU LP	AACACAACCTGCCAACATTTC	
	SEU RP	CTTGTGGAATGAAATTTTGCG	
	KNAT1 LP	GAGTTTCCAGCTTCTGACACG	
	KNAT1 RP	TCCAATCAACAAACAATGCAG	
	LUG LP	TTAACATGGAGACGCAAAACC	
	LUG RP	TGGGTTGAAGATTCTGAATGC	
	YAB5 LP	GTGTAGGTGAATGTCCCATGC	
	YAB5 RP	GTACGCAGAAGGTACTCGCTG	
	GIK LP	TCACCAACTACGTTACCTCCG	
	GIK RP	AATCCCATTTTAGTCCGTGTTG	
	INO LP	AAGCTCTGCCTTTCCTTTGTC	
	INO RP	TGTCATTTTCCAAAGCAAACC	
	ULT1 LP	TTTGACAATGGAACCTTTTCG	
	ULT1 RP	TCTTCTCTTCTCCCGAAAAGC	
	NGA2 LP	GTCGTCAGGTCCTAACGTTTC	
	NGA2 RP	ATGGTGGTGGATGAGATTGAC	
Expression analysis via qRT-PCR	qPCR AtKAN1 Fw	GCCATGAAAGAGCAACTCCA	
	qPCR AtKAN1 Rv	GAACTTCGTTTCCATTTATGCCC	
	qPCR AtKAN2 Fw	GCCATGAAAGAGCAACACCT	
	qPCR AtKAN2 Rv	CTTTGTCGGTTGTCTTCACTG	
	qPCR AtKAN3 Fw	TCACATTGGCTCATGTTAAATCCC	
	qPCR AtKAN3 Rv	AACCGAGCTTCACTTGAGGA	
	qPCR AtWOX1 Fw	AAAGATCCTCCAGGTTACAAGGT	
	qPCR AtWOX1 Rv	CTCCACCCGTATATTCGCTG	
	qPCR PRS Fw	CCCATGTGTCTTCCTCATCAG	
	qPCR PRS Rv	TCATCATCCAATCTCGACCGT	

	qPCR Ec mir166 A Fw	GGAAGCTATCTTTTTTGAGG	
	qPCR Ec mir166 A Rv	GGAAACAATCAAGAAATCAATCTTT	
	qPCR Ec mir166 D Fw	AGTTGAGGGGAATGTTGTCTGG	
	qPCR Ec mir166 D Rv	AATGAAGCCTGGTCCGAAATC	
	qPCR Ec mir166 A Fw	GAGGGGAATGTTGTCTGGC	
	qPCR Ec mir165 A Rv	GCCTGGTCCGAAATCATTC	
	qPCR mir166 G Fw	GGGTTTAGAGGAATGTTGTTTGG	
	qPCR mir166 G Rv	GGGAATGAAGCCTGGTCC	
	qPCR mir166 F Fw	GTGAATGATGCCTGGCTCG	
	qPCR mir166 F Rv	GGGAATGAAGCCTGGTCC	
	qPCR mir165 B Fw	GGAATGTTGTTTGGATCGAGG	
	qPCR mir165 B Rv	GTCCGACGATACCATGTGG	
	165A-qFn	GATCGATTATCATGAGGGTTAAGC	Tatematsu *et al.* (2015)
	165A-qRn	CTATAATATCCTCGATCCAGACAAC	Tatematsu *et al.* (2015)
	166A-qFn	GGGGCTTTCTCTTTTGAGG	Tatematsu *et al.* (2015)
	166A-qRn	CGAAAGAGATCCAACATGAATAG	Tatematsu *et al.* (2015)
	166B-qFn	GATTTTTCTTTTGAGGGGACTGTTG	Tatematsu *et al.* (2015)
	166B-qRn2	CTGAATGTATTCAAATGAGATTGTATTAG	Tatematsu *et al.* (2015)
	166C-qFn	GCGATTTAGTGTTGAGAGGATTG	Tatematsu *et al.* (2015)
	166C-qRn	GTTCTTCCAAATTAATTCGAGTG	Tatematsu *et al.* (2015)
	166D-qFn	GGTTGAGAGGAATATTGTCTGG	Tatematsu *et al.* (2015)
	166D-qRn	TTTAGGGATTTCACTCTTTAAAATG	Tatematsu *et al.* (2015)
	166E-qFn	GAGGGGAATGTTGTCTGG	Tatematsu *et al.* (2015)
	166E-qRn2	GAAGAGACATATATATATAATCAAATATAGATC	Tatematsu *et al.* (2015)
	qPCR AtPHB Fw	CAACTTCACACTGCTTCTGG	
	qPCR AtPHB	GGCTTCATCCCAATCATCTG	

	Rv		
	qPCR AtREV Fw	CTCATTAAAGCCACAGCCAG	
	qPCR AtREV Rv	CAAACACTTTCCAAGCAACAG	
	qPCR AtATHB8 Fw	GCCTTGTGATATGCGAACGA	
	qPCR AtATHB8 Rv	TTTGGGCGAGTAAAGTGGAG	
	qPCR AtPHV Fw	CCCGTAGTTACAGTATTCATACAG	
	qPCR AtPHV Rv	CAAGTGTAGTTTCAAGCATGTC	
	qPCR AtCNA Fw	TTCCTTCTTCAACTTTGTAGCGG	
	qPCR AtCNA Rv	GAACCAATTTCCAGTGCCGA	
	qPCR AtCRC Fw	CTCTCGTTTCTCACCACAACTC	Gross *et al.* (2018)
	qPCR AtCRC Rv	GCTTCTTCTCAGGAGGTTTGAC	Gross *et al.* (2018)
	RTq-At-Actin_Fw	AGTGGTCGTACAACCGGTATTGT	Gross *et al.* (2018)
	RTq-At-Actin_Rv	GATGGCATGGAGGAAGAGAGAAAC	Gross *et al.* (2018)
	GAPDH QRT Fw	GCTTCCTTCAACATCATTCC	Tekleyohans (2014)
	GAPDH QRT Rev	AGTTGCCTTCTTCTCAAGTC	Tekleyohans (2014)
	EcCRC RTQ fw	CAGCCAAAAATTGGGCTAGAT	Orashakova *et al.* (2009)
	EcCRC RTQ rv	ACATAACTAGAGGAACTAAAACT	Orashakova *et al.* (2009)

Vector Maps

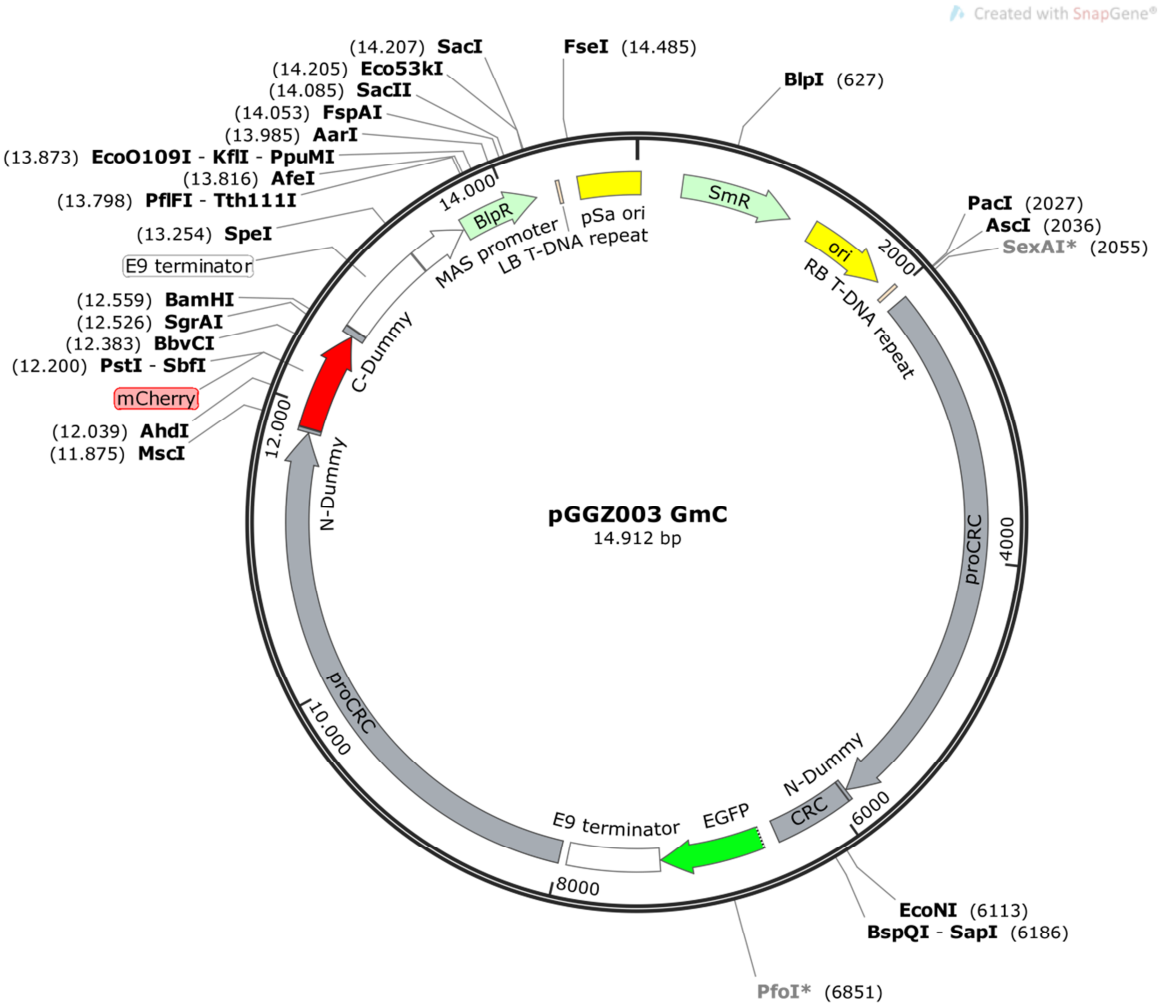

Figure 37: Vectormap of pGGZ003 proCRC:CRC-GFP; proCRC:mCherry.

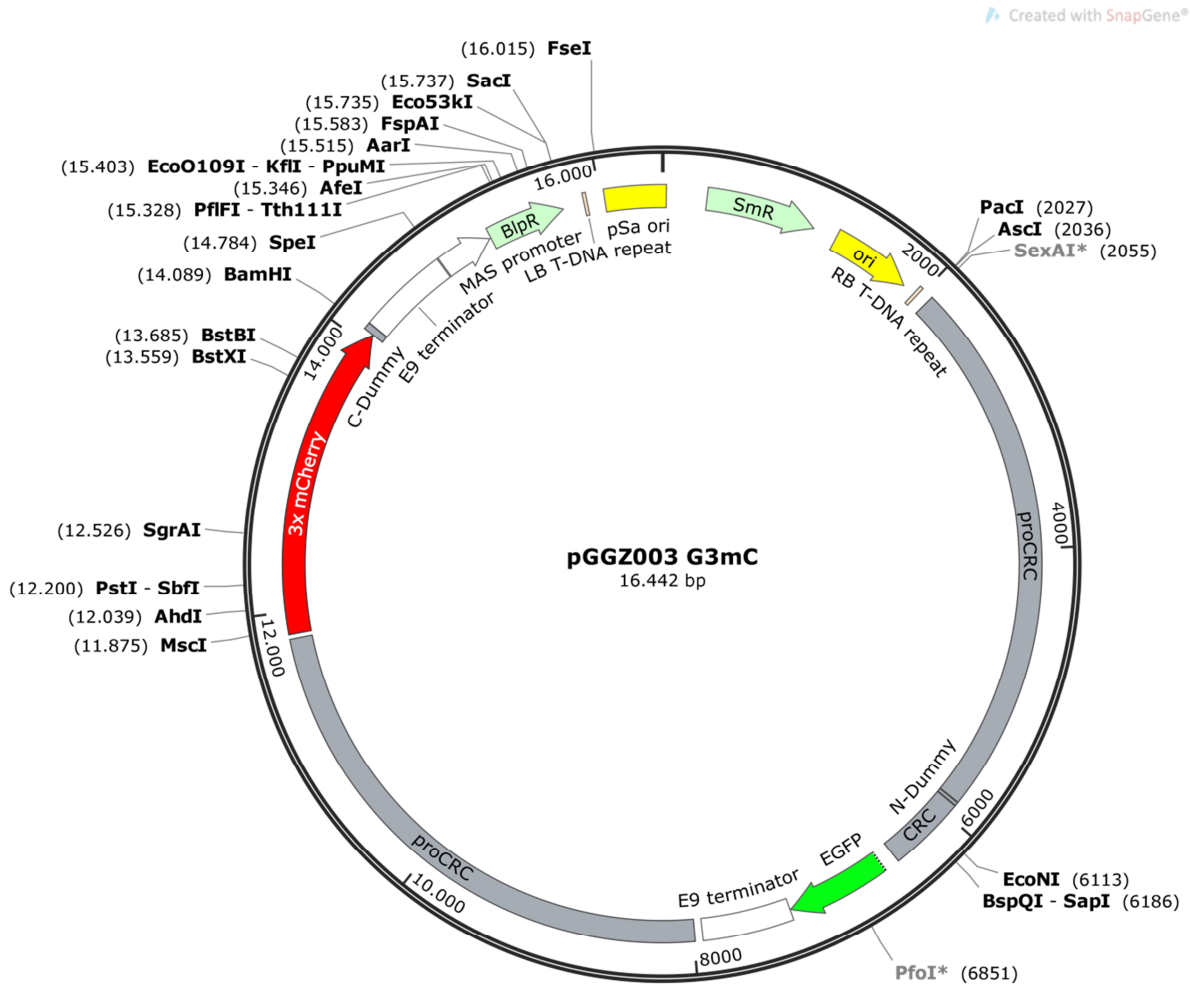

Figure 38: Vector map of pGGZ003 proCRC:CRC-GFP; proCRC:3xmCherry.

Composition of Y1H Libraries

Table 14: Composition library 2 (the „de Folter“ library).

Locus	Gene	Yeast growth marker
AT1G01030	NGA3	Trp
AT2G33860	ETT	Trp
AT2G35270	GIK	Trp
AT3G61970	NGA2	Trp
AT4G08150	BP	Trp
AT4G36930	SPT	Trp
AT5G02030	RPL	Trp
AT5G60450	ARF4	Trp

Table 15: Composition of library 3.

Locus	Gene	Yeast growth marker
AT1G08465	YAB2	Leu
AT1G13400	NUB	Leu
AT1G23420	INO	Leu
AT1G24260	SEP3	Leu
AT1G30330	ARF6	Leu
AT1G30490	PHV	Leu
AT1G43850	SEU	Leu
AT1G52150	CNA	Leu
AT1G69180	CRC	Leu
AT2G03710	SEP4	Leu
AT2G26580	YAB5	Leu
AT2G34710	PHB	Leu
AT3G47730	ATH1	Leu
AT4G00180	YAB3	Leu
AT4G01500	NGA4	Leu
AT4G18960	AG	Leu
AT4G25520	SLK1	Leu
AT4G28190	ULT1	Leu
AT4G32551	LUG	Leu
AT5G60690	REV	Leu
AT5G62090	SLK2	Leu

A. thaliana Mutant and Salk Lines

Table 16: Mutant lines and Salk lines which were crossed with *proCRC:GUS* reporter line.

Polymorphism	Locus	Gene
SALK_027284	AT1G10120	CIB4
SALK_116219C	AT1G23420	INO
hbb	AT1G25330	HAF
cal-1	AT1G26310	CAL
SALK_061829	AT1G43850	SEU
jag-jr	AT1G68480	JAG
SALK_135188C	AT1G68920	CIL1
SALK_041504C	AT2G26580	YAB5
SALK_005658C	AT2G33860	ETT
SALK_094394C	AT2G35270	GIK
SALK_108199	AT2G37060	NF-YB8
SALK_115813	AT2G42400	VOZ2
SALK_138286	AT3G16500	PAP1
SALK_002235	AT3G20910	NF-YA9
SALK_013517C	AT3G25710	TMO5

SALK_046567	AT3G25730	EDF3
SALK_122884	AT3G28910	MYB30
SALK_026607	AT3G55560	AGF2
SALK_137356C	AT3G61970	NGA2
SALK_208784	AT4G02670	IDD12
SALK_137958	AT4G08150	KNAT1/BP
SALK_006502	AT4G16780	HAT4
SALK_074642C	AT4G28190	ULT1
SALK_044923	AT4G31420	REIL1
SALK_113012C	AT4G32551	LUG
SALK_087493C	AT4G38960	BBX19
SALK_024956	AT4G40060	ATHB16
SALK_040126	AT5G02030	PNY
SALK_118847	AT5G02840	RVE4
SALK_061991	AT5G04340	ZAT6
SALK_027141	AT5G37020	ARF8
SALK_033647	AT5G60910	FUL
SALK_014881	AT5G65310	ATHB5

Electronic Appendix

Additional Publications

During this project, two additional not-project-related publications were published with my contribution:

Bolouri Moghaddam M-R, **Gross T**, Becker A, Vilcinskas A, Rahnamaeian M (2017). The selective antifungal activity of *Drosophila melanogaster* metchnikowin reflects the species-dependent inhibition of succinate–coenzyme Q reductase. *Scientific Reports* 7, doi:10.1038/s41598-017-08407-x

Abstract

Insect-derived antifungal peptides have a significant economic potential, particularly for the engineering of pathogen-resistant crops. However, the nonspecific antifungal activity of such peptides could result in detrimental effects against beneficial fungi, whose interactions with plants promote growth or increase resistance against biotic and abiotic stress. The antifungal peptide metchnikowin (Mtk) from Drosophila melanogaster acts selectively against pathogenic Ascomycota, including Fusarium graminearum, without affecting Basidiomycota such as the beneficial symbiont Piriformospora indica. Here we investigated the mechanism responsible for the selective antifungal activity of Mtk by using the peptide to probe a yeast two-hybrid library of F. graminearum cDNAs. We found that Mtk specifically targets the iron-sulfur subunit (SdhB) of succinate–coenzyme Q reductase (SQR). A functional assay based on the succinate dehydrogenase (SDH) activity of mitochondrial complex II clearly demonstrated that Mtk inhibited the SDH activity of F. graminearum mitochondrial SQR by up to 52%, but that the equivalent enzyme in P. indica was unaffected. A phylogenetic analysis of the SdhB family revealed a significant divergence between the Ascomycota and Basidiomycota. SQR is one of the key targets of antifungal agents and we therefore propose Mtk as an environmentally sustainable and more selective alternative to chemical fungicides.

Contribution

I performed a BiFC analysis of Mtk binding to SDH and added this part in material and methods and results.

Dommes AB, **Gross T**, Herbert DB, Kivivirta KI, Becker A. (2019) Virus-induced gene silencing: empowering genetics in non-model organisms. J Exp Bot. 2019 70(3):757-770. doi: 10.1093/jxb/ery411

Abstract

Virus-induced gene silencing (VIGS) is an RNA interference-based technology used to transiently knock down target gene expression by utilizing modified plant viral genomes. VIGS can be adapted to many angiosperm species that cover large phylogenetic distances, allowing the analysis of gene functions in species that are not amenable to stable genetic transformation. With a vast amount of sequence information already available and even more likely to become available in the future, VIGS provides a means to analyze the functions of candidate genes identified in large genomic or transcriptomic screens. Here, we provide a comprehensive overview of target species and VIGS vector systems, assess recent key publications in the field, and explain how plant viruses are modified to serve as VIGS vectors. As many reports on the VIGS technique are being published, we also propose minimal reporting guidelines for carrying out these experiments, with the aim of increasing comparability between experiments. Finally, we propose methods for the statistical evaluation of phenotypic results obtained with VIGS-treated plants, as analysis is challenging due to the predominantly transient nature of the silencing effect.

Contribution

I wrote the chapter about “Development of VIGS-suitable vector systems from plant viruses”, including figure 2.

Declaration

I declare that I have completed this dissertation single-handedly without the unauthorized help of a second party and only with the assistance acknowledged therein. I have appropriately acknowledged and cited all materials that are derived literally from or are based on the content of published or unpublished work of others, and all information that relates to verbal communications. I have abided by the principles of good scientific conduct laid down in the charter of the Justus-Liebig University of Giessen in carrying out the investigations described in the dissertation.

Date Signature